UNIVERSIDADE ESTADUAL DO NORTE FLUMINENSE DARCY RIBEIRO – UENF

JACKELLINNE CAETANO DOUÉTTS PERES

Identificação e caracterização da AaMps1 e análise proteômica comparativa durante o controle do ciclo celular na embriogênese somática de *Araucaria angustifolia* (Bertol.) Kuntze

CAMPOS DOS GOYTACAZES – RJ
OUTUBRO/2016

Identificação e caracterização da AaMps1 e análise proteômica comparativa durante o controle do ciclo celular na embriogênese somática de *Araucaria angustifolia* (Bert.) O. Ktze.

JACKELLINNE CAETANO DOUÉTTS PERES

"Tese apresentada ao Centro de Biociências e Biotecnologia da Universidade Estadual do Norte Fluminense Darcy Ribeiro, como parte das exigências para obtenção do título de Doutora em Biociências e Biotecnologia".

Orientadora: Profª. Dra. Claudete Santa Catarina

Co-orientador: Prof. Dr. Marco Antonio Lopes Cruz

CAMPOS DOS GOYTACAZES – RJ

OUTUBRO/2016

Identificação e caracterização da AaMps1 e análise proteômica comparativa durante o controle do ciclo celular na embriogênese somática de *Araucaria angustifolia* (Bert.) O. Ktze.

JACKELLINNE CAETANO DOUÉTTS PERES

"Tese apresentada ao Centro de Biociências e Biotecnologia da Universidade Estadual do Norte Fluminense Darcy Ribeiro, como parte das exigências para obtenção do título de Doutora em Biociências e Biotecnologia".

Aprovada em 24 de outubro de 2016.

Comissão Examinadora:

_____

Profª. Drª. Elane da Silva Ribeiro (D.Sc., Biociências e Biotecnologia) – UFRJ/Macaé

_____

Profª. Drª. Maura da Cunha (D.Sc., Ciências Biológicas) – UENF

_____

Profª. Drª. Antônia Elenir Amâncio Oliveira – (D.Sc., Biociências e Biotecnologia) - UENF

_____

Prof. Dr. Marco Antônio Lopes Cruz (D.Sc. Biociências e Biotecnologia) – UFRJ/Macaé
(Co-orientador)

_____

Profª. Dra. Claudete Santa Catarina (D.Sc. Biotecnologia) – UENF
(Orientadora)

A minha família que são meu apoio e sustentação em todos os momentos.
Dedico e ofereço

AGRADECIMENTOS

A Universidade Estadual Do Norte Fluminense pela oportunidade de Educação gratuita e de qualidade.

Agradeço a FAPERJ pela bolsa e ao CNPq e a CAPES pelo apoio financeiro.

Agradeço em especial a minha orientadora Professora Claudete Santa-Catarina, pela confiança no meu trabalho, paciência e apoio nesta jornada. Agradeço também, pelos valiosos ensinamentos e por estar presente sempre que necessário.

Ao meu coorientador Professor Marco Antônio Lopes Cruz (UFRJ/Macaé) pela paciência, colaboração e conselhos.

Ao Professor Vanildo Silveira pelo suporte para a realização deste trabalho.

A Victor, Kariane, Joviana, Ellen e Ricardo pela amizade que sempre me fortalece e que pretendo cultivar para o resto da vida.

Aos amigos do Laboratório, Poliana, Rosana, Pollyara, Ângelo, Lucas, Bianca, Felipe e Tatiana por toda a ajuda e por tornarem mais agradáveis as aulas, os experimentos e os dias nesta Universidade.

Agradeço a minha família, pois todos de alguma forma contribuíram para minha trajetória até o presente momento.

A minha mãe Telma, e as tias Gianni e Rita que sempre me incentivaram e apoiaram em todos momentos da vida.

A minha avó Genilsa, carinhosamente chamada de mãezinha, pelos valiosos ensinamentos ao longo desta vida.

As amigas e irmãs de coração Rosiane, Karine, Marcelly e Adriana por não desistirem de mim, mesmo quando não posso “aparecer” e por todos momentos de descontração em meio a tantos contratempos.

A minha cunhada/amiga Patrícia pelo incentivo a minha vida acadêmica e pela empolgação frente aos meus avanços.

Ao meu amado marido Felippe, por tudo que enfrenta ao meu lado, por ser meu companheiro nesta luta diária que é a vida, por nossos filhos Marianna e Eduardo que trazem alegria para minha vida.

A Deus que me ampara e permite que eu possa atingir os objetivos traçados para a vida.

Sumário

RESUMO

A *Araucaria angustifolia* é uma espécie nativa brasileira, que devido a sua importância econômica, foi intensamente explorada ao longo dos anos, encontrando-se atualmente ameaçada de extinção na categoria criticamente em perigo. O uso de técnicas biotecnológicas, como a embriogênese somática, tem sido aplicada à espécie, visando estabelecer metodologias alternativas de propagação que possam contribuir para a conservação da espécie, e também servir de modelo para estudos básicos. Um sistema de embriogênese somática da espécie foi desenvolvido, entretanto, a conversão de embriões somáticos ainda é uma etapa limitante. Desta forma, o objetivo deste trabalho foi identificar e caracterizar a proteína alvo do inibidor da Mps1 e avaliar o efeito da inibição desta proteína sobre proteínas diferencialmente abundantes em culturas embriogênicas de *A. angustifolia*. Inicialmente, foi realizada a identificação e caracterização da Mps1 utilizando banco de dados de transcriptoma de Araucaria e espectrometria de massas, bem como foi avaliado o efeito da inibição da Mps1 sobre o crescimento e morfologia de culturas embriogênicas de *A. angustifolia*. Para tanto, culturas embriogênicas foram tratadas ou não com 10 µM de SP600125, inibidor da Mps1, durante 15 dias. Posteriormente, foi avaliado o efeito da inibição da AaMps1 sobre as proteínas diferencialmente expressas. Para a análise em espectrometria de massas, as proteínas foram extraídas com tampão Ureia/Tiureia, digeridas com tripsina e posteriormente analisadas com ESI-LC-MS/MS. Um banco de dados de *A. thaliana* e *A. angustifolia* foram utilizados para identificação das proteínas, e o BlastGo foi utilizado para a classificação funcional das proteínas que foram diferencialmente abundantes (pelo menos 1,5 vezes). Na primeira etapa, foi identificado um gene de cópia única da proteína Mps1 (AaMps1) a partir do banco de dados do transcriptoma de *A. angustifolia*, e através de espectrometria de massa, AaMps1 foi identificada e quantificada em culturas embriogênicas. O inibidor da Mps1 inibiu o crescimento celular e alterou a morfologia das massas pró-embriogênicas (PEMs), bem como resultou em redução nos níveis de proteína AaMps1 em culturas embriogênicas. Na segunda etapa, verificou que a inibição da AaMps1 afetou a abundância de outras proteínas. Proteínas relacionadas com o ciclo celular e proliferação, e abundantes na fase de intensa divisão celular, foram down-reguladas com a utilização do inibidor. Proteínas relacionadas com organização do citoesqueleto, expansão celular e proteção contra dessecação foram up-reguladas quando tratadas. Este trabalho auxiliará no esclarecimento dos mecanismos relacionados com a inibição de proliferação e diferenciação das culturas embriogênicas visando a formação de embriões somáticos em plantas.

Palavras-chaves: Biotecnologia, Domínio quinase, Proteínas.

ABSTRACT

Araucaria angustifolia is a Brazilian native species, which because of its economic importance, has been heavily exploited over the years, meeting currently threatened with extinction in the critically endangered category. The use of biotechnological techniques such as somatic embryogenesis, has been applied to the species, to establish alternative methods of propagation that can contribute to the conservation of the species, and also serve as a model for basic studies. A system of somatic embryogenesis was developed for this species, however, the conversion of somatic embryos is still a limiting step. Thus, the objective of this study was to identify and characterize the target protein of Mps1 inhibitor and evaluate the effect of its inhibition on differentially abundant proteins in embryogenic cultures of *A. angustifolia*. Initially, the identification and characterization of Mps1 using transcriptome database of Araucaria and mass spectrometry was performed, as well as the effect of Mps1 inhibition on the growth and morphology of the embryogenic cultures of *A. angustifolia* were realized. To this end, embryogenic cultures were treated with or without 10 μM of SP600125, the Mps1 inhibitor, during 15 days. Further, the effect of the AaMps1 inhibition on the differentially expressed proteins was performed. For the analysis of mass spectrometry, proteins were extracted with urea/thiourea buffer, digested with trypsin and analyzed with LC-ESI-MS/MS. An *A. thaliana* and *A. angustifolia* database were used for identification of proteins, and BlastGo was used for the functional classification of proteins that were differentially abundant (at least 1.5 times). In the first step, we identified a single copy gene Mps1 protein (AaMps1) from the transcriptome database of *A. angustifolia* and through a mass spectrometric approach, AaMps1 was identified and quantified in embryogenic cultures. The inhibitor Mps1 inhibited cell growth and change the morphology of pro-embryogenic masses (PEMs), as well as inhibition of AaMps1 resulted in a reduction in protein levels in embryogenic cultures. In the second step, the inhibition of AaMps1 affect the abundance of other proteins. Proteins related to the cell cycle and proliferation, intense and abundant in the cell division phase, were down-regulated using the inhibitor. Proteins related to cytoskeletal organization, cell expansion and desiccation protection were up-regulated when treated. This work helps to clarify the mechanisms related to inhibition of proliferation and differentiation of embryogenic cultures aiming at the formation of somatic embryos in plants.

Key-words: Biotechnology, Kinase domain, Proteins.

1 INTRODUÇÃO

O estabelecimento de estratégias de conservação das espécies florestais nativas, como a *Araucaria angustifolia*, exige informações sobre a biologia reprodutiva e a ecologia, bem como, estudos básicos sobre sistemas alternativos de propagação comparado com os métodos tradicionais. Neste contexto, a aplicação de técnicas biotecnológicas como a embriogênese somática pode ser uma alternativa para a manutenção de espécies nativas (Bunn et al., 2011), em especial aquelas ameaçadas de extinção, como é o caso da *A. angustifolia* (IUCN, 2015).

Um sistema de embriogênese somática foi desenvolvido para esta espécie e vários aspectos associados ao controle deste processo foram estudados até o momento, incluindo o efeito de poliaminas (PAs), óxido nítrico (NO) e agentes de maturação, visando identificar marcadores da competência para a embriogênese somática (Guerra et al., 2000; Silveira et al., 2006; Steiner et al., 2008; Osti et al., 2010; Vieira et al., 2012; Farias-Soares et al., 2014), Adicionalmente, alguns estudos demonstraram que a diferença no perfil protéico, via análise proteômica, pode auxiliar na busca de marcadores moleculares associados ao desenvolvimento vegetal, e a identificação de proteínas especificas também pode auxiliar o entendimento da competência celular para a evolução morfogenética das culturas embriogênicas (Balbuena et al., 2011; Jo et al., 2014; Dos Santos et al., 2016; Fraga et al., 2016).

Recentemente, foi verificado que o controle do ciclo celular, utilizando o inibidor da Monopolar Spindle 1 (Mps1), o SP600125, influencia o crescimento e a morfologia das culturas embriogênicas, assim como o metabolismo endógeno de carboidratos, PAs e NO (Douétts-Peres, 2013). Em continuidade aos estudos iniciados torna-se necessário identificar a expressão e caracterizar a proteína alvo do inibidor, a Mps1 em *A. angustifolia* (AaMps1), e analisar o perfil de proteínas diferencialmente abundantes, via proteômica comparativa, sob influência do inibidor da Mps1. Estes estudos

possibilitarão o melhor entendimento do controle do ciclo celular sobre a embriogênese somática em *A. angustifolia*.

Neste sentido, o intuito do presente trabalho é investigar os efeitos da inibição do ciclo celular nas culturas embriogênicas e como esta inibição pode influenciar o perfil proteico durante a cultura *in vitro* de culturas embriogênicas. Desta forma, a embriogênese somática aliada a análise proteômica podem ser ferramentas importantes para ajudar na compreensão dos eventos ocorridos durante a embriogênese somática. Assim poderemos colaborar no esclarecimento dos mecanismos relacionados com a inibição de proliferação e início da diferenciação das culturas embriogênicas visando a formação de embriões somáticos e contribuindo para o estabelecimento de metodologias alternativas para a propagação e conservação desta espécie.

No primeiro capítulo, visamos identificar e realizar uma caracterização estrutural e funcional de AaMps1 e analisar os efeitos da inibição desta proteína sobre o crescimento celular e a morfologia das Massas Pro-Embriogênicas (PEMs) em culturas embriogênicas de *A. angustifolia* e, no segundo capítulo, estudar os efeitos da inibição da proteína AaMps1 sobre os perfis proteômicos de culturas em suspensão embriogênicas de *A. angustifolia*.

2 REVISÃO DE LITERATURA

2.1 Espécie de estudo

Araucaria angustifolia constitui o dossel superior da Floresta Ombrófila Mista e apresenta um caráter dominante na vegetação (Longhi, 1980; Leite e Klein, 1990). O gênero de Araucária só ocorre no hemisfério Sul, no Brasil sua área de distribuição ocupava originalmente uma superfície de cerca de 200.000 km^2, ocorrendo no Paraná (40% da superfície), Santa Catarina (31%) e Rio Grande do Sul (25%) e em manchas esparsas no Sul de São Paulo (3%), até o Sul de Minas Gerais e do Rio de Janeiro (1%) (Carvalho, 1994).

Por possuir um alto valor econômico, madeireiro, resinífero e alimentar, tem havido uma progressiva extração das populações naturais de *A. angustifolia* ao longo dos anos, e estimativas apontam a existência de aproximadamente 1 a 2% das áreas originais cobertas pela floresta com Araucária (Koch e Corrêa, 2002). Neste sentido, a espécie foi incluída na "Lista de espécies que necessitam atenção" elaborada pela "Food and Agriculture Organization" (FAO, 1986) e na "Lista oficial de espécies da flora brasileira ameaçadas de extinção", como uma espécie vulnerável (IBAMA, 1992). Recentemente, de acordo com a Red list 2015 organizada pela "International Union for Conservation of Nature" (IUCN, 2015), a *A. angustifolia* se encontra criticamente em perigo na listagem de espécies ameaçadas de extinção.

Outro fator que vem contribuindo para a vulnerabilidade da espécie é o fato das sementes serem recalcitrantes (Farias-Soares et al., 2013), tendo curta longevidade natural, com perda total de viabilidade em até um ano após a coleta (Aquila e Ferreira, 1984). Estudos mostram que os embriões de *A. angustifolia* apresentam alterações estruturais e tornam-se inviáveis quando o teor hídrico atinge valores inferiores a 70 %

(Tompsett, 1984; Farrant et al., 1989). Estudos visando o aprimoramento de técnicas alternativas de propagação são importantes para a manutenção da espécie e dos recursos naturais. Neste contexto, técnicas biotecnológicas, como a embriogênese somática, têm sido utilizadas visando diferentes objetivos, que vão desde a obtenção de um modelo de referência para estudos básicos em fisiologia, bioquímica e biologia celular e molecular, até a propagação clonal, incluindo a conservação em várias espécies (Park et al., 1998; Guerra et al., 2000; Bunn et al., 2011; Pinhal et al., 2011).

Comparativamente à micropropagação, a embriogênese somática é considerada mais vantajosa, pois permite a obtenção de uma grande quantidade de propágulos (embriões somáticos), um alto grau de automatização que reduz os custos por unidade produzida, os embriões somáticos podem ser produzidos de forma sincronizada, com alto grau de uniformização e pureza genética. Além disso, a embriogênese somática pode ser utilizada como uma ferramenta integrada a programas de melhoramento genético florestal, em especial, quando associada à técnica de criopreservação (Merkle e Dean, 2000).

2.2 A embriogênese somática em *A. angustifolia*

A embriogênese somática é um processo pelo qual, células somáticas se diferenciam em embriões somáticos (Tautorus et al., 1991), passando por estádios de desenvolvimento morfologicamente semelhantes aos do embrião zigótico, que são derivados da fusão de células gaméticas (Termignoni, 2005). Neste sentido, denomina-se embrião somático aquele derivado de células somáticas adultas, já diferenciadas (Termignoni, 2005). Como modelo para estudo de um processo morfogenético, a embriogênese somática é ideal para investigar o processo de diferenciação em plantas, bem como a expressão de mecanismos de totipotencialidade da célula vegetal (Andrade, 2010).

Um sistema de embriogênese somática foi desenvolvido para *A. angustifolia* e a estratégia empregada no estabelecimento da embriogênese somática nesta espécie consiste em: um ciclo de indução/multiplicação de culturas embriogênicas originadas a partir do embrião zigótico imaturo pela utilização de auxinas e citocininas; e um ciclo de maturação, promovido por alterações no balanço de reguladores de crescimento e fontes de carbono adicionado ao meio de cultura (Figura 1). Os resultados destas etapas levam à formação de embriões somáticos (Steiner et al., 2005; Guerra et al., 2008; Steiner et al., 2008). Adicionalmente, sabe-se que as rotas morfogenéticas na multiplicação e maturação podem ser influenciadas pela adição de ácido abscísico (ABA), agentes osmóticos, carvão ativado, PAs, glutationa e NO aos meios de cultura (Astarita, 2000; Silveira et al., 2002; Steiner et al., 2005; Silveira et al., 2006; Steiner et al., 2007; Osti et al., 2010; Vieira et al., 2012). Recentemente em trabalhos preliminares , foi possível observar que a inibição da divisão celular em culturas embriogênicas *de A. angustifolia*, usando o inibidor da Mps1, afeta a morfologia e crescimento, assim como o metabolismo endógeno de carboidratos, PAs e NO (Douétts-Peres, 2013). Desta forma, a continuidade dos estudos visando entender melhor o papel da inibição da divisão celular e o padrão da expressão diferencialmente abundante de proteínas em Araucária é fundamental para melhor entender do controle do ciclo celular na embriogênese somática nesta espécie.

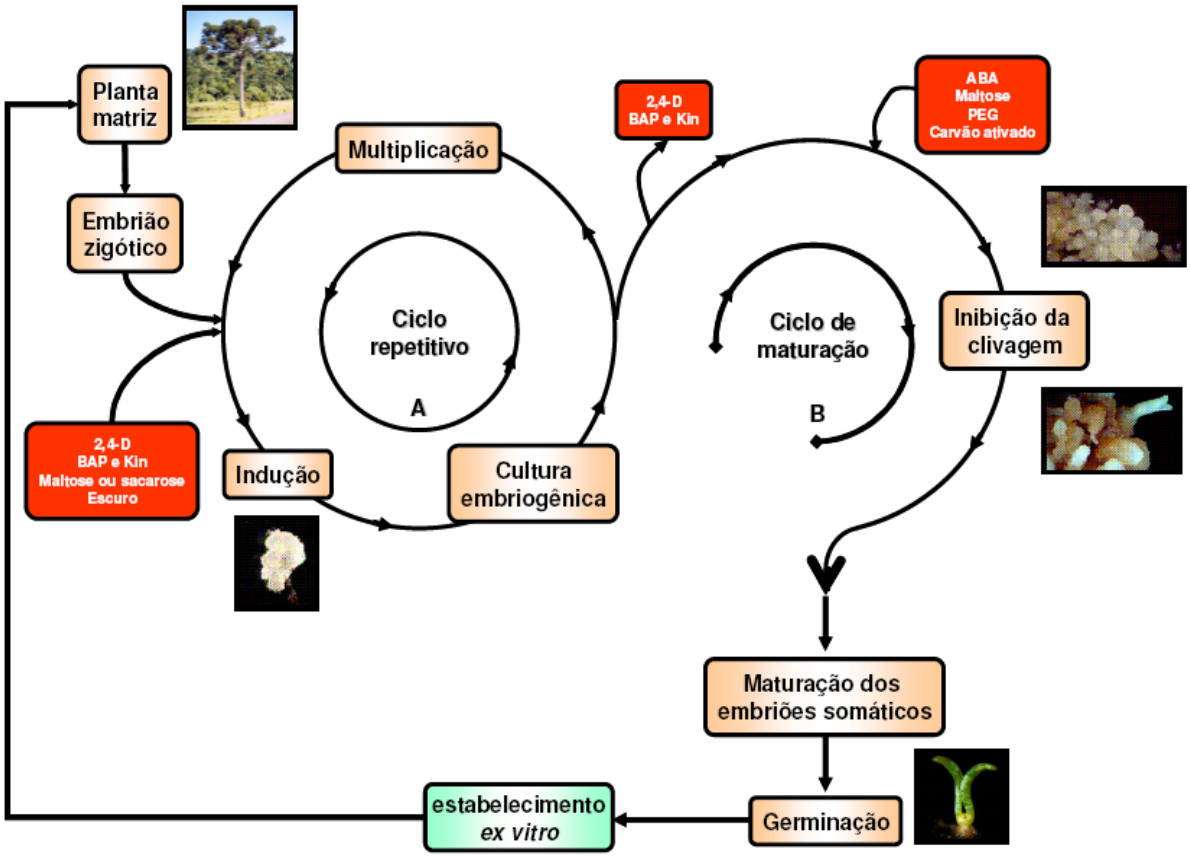

Figura 1: Representação esquemática dos ciclos de multiplicação e maturação que compõem o processo de embriogênese somática em *A. angustifolia*. 2,4 D: ácido 2,4 diclorofenoxiacético; BAP: benzilaminopurina; Kin: cinetina; ABA: ácido abscísico; PEG: polietileno glicol. Fonte: Balbuena (2009).

2.3 O ciclo celular na embriogênese somática

A divisão celular compreende quatro fases sequenciais ordenadas temporalmente que resulta na formação de duas células filhas. Na primeira fase denominada G1, a célula percebe sinais relevantes que iniciam os processos de divisão celular. Posteriormente, a célula passa para a fase S, ocorrendo a replicação do DNA e dos outros componentes celulares, em seguida, entra na fase G2 que separa a fase S da fase M subsequente. As células em G2 são, portanto, diferentes das células G1 por possuirem um conteúdo de DNA e volume celular duplicado. As fases G1 e G2 são pontos de checagem fundamentais, pois permitem o funcionamento dos controles

que garantem que a fase anterior tenha sido completada de forma precisa antes de iniciar a próxima fase (Vantard et al., 2000; Dewitte e Murray, 2003).

O ponto de verificação, também conhecido como ponto de verificação de montagem do fuso, impede avanço do ciclo celular da metáfase para anáfase, antes da fixação de cada cromossomo aos microtúbulos do fuso (Musacchio e Salmon, 2007). Alguns autores ressaltam que a segregação cromossômica precisa durante a meiose é essencial para a divisão celular normal, e a formação de um fuso bipolar é necessária (Dawe, 1998; Compton, 2000; Chen et al., 2002). Adicionalmente, estudos posteriores demonstraram que os genes necessários para a meiose também desempenham um papel na formação do fuso mitótico (Marcus et al., 2003; Ambrose et al., 2005).

As células eucarióticas desenvolveram uma complexa rede de proteínas reguladoras que governa sua progressão. O ciclo celular eucariótico é regulado em múltiplos pontos e a maioria deles, senão todos, se estabelecem devido a ativação de uma classe especial de proteínas quinases. Estas proteínas são funcionais a partir da ligação com uma proteína reguladora conhecida como ciclina e são, portanto, chamadas quinases dependentes de ciclina (Dewitte e Murray, 2003). Na ausência de um ponto de verificação mitótico funcional, as células sofrem aneuploidia e posteriormente morrem. Isso ocorre, por exemplo, quando a função de uma proteína do fuso monopolar, chamada Mps1, é perdida (Lan e Cleveland, 2010).

A Mps1 é uma fosfoproteína quinase dual-específica, descrita primeiro em leveduras (Winey et al., 1991) e depois em humanos (Mills et al., 1992), é caracterizada como um regulador conservado evolutivamente em eucariotos (Fisk e Winey, 2004). Esta proteína desempenha um papel crucial no controle da exatidão de segregação cromossômica no ponto de verificação mitótico. A proteína Mps1 consiste de uma região N-terminal não catalítica e um domínio C-terminal catalítico, o qual expõe homologia fraca com outras quinases humanas, porém é altamente conservada entre

ortólogos eucarióticos (Liu e Winey, 2012). Em genomas vegetais, De Oliveira et al. (2012) verificaram um homólogo altamente semelhante, a AtMps1 em *Arabidopsis thaliana*, mostrando que as características estruturais, como o sítio catalítico, observado em Mps1 de outros eucariotos, são claramente conservadas em Mps1 de plantas. A Mps1 é um componente importante do ponto de verificação da montagem do fuso, fazendo parte do Spindle Assembly Checkpoint (SAC) e também é necessária para a correta localização de outras proteínas relacionadas com a montagem do fuso mitótico. A lista de funções da Mps1 também inclui papéis na meiose e citocinese (Fisk e Winey, 2004; Zhao e Chen, 2006; Musacchio e Salmon, 2007).

Neste sentido, a manipulação do funcionamento do ciclo celular pode ser uma importante ferramenta para estudos relacionados a diversos aspectos que ocorrem ao longo do desenvolvimento vegetal. Diversos compostos, ou agentes químicos, atuam como inibidores do ciclo celular e são utilizados para sincronizar células vegetais em estudos associados à progressão do ciclo celular em plantas. Os agentes químicos atuam bloqueando o ciclo celular, agindo sobre vários aspectos, como a condução de forças motoras do ciclo celular (Planchais et al., 2000). A concentração ótima de um inibidor, a duração do tratamento e tempo necessário para voltar a entrar no ciclo celular têm de ser estabelecido para cada espécie vegetal (Binarová et al., 1998; Planchais et al., 2000).

Vários são os agentes químicos utilizados para inibição do ciclo de divisão celular, como a roscovitina (Binarová et al., 1998) hidroxiuréia, mimosina e afidicolina (Young e Hodas, 1964; Mironov et al., 1999; Planchais et al., 2000). Dentre os inibidores químicos, o SP600125 é um inibidor de proteínas quinase originalmente descrito como um inibidor de proteínas Jun N-terminal kinase (JNK) em animais (Bennett et al., 2001), o qual também tem sido valioso para validar as funções celulares de Mps1 (Schmidt et al., 2005; Jelluma et al., 2008). Foi demonstrado que na proteína

Mps1 humana, que apresenta uma conformação típica de proteína quinase, o SP6000125 atua como um inibidor ATP competitivo, ficando alojado no sítio de ligação do ATP onde é estabilizado por interações hidrofóbicas, verificando-se que a inibição da Mps1 no domínio catalítico purificado foi 90% na presença deste inibidor (Chu et al., 2008). Adicionalmente, alguns resultados indicam que o inibidor SP600125 bloqueia a transição das fases G2-M em *Arabidopsis* por inibir especificamente a atividade da AtMps1 (De Oliveira et al., 2012).

2.4 Análises proteômicas na embriogênese somática

O perfil de proteínas expressas em uma determinada célula, tecido ou organismo pode ser evidenciado através de uma técnica denominada proteômica (Wasinger et al., 1995).

Além das diversas funções que as proteínas possuem, vários estudos mostram que estas atuam como marcadores moleculares do desenvolvimento das plantas (Campalans et al., 2000). O desenvolvimento de um número de métodos proteômicos tem facilitado ainda mais a compreensão da embriogênese somática em plantas (Correia et al., 2016). Além disso a expressão de determinadas proteínas pode ser relacionada com a competência das culturas embriogênicas para formar embriões somáticos (Ventosa, 2010; Almeida et al., 2012; Noah et al., 2013; Jo et al., 2014). Além disso, um perfil diferenciado de proteínas expressas foi observado para os diferentes estádios de desenvolvimento dos embriões somáticos em *Mendicago truncatula* (Almeida et al., 2012). Recentemente, a identificação de algumas proteínas, pela proteômica, também possibilitou o entendimento de processos celulares, como a morte celular programada, que ocorrem durante o desenvolvimento de embriões somáticos em *A. thaliana* e *Picea abies* (Smertenko e Bozhkov, 2014).

Investigação de alterações na expressão de proteínas são focados principalmente em três aspectos da embriogênese somática: mudanças de expressão de proteína durante os estágios iniciais da embriogênese, proteínas diferencialmente expressas em células embrionárias e não embrionárias, e proteínas diferencialmente expressas em embriões somáticos e zigóticos (Guan et al., 2016). Durante a fase de indução de embriões somáticos, calos embriogênicos e não embriogênicas têm sido utilizados para identificar alterações na expressão de proteínas e estes estudos tem associado um perfil proteico diferenciado em culturas com diferentes potenciais embriogênicos identificando classes de proteínas ou proteínas chaves que promovam uma melhor eficiência na formação dos embriões (Guan et al., 2016).

O perfil proteico na embriogênese somática de Araucária já vem sendo utilizado para a elucidação de alguns aspectos como a capacidade de maturação de culturas embriogênicas. Nas diferentes fases de desenvolvimento do embrião somático (Steiner, 2005), a diferença no perfil proteico, via análise proteômica, tem auxiliado na busca de marcadores moleculares associados ao desenvolvimento vegetal. Além disso, a identificação de proteínas especificas também podem auxiliar no entendimento da competência celular para a evolução morfogenética das culturas embriogênicas. Estudos em linhagens de células de *A. angustifolia* com diferentes capacidades de desenvolver embriões somáticos demonstraram, por exemplo, que a enzima S-adenosilmetionina sintase é uma proteína importante relacionada com a promoção do desenvolvimento dos embriões somáticos em culturas embriogênicas (Jo et al., 2014). De modo geral, para esta espécie, um aumento na abundância de proteínas relacionadas à defesa celular e à respostas a diferentes tipos de estresse (oxidativo, hormonal e osmótico), são observadas em células com maior potencial embriogênico (Dos Santos et al., 2016; Fraga et al., 2016). Baseado nestes relatos, a embriogênese somática também pode ser utilizada como modelo para o estudo do controle do ciclo

celular na fase de proliferação associado ao perfil de proteínas diferencialmente abundantes durante este processo.

3 OBJETIVOS

3.1 Objetivo geral

O objetivo deste estudo é identificar e caracterizar a proteína alvo do inibidor da Mps1 e avaliar o efeito desta inibição sobre a abundância diferencial de proteínas em culturas embriogênicas de *A. angustifolia*.

3.2 Objetivos específicos

1) Identificar a sequência da proteína homóloga a Mps1 no banco de transcriptoma de *A. angustifolia* (AaMps1).
2) Caracterizar estrutural e funcionalmente a sequência da AaMps1 em *A. angustifolia.*
3) Identificar e quantificar a proteína AaMps1 em culturas embriogênicas de *A. angustifolia* mantidas em suspensão.
4) Analisar os efeitos da inibição desta proteína sobre o crescimento celular e morfologia das massas pró-embriogênicas (PEMs) em culturas embriogênicas de *A. angustifolia*.
5) Analisar os efeitos da inibição desta proteína sobre o conteúdo da AaMps1 em culturas embriogênicas de *A. angustifolia* mantidas em suspensão.
6) Estudar os efeitos da inibição da proteína AaMps1 em perfis proteômicos de culturas embriogênicas de *A. angustifolia* em suspensão.

4 CAPÍTULOS

4.1 Capítulo 1

Mps1 (Monopolar Spindle 1) Protein Inhibition Affects Cellular Growth and Pro-Embryogenic Masses Morphology in Embryogenic Cultures of Araucaria angustifolia (Bertol.) Kuntze (Araucariaceae)*

Abstract

Somatic embryogenesis has been shown to be an efficient tool for studying processes based on cell growth and development. The fine regulation of the cell cycle is essential for proper embryo formation during the process of somatic embryogenesis. The aims of the present work were to identify and perform a structural and functional characterization of Mps1 and to analyze the effects of the inhibition of this protein on cellular growth and proembryogenic mass (PEM) morphology in embryogenic cultures of *A. angustifolia*. A single copy Mps1 gene named AaMps1 was retrieved from *the A. angustifolia* transcriptome database, and through a mass spectrometry approach, AaMps1 was identified and quantified in embryogenic cultures. The Mps1 inhibitor SP600125 (10 μM) inhibited cellular growth and changed PEMs, and these effects were accompanied by a reduction in AaMps1 protein levels in embryogenic cultures. Our work has identified the Mps1 protein in a gymnosperm species for the first time, and we have shown that inhibiting Mps1 affects cellular growth and PEM differentiation during *A. angustifolia* somatic embryogenesis. These data will be useful for better understanding cell cycle control during somatic embryogenesis in plants.

*Este capitulo foi publicado em 11 de abril de 2016, na revista PLoS One 11(4): e0153528.Doi:10.1371/journal.pone.0153528 (Anexo 1).

4.1.1 Introduction

The transition from a somatic cell into a somatic embryo, during somatic embryogenesis, is a complex event, consisting of the following crucial steps: induction, cell dedifferentiation, and competence acquisition; multiplication, with intense cell division; maturation, which determines fate; and the germination of somatic embryos [1].

During somatic embryo formation, the correct performance of the cell cycle is crucial, and adequate levels of certain signaling molecules, such as polyamines, carbohydrates, and nitric oxide (NO), are required [2–4]. The maturation induction of somatic embryogenic cultures with maturation promoters, such as abscisic acid (ABA), or with osmotic agents, such as polyethylene glycol (PEG) and maltose, induce cell growth inhibition, preventing division and promoting the differentiation of cell cultures [5–8]. However, other compounds, such as auxins, NO, and putrescine, promote cell division, thereby increasing growth and inhibiting cell differentiation into somatic embryos [4,6,7]. Embryogenic suspension culture systems have been developed for *Araucaria angustifolia*, and they have been shown to be efficient systems for studying the effects of signaling molecules in gymnosperms [4,9,10]. Cell cycle regulation can be used as a tool for the elucidation of metabolism-related events, and it involves signaling compounds that are important for various processes in plant development [11], including somatic embryogenesis [12].

Cell division in eukaryotes is controlled by a complex mechanism that involves cyclin dependent kinases (CDKs) as key regulators [13,14]. One of these kinases is Mps1 (Monopolar Spindle 1), which has been described in

humans and is characterized as a cell cycle regulator that is evolutionarily conserved in eukaryotes [15]. Mps1 is a dual-specificity protein kinase that plays a critical role in monitoring the accuracy of chromosome segregation at the mitotic checkpoint, and it is an important component of the Spindle Assembly Checkpoint (SAC) [16]. Among chemical inhibitors, SP600125 acts on Jun N-terminal kinase (JNK) proteins in humans [17] and has been valuable in validating the cellular functions of Mps1. In plants, a protein was found that was highly similar to human Mps1 in terms of structural characteristics, such as its catalytic site, and it was conserved relative to the Mps1 protein found in *A. thaliana* [18]. The inhibitor SP600125 blocks the G2-M transition in Arabidopsis by specifically inhibiting the activity of AtMps1 [18]. However, the role of Mps1 in gymnosperm species, such as *A. angustifolia*, has not yet been shown.

The aims of the present work were to identify and perform a structural and functional characterization of Mps1 and to analyze the effects of the inhibition of this protein on cellular growth and pro-embryogenic mass (PEM) morphology in embryogenic cultures of *A. angustifolia*.

4.1.2 Materials and Methods

4.1.2.1 Plant Material

Embryogenic suspension cultures of *A. angustifolia* were induced according to the methodology established by Steiner et al. [19] and then used for these experiments. Embryogenic cell suspension cultures are formed by PEMs made of embryogenic cells (which are rounded, with a dense cytoplasm) and suspensor cells (which are highly vacuolated and elongated) [6,20].

4.1.2.2 Mps1 Sequence Identification and Structural Analyses

To identify a putative Mps1 from *A. angustifolia*, we performed a tBLASTn search [21] by using the Mps1 protein sequence of *A. thaliana* (AT1G77720) as a query against the *A. angustifolia* transcriptome database [22,23], with the following parameters: E-value > E-10 and a minimum coverage threshold of 30% (query and hit). The complete sequence is available at GenBank under accession number KU600448. Other sequences that were homologous to their *A. thaliana* counterpart were identified by searching the Phytozome 10.2 database (http://www.phytozome.net/), NCBI (http://www.ncbi.nlm.nih.gov/), TAIR (https://www.arabidopsis.org), and SustainPineDB (http://www.scbi.uma.es/sustainpinedb) using BLAST. All the sequences obtained here and the putative AaMps1 were aligned with MEGA software, version 6.0 [24] using MUSCLE/CLUSTALW with default parameters. The alignment was analyzed using the Neighbor-Joining method, and the distances were calculated according to the best model identified by the program. The model parameter and tree estimates were performed with PhyML [25], and the tree topology was evaluated with 1500 bootstrap replications. Detailed information on all the sequences used for analysis is available in S1 Table.

A template identification using the Mps1 sequence from *A. angustifolia* was performed using the template identification tool from SWISS-MODEL [26–28] to find the most accurate templates (by considering the sequence identity, coverage, and crystal resolution). Additionally, we performed a motif search analysis with the aid of the Eukaryotic Linear Motif (ELM) server [29] to find interaction sites with other cell cycle regulation elements.

Molecular modeling was performed using MODELLER v9.14 [30,31] with the following structures as templates: 2ZMD [32], 3DBQ [33], 3HMN [34], and 3VQU (http://dx.doi.org/10.2210/pdb3vqu/pdb). All four crystals are representations of the human Mps1 protein. Molecular docking experiments with the *A. angustifolia* Mps1 3D model were performed with Autodock v4.6.2 [35]. Experimental conditions were set using the oxygen atom (position 838) from the GLU-790 residue inside a 45x45x45 (XYZ dimensions) grid box centered at approximately 0.9460/- 32.2960/-9.4240 (x/y/z coordinates). The molecular docking and modeling solutions were visualized and registered with PyMOL v1.3 (Schrödinger, LCC), using the Autodock plugin [36].

Linear protein interaction motifs were detected with the ELM Database (http://elm.eu.org/) [29]. The Mps1 proteins analyzed here were from the species *A. angustifolia* (AaMps1), *Amborella trichopoda* (AbMps1 –gi | 586646077), *Eucalyptus grandis* (EgMps1 –gi | 702379945), *Carica papaya* (CpMps1 -| evm.TU.supercontig_36.11), and *Medicago truncatula* (MtMps1 gi | 357461629). Phosphorylation sites were predicted with PlantPhos, a tool that was developed to predict phosphorylation sites in plant proteins [37].

4.1.2.3 Suspension Culture Conditions

To obtain cell suspensions, embryogenic cultures were multiplied and maintained in the basic liquid culture medium MSG [38] supplemented with 30 g l-1 sucrose, 1.4 g l-1 L-glutamine (Sigma-Aldrich, St. Louis, USA), and 0.1 g l-1 myo-inositol (Merck KGaA, Darmstadt, Germany), and the pH of the culture medium was adjusted to 5.7 before autoclaving at 121°C for 20 min, 1.5 atm. The embryogenic cell suspension cultures were subcultured every 15 days by adding 10 ml of the old suspension culture to 60 ml of fresh liquid medium.

Embryogenic cell suspension cultures were kept on an orbital shaker (Cientec, Minas Gerais, Brazil) at 100 rpm in the dark, at 25 ± 2°C.

To analyze the effect of Mps1 inhibition on cellular growth and the PEM morphology, embryogenic cell suspension cultures were grown in basic MSG culture medium supplemented with 30 g l-1 sucrose, 1.4 g l-1 L-glutamine, and 0.1 g l-1 myo-inositol, and with or without Mps1 inhibitor SP600125 (Sigma-Aldrich). The Mps1 inhibitor was filter-sterilized through a 0.2-µm PVDF membrane (Millipore, São Paulo, Brazil) before being added to the culture medium. After the inoculation of embryogenic cell culture with 15-day-old cell suspensions, the flasks were maintained on an orbital shaker at 100 rpm in the dark, at 25 ± 2°C.

4.1.2.4 Effects of Mps1 Inhibition on Cellular Growth

The cellular growth in suspension cultures was measured using settled cell volume (SCV) according to Osti et al. [4] to establish the growth curve for different concentrations (0, 1 and 10 µM) of Mps1 inhibitor. The SCV was determined by cell sedimentation in the side arm of the adapted flasks and was evaluated every three days until day 30 of the culture. Each treatment was performed in triplicate. From the resulting growth curve, the initial time, lag phase, early exponential phase, exponential phase, and stationary phase were established as days 0, 6,15, 21, and 27, respectively, of the incubation.

To analyze cellular growth based on increases in fresh matter (FM) and dry matter (DM), 60 mg aliquots of 15-day-old embryogenic suspension cultures were inoculated into 12-well tissue culture plates (TPP1) containing 2 ml/well of basic MSG culture medium without (control) or with (10 µM) Mps1 inhibitor. The

* A metodologia dos itens 4.1.2.4 e 4.1.2.5 foram detalhadas em um protocolo publicado em 05 de dezembro de 2016, na revista Bio-Protocol 6(23): DOI: https://doi.org/10.21769/BioProtoc.2031 (Anexo 2).

application of Mps1 inhibitor (10 μM) inhibited the cellular growth according toSCV analyses. Six samples (corresponding to six wells) from each treatment were obtained to measure the FM before (0) and after 6, 15, 21, and 27 days of incubation. The DM was obtained by drying the FM samples at 70°C for 48 h.

4.1.2.5 Effects of Mps1 Inhibition on PEM Morphology

The analyses of PEM morphology were performed by measuring the area and size of embryogenic cells and suspensor cells. For both analyses, samples were collected before (0) and after 6, 15, 21, and 27 days of incubation without (control) or with (10 μM) Mps1 inhibitor, which showed cellular growth inhibition in the SCV analyses. Samples were collected and prepared on slides, followed by examination under an Axioplan light microscope (Carl Zeiss, Jena, Germany) equipped with an AxioCam MRC5 digital camera (Carl Zeiss). After the images were obtained, area and size were measured using AxioVision LE software, version 4.8 (Carl Zeiss).

The area measurements were performed from PEMs, from the group of embryogenic-type cells that form the embryonal head, and from the suspensor-type cells. For these analyses, for each treatment and each incubation time, three slides were prepared, and at least ten images of PEMs were obtained.

For the cell size analyses, the PEMs were treated with cellulase (Fluka Analytical, Buchs, Switzerland) 0.1% for 3 h to dissociate the embryogenic and suspensor cells of PEM. As embryogenic-type cells are isodiametric, the size was measured based on the diameter, and as suspensor-type cells are elliptic and elongated, the size was measured using the length and width (at the middle of the cell). For these analyses, for each treatment and each incubation time,

three slides were prepared, and fifty images from each cell type (embryogenic or suspensor) were obtained.

4.1.2.6 Identification and Quantification of the AaMps1 Protein

The AaMps1 protein was identified and quantified using embryogenic suspension cultures before (time 0) and after 15 days of incubation (the period of cellular growth) without (control) and with Mps1 inhibitor (10 μM), which inhibited cellular growth. This analysis was performed to confirm the presence of this protein in the embryogenic suspension cultures and to observe the effect of the inhibitor on the protein concentration in the two treatments.

Protein extractions were performed according to Balbuena et al. [39] with some modifications. Samples containing 300 mg FM were ground in liquid nitrogen and transferred into clear 2 ml microtubes containing 1.0 ml of extraction buffer made of 7 Murea (GE Healthcare, Freiburg, Germany), 2Mthiourea (GE Healthcare), 1% dithiothreitol (DTT; GE Healthcare), 2% Triton X-100 (GE Healthcare), 0.5% pharmalyte (GE Healthcare), 1 mM phenylmethanesulfonyl fluoride (PMSF; Sigma-Aldrich), and 5 μMpepstatin (Sigma-Aldrich). All extracts were vortexed for 2 min and kept in the extraction buffer on ice for 30 min, followed by centrifugation at 12,000 x g for 10 min at 4°C. The supernatants were transferred to clear microtubes; then, the proteins were precipitated in ice for 30 min in 10% trichloroacetic acid (TCA; Sigma-Aldrich) and were washed three times with cold acetone (Merck). Finally, the proteins were resuspended and concentrated in 1 ml of the same extraction buffer. The protein concentration was estimated using a 2-D Quant Kit (GE Healthcare). Sample preparation and HDMSE (data independent acquisition,

with ion mobility) mass spectrometry analyses were performed according to Reis et al. [40].

MS data processing and database searching were performed using Progenesis QI for Proteomics Software V. 2.0 (Non linear Dynamics, Newcastle, UK). The analysis used the following parameters: 1 missed cleavage; minimum fragment ion per peptide equal to 1; minimum fragment ion per protein equal to 3; minimum peptide per protein equal to 1; variable modifications by carbamidomethyl (C), acetyl N-terminal, and oxidation (M); a default false discovery rate (FDR) value with a 4% maximum; a score greater than 5; and a maximum of 10 ppm for mass errors. This program compares the AtMps1 (A. thaliana) sequence—gi | 28416703 and the AaMps1 (A. angustifolia) predicted protein sequence obtained by BLAST with the A. angustifolia transcriptome database [22, 23] for protein identification.

4.1.2.7 Data Analysis

The data presented here were statistically analyzed using analysis of variance (ANOVA) ($P<0.01$) followed by Tukey's test using R software (Foundation for Statistical Computing, version 3.0.3, 2014, Vienna, Austria). Nucleotide sequence data from this article can be found in the GenBank under accession number KU600448.

4.1.3 Results

4.1.3.1 Mps1 Sequence Identification and Structural Analyses

Using AtMps1 as a query, we identified a single-copy gene in *A. angustifolia*, and its protein was designated AaMps1 (Fig 1 and Table 1). This sequence presented higher homology with AbMps1 protein in *Amborella*

trichopoda, EgMps1 in *Eucalyptus grandis*, CpMps1 in *Carica papaya*, and MtMps1 in *Medicago truncatula* (Fig 2).

A kinase domain with 293 amino acid residues could be identified, with approximately 91% of these amino acids being common between the different species, thus showing that this kinase domain is conserved among the analyzed species (Fig 2). Tridimensional modeling of the AaMps1 kinase domain (Fig 3A) presents two subdomains that are connected by a flexible loop. The larger subdomain is composed of five α-helices and four β-sheets, and the smaller subdomain contains one α-helix and five β-sheets (Fig 3A). The alignment of the AaMps1 kinase domain reveals a structure that is similar to that of hMps1 (Fig 4) and AtMps1 (Fig 5). A tridimensional analysis of the AaMps1 kinase domain also showed that an Asp-Phe-Gly (DFG) motif (Fig 3B) and a threonine triad (T870, T871 and T881) related to autophosphorylation (Fig 3C) were highly conserved in other analyzed plant species (Fig 2).

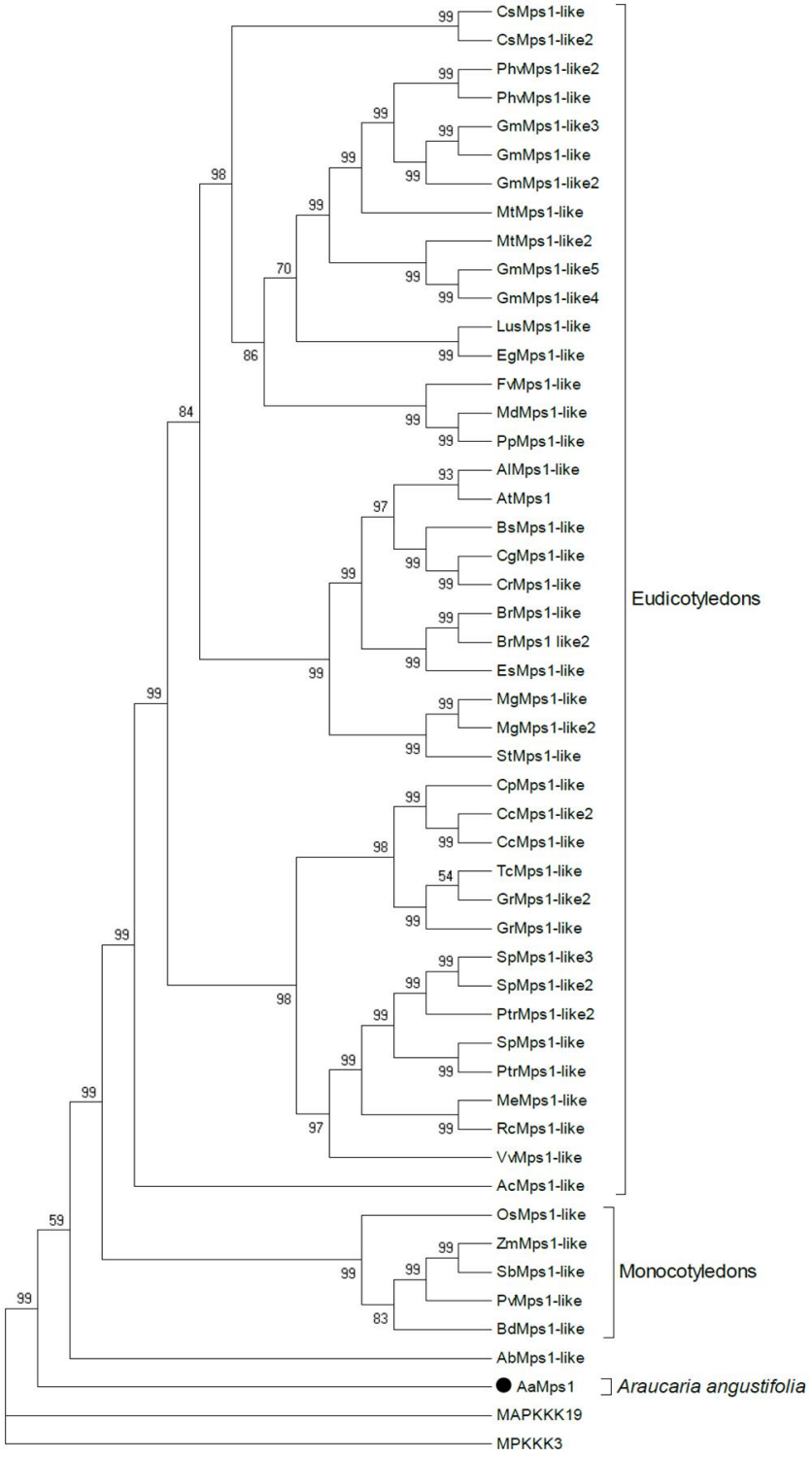

Fig 1. Phenogram of Mps1. Sequence data details are listed in S1 Table. The topology of the tree was consistent with the phylogenetic distribution of the species. Mps1 is encoded by a single-copy gene in monocotyledons and *Araucaria angustifolia*. Paralogs were found in some species inside the Eudicotyledons clade, indicating species-specific duplications. The bootstrap values are shown on the branches. The tree was rooted with MAPKs of Arabidopsis thaliana as the outgroup. *Amborella trichopoda* (Ab), *Aquilegia coerulea* (Ac), *Arabidopsis lyrata* (Al), *Arabidopsis thaliana* (At), *Araucaria angustifolia* (Aa), *Boechera stricta* (Bs), *Brachypodium distachyon* (Bd), *Brassica rapa* (Br), *Capsella grandiflora* (Cg), *Capsella rubella* (Cr), *Carica papaya* (Cp), *Citrus clementina* (Cc), *Cucumis sativus* (Cs), *Eucalyptus grandis* (Eg), *Eutrema salsugineum* (Es), *Fragaria vesca* (Fv), *Glycine max* (Gm), *Gossypium raimondii* (Gr), *Linum*

usitatissimum (Lu), *Malus domestica* (Md), *Manihot esculenta* (Me), *Medicago trunculata* (Mt), *Mimulus guttatus* (Mg), *Oryza sativa* (Os), *Panicum virgatum* (Pv), *Phaseolus vulgaris* (Phv), *Pinus pinaster* (Ppi), *Populus trichocarpa* (Pt), *Prunus persica* (Pp), *Ricinus communis* (Rc), *Salix purpurea* (Sp), *Solanum tuberosum* (St), *Sorghum bicolor* (Sb), *Theobroma cacao* (Tc), *Vitis vinifera* (Vv), and *Zea mays* (Zm).

Table 1. Sequence information.

Species	Name	Accession number	Database
Amborella trichopoda	AbMps1-like	586646077	NCBI
Aquilegia coerulea	AcMps1-like	22026026	Phytozome
Arabidopsis lyrata	AlMps1-like	55089163	Phytozome
Arabidopsis thaliana	AtMps1	19651099	Phytozome
Arabidopsis thaliana	MPKKK3	AT1G53570.1	TAIR
Arabidopsis thaliana	MAPKKK19	AT5G67080.1	TAIR
Araucaria angustifolia	AaMps1	comp44392_c0_seq1	Araucaria
Boechera stricta	BsMps1-like	30674076	Phytozome
Brachypodium distachyon	BdMps1-like	31132433	Phytozome
Brassica rapa	BrMps1_like2	30632638	Phytozome
Brassica rapa	BrMps1-like	30635976	Phytozome
Capsella grandiflora	CgMps1-like	28896987	Phytozome
Capsella rubella	CrMps1-like	20905877	Phytozome
Carica papaya	CpMps1-like	16418293	Phytozome
Citrus clementina	CcMps1-like	20785857	Phytozome
Citrus clementina	CcMps1-like2	20785858	Phytozome
Cucumis sativus	CsMps1-like	16971492	Phytozome
Cucumis sativus	CsMps1-like2	16971493	Phytozome
Eucalyptus grandis	EgMps1-like	23584928	Phytozome
Eutrema salsugineum	EsMps1-like	20192414	Phytozome
Fragaria vesca	FvMps1-like	27261715	Phytozome
Glycine max	GmMps1-like	30487385	Phytozome
Glycine max	GmMps1-like2	30553833	Phytozome
Glycine max	GmMps1-like3	30487385	Phytozome
Glycine max	GmMps1-like4	30504360	Phytozome
Gossypium raimondii	GmMps1-like5	30533762	Phytozome
Gossypium raimondii	GrMps1-like	26765252	Phytozome
Gossypium raimondii	GrMps1-like2	26760976	Phytozome
Linum usitatissimum	LusMps1-like	23181249	Phytozome
Malus domestica	MdMps1-like	22634014	Phytozome
Manihot esculenta	MeMps1-like	17993060	Phytozome
Medicago trunculata	MtMps1-like	31054629	Phytozome
Medicago trunculata	MtMps1-like2	31091020	Phytozome
Mimulus guttatus	MgMps1-like	28944327	Phytozome
Mimulus guttatus	MgMps1-like2	28926427	Phytozome
Oryza sativa	OsMps1-like	24124978	Phytozome
Panicum virgatum	PvMps1-like	30239330	Phytozome
Phaseolus vulgaris	PhvMps1-like	27146011	Phytozome
Phaseolus vulgaris	PhvMps1-like2	27146012	Phytozome
Populus trichocarpa	PtrMps1-like	27024355	Phytozome
Populus trichocarpa	PtrMps1-like2	27029976	Phytozome
Prunus persica	PpMps1-like	17662821	Phytozome
Ricinus communis	RcMps1-like	16813011	Phytozome
Salix purpurea	SpMps1-like	31403193	Phytozome
Salix purpurea	SpMps1-like2	31428444	Phytozome
Salix purpurea	SpMps1-like3	31407206	Phytozome
Solanum tuberosum	StMps1-like	24407254	Phytozome
Sorghum bicolor	SbMps1-like	28395238	Phytozome
Theobroma cacao	TcMps1-like	27459214	Phytozome
Vitis vinifera	VvMps1-like	17821444	Phytozome
Zea mays	ZmMps1-like	31017286	Phytozome

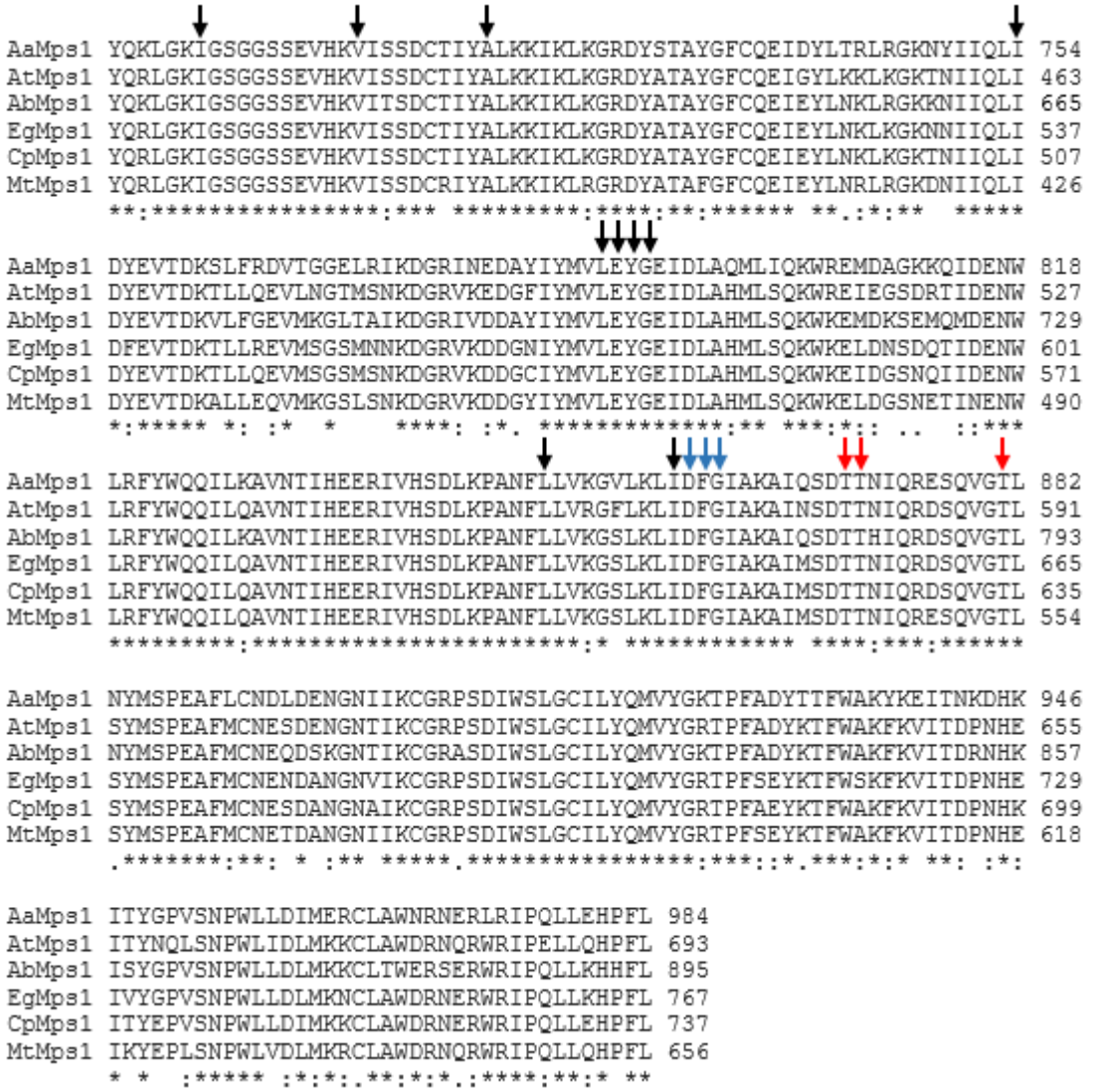

Fig 2. Multiple sequence alignment. Kinase domain in Mps1 proteins from *A. angustifolia* (AaMps1), *A. thaliana* (AtMps1), *A. thicopoda* (AbMps1), *E. grandis* (EgMps1), *C. papaya* (CpMps1), and *M. truncatula* (MtMps1). The black arrows indicate amino acids important for interaction with the inhibitor that are also conserved between hMps1, AaMps1 and other plant species. The blue arrow indicates the conserved DFG motifs. The red arrow indicates the conserved threonine residues.

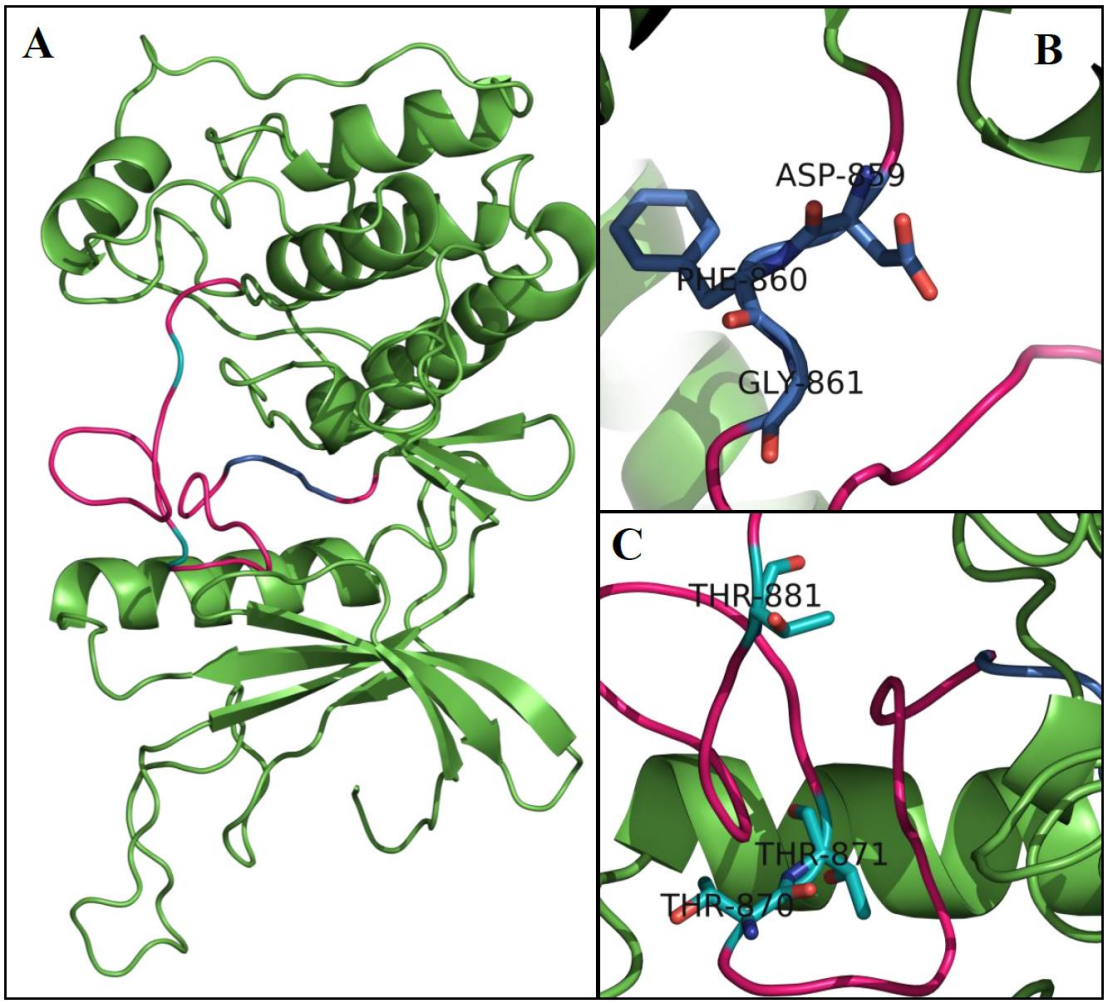

Fig 3. A 3D model of the AaMps1 kinase domain. (A) An overview of the kinase domain. Rose: activation loop; Blue: DFG motif; and Cyan: threonines. (B) A detailed view of the DFG motif. (C) A detailed view of the threonine residues (T870, T871, and T881) that are related to autophosphorylation.

Fig 4. Tridimensional modeling and overlap of AaMps1 kinase domains and AtMps1. AaMps1 (cyan) in A. angustifolia and AtMps1 (green) in A. thaliana.

Fig 5. Tridimensional modeling and overlap of AaMps1 kinase domains and hMps1. AaMps1 (cyan) in A. angustifolia and hMps1 (pink) in humans.

The phosphorylation sites in the kinase domain of the Mps1 protein were predicted (Table 2) using the AtMps1 sequence in PlantPhos, leading to the identification of 18 sites in AaMps1 that are analogous to the phosphorylation sites observed in AtMps1. In comparison with the AaMps1 sequence, 16 phosphorylation sites were predicted in EgMps1, 18 in CpMps1, and 17 in MtMps1.

Table 2. Phosphorylation sites of the kinase domain.

	Residue Position	Residue Substrate	*A. angustifolia*	*A. thaliana*	*E. grandis*	*C. papaya*	*M. truncatula*
Kinase Domain	691	Y	X	X	X	X	X
	699	S	X	X	-	X	X
	702	S	X	X	X	X	X
	703	S	X	X	X	X	X
	710	S	X	X	X	X	X
	711	S	X	X	X	X	X
	714	T/S	X	X	X	X	-
	716	Y	X	X	X	X	X
	728	Y	X	X	X	X	X
	732	Y	X	X	X	X	-
	756	Y	X	X	-	X	-
	786	Y	X	X	X	-	X
	870	T ←	-	-	-	-	X
	871	T ←	X	X	X	X	X
	881	T ←	X	X	X	X	X
	884	Y	X	X	X	X	X
	922	Y	X	X	X	X	X
	941	T	X	-	X	X	X
	949	Y	X	X	-	X	X
	953	S	X	X	X	X	X

Phosphorylation sites of the kinase domain in *A. angustifolia* AaMps1 analyzed by PlantPhos and compared with *A. thaliana* (AtMps1), *E. grandis* (EgMps1), *C. papaya* (CpMps1), and *M. truncatula* (MtMps1). Arrows indicate conserved threonine triads in the species. Y = tyrosine; S = serine; T = threonine; X = presence; and - = absence.

The AaMps1 sequence revealed 1036 residues, and the proteins AbMps1, EgMps1, CpMps1 and MtMps1 contained 950, 851, 821 and 742 residues, respectively (Fig 6A). The linear protein interaction motifs of Mps1 were analyzed with ELM prediction tool motifs to compare AaMps1 with Mps1 proteins from other species. AaMps1 had the characteristic motifs of the Mps1 protein kinase (Fig 6A), which were observed in *A. trichopoda*, *E. grandis*, *C. papaya*, and *M. truncatula*. The motifs that were found to be conserved in these species include the Mitotic arrest-deficient 2 (MAD2) binding motif LIG_MAD2, the Cyclin recognition site DOC_CYCLIN_1, the MAPK docking motif DOC_MAPK_1, the Nuclear Export Signal TRG_NES_CRM1_1, the Nuclear Localization Signal TRG_NLS_MonoExtC_3, the Protein phosphatase-1 (PP1) regulation site DOC_PP1_RVXF_1, a motif phosphorylated by phosphoinositide-3-OH-kinase (PIKK) family members, MOD_PIKK_1, and a motif for the DFG structural conformation. These motifs were present in at least four species among those analyzed here (AaMps1, AbMps1, EgMps1, CpMps1, and MtMps1). The structures of the DOC_CYCLIN_1, DOC_MAPK_1, and LIG_MAD2 motifs in AaMps1 were observed by tridimensional model analyses (Fig 6B).

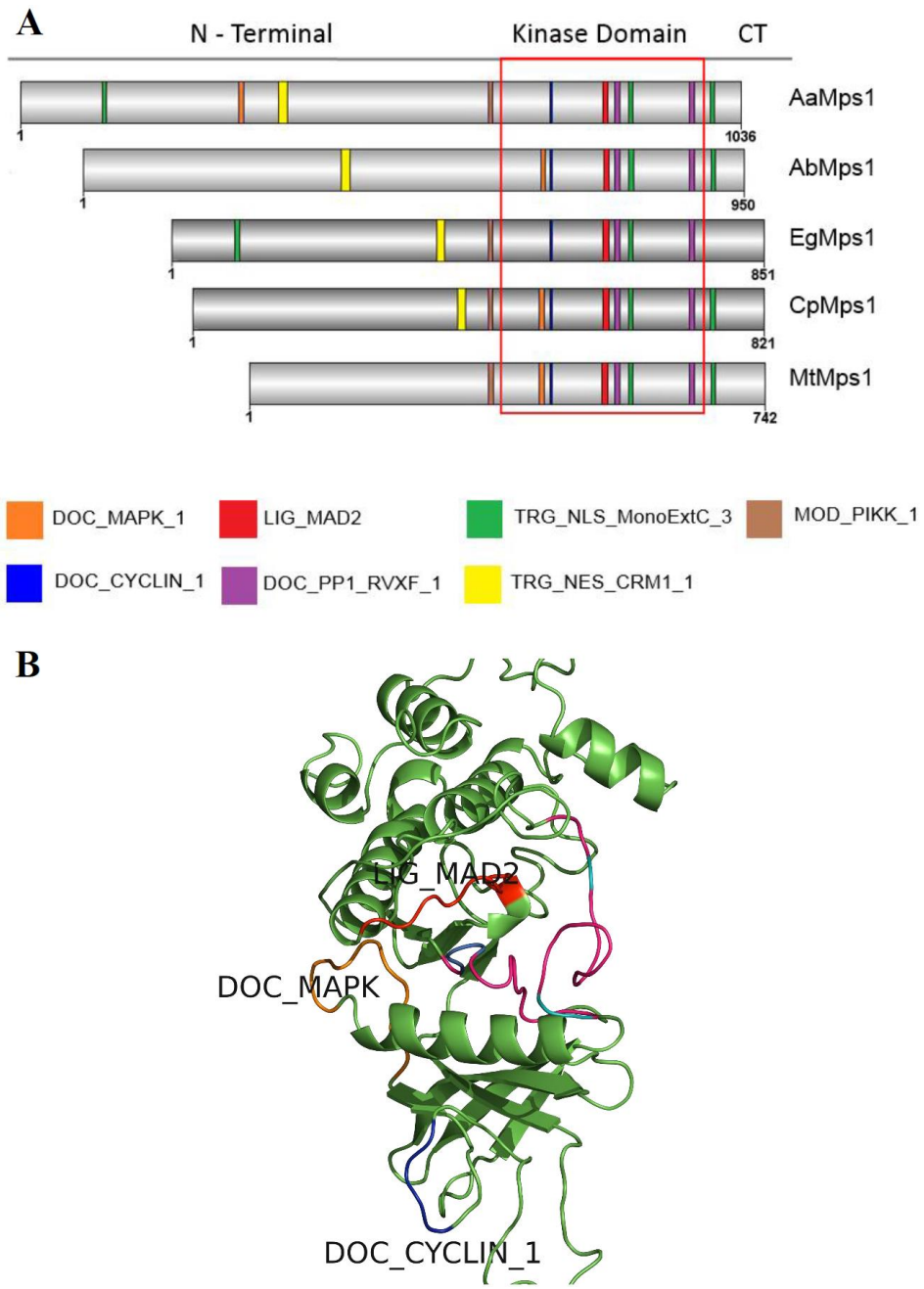

Fig 6. Mps1 motifs related to the cell cycle in plants. (A) Linear motifs of several Mps1 orthologs that were observed in *A. angustifolia* (AaMps1), *A. thicopoda* (AbMps1), *E. grandis* (EgMps1), *C. papaya* (CpMps1), and *M. truncatula* (MtMps1). (B) The 3D model of relevant interaction motifs DOC_CYCLIN_1, DOC_MAPK and LIG_MAD2 in AaMps1.

4.1.3.2 Effects of Mps1 Inhibition on Cellular Growth of Embryogenic Suspension Cultures

Through SCV analysis (Fig 7), it was possible to observe the inhibition of cellular growth in *A. angustifolia* embryogenic suspension cultures treated with

the Mps1 inhibitor at 10 µM, without significant differences in the incubation times. However, the cellular growth of embryogenic suspension cultures incubated in the control and 1 µM Mps1 inhibitor treatments increased during the incubation times, enabling the identification of the lag (until the 12th day), exponential (from the 15th day), and stationary (27 days) phases (Fig 7).

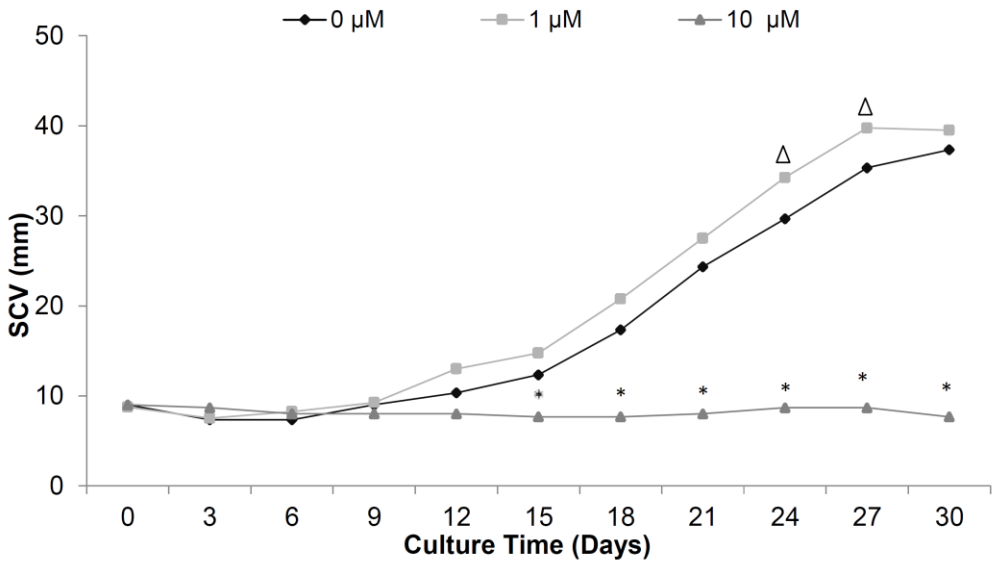

Fig 7. Cellular growth curve. Growth curve by settled cell volume (SCV) analyzes in embryogenic suspension cultures of *A. angustifolia* incubated with different concentrations (0, 1, and 10 µM) of Mps1 inhibitor SP600125, during 30 days of incubation. Triangles denote significant differences (P < 0.01) between control and 1 µM Mps1 inhibitor, and asterisks denote significant differences (P < 0.01) comparing 10 µM Mps1 inhibitor with the control and 1 µM Mps1 inhibitor treatments according to Tukey's test (n = 3; coeficiente of variation = 14.5%).

Cellular growth, in terms of the FM and DM increments in embryogenic suspension cultures during incubation, was affected by the Mps1 inhibitor. Beginning at 15 days of incubation, growth inhibition according to FM (Fig 8A) and DM (Fig 8B) analysis was observed in the presence of the Mps1 inhibitor. In addition, embryogenic suspension cultures showed a significant increase in

the FM increment beginning on the 15th day of incubation in the control treatment (Fig 8A). The DM increment in the control treatment was significant and progressive from the 6th day until the end of incubation (Fig 8B).

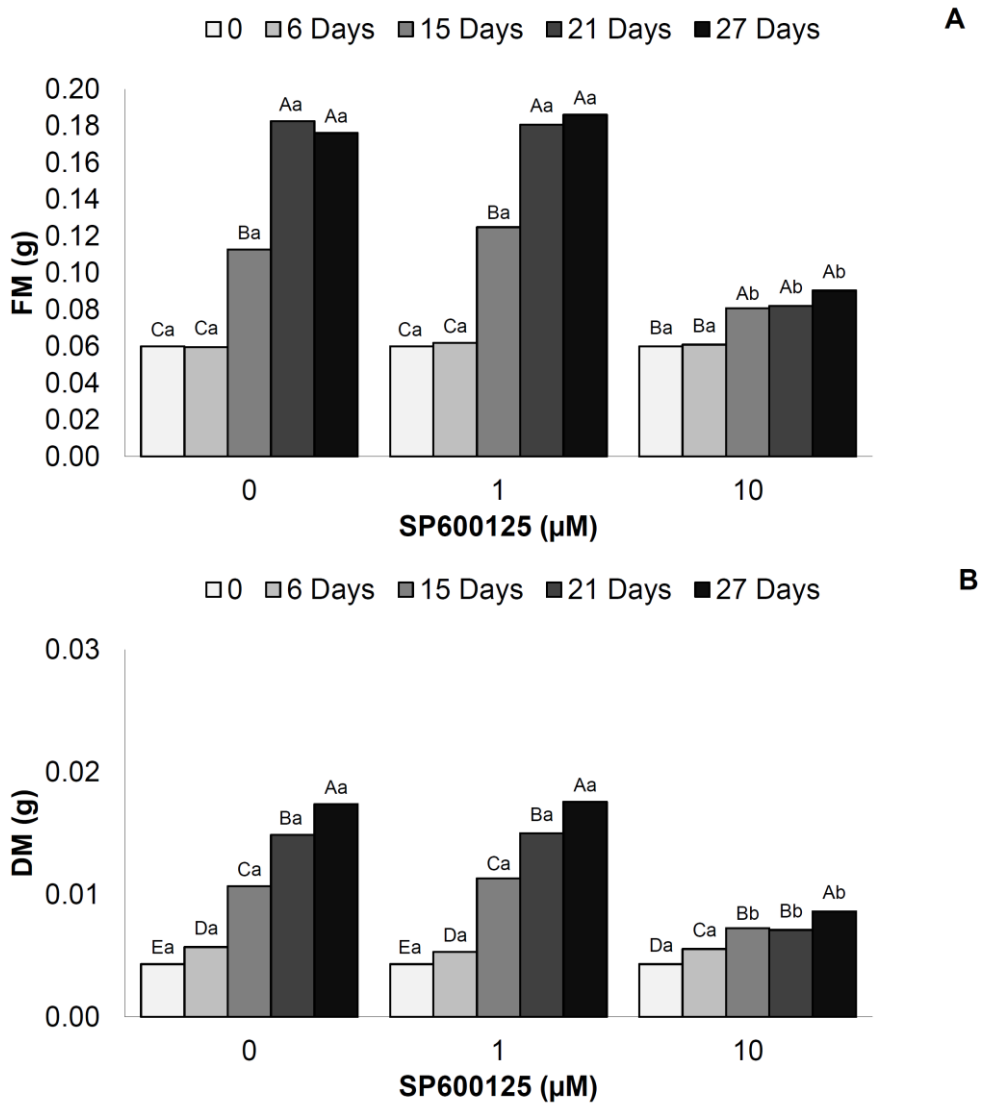

Fig 8. Mass increment (g) in *A. angustifolia* embryogenic suspension cultures. (A) FM and (B) DM values in embryogenic suspension cultures before (0) and after 6, 15, 21, and 27 days of incubation in MSG basic culture medium with (10 µM) or without Mps1 inhibitor SP600125. Lowercase letters denote significant differences ($P < 0.01$) between treatments for each day of incubation. Capital letters denote significant differences ($P < 0.01$) in the same treatment during incubation. Means followed by different letters are significantly different ($P < 0.01$) according to Tukey's test. CV = coefficient of variation (n = 6; CV FM = 10.3%; CV DM = 7.3%).

4.1.3.3 Effects of Mps1 Inhibition on PEM Morphology

The morphology of PEMs was affected by the addition of 10 μM Mps1 inhibitor compared to the control treatment (Fig 9). These PEMs contain two types of cells: embryogenic cells (EC), which are grouped to form the embryonal head (HC), and the suspensor cells (SC). Embryogenic cells are isodiametric, with an evident nucleus, while suspensor cells are elliptic, being elongated and oblong (Fig 9).

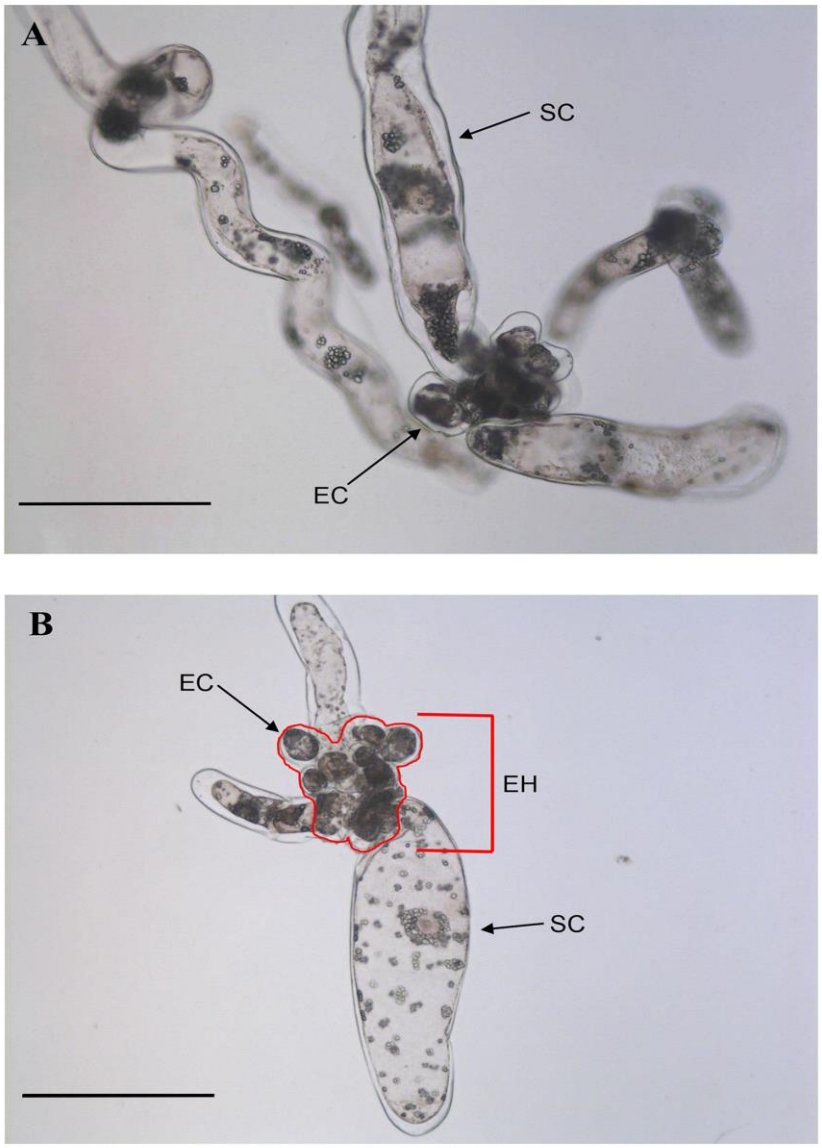

Fig 9. The morphology of *A. angustifolia* PEMs in cell suspension culture. Morphological features of PEMs after 15 days of incubation in MSG basic culture medium without (A) or with the Mps1 inhibitor SP600125 (10 μM) (B). EH = embryonal head; EC = embryogenic cells; SC = suspensor cells. Bars = 200 μm.

The embryogenic cells from the embryonal head of PEMs had significantly greater area from the 15th to 27th day in the control compared with those treated with 10 µM Mps1 inhibitor (Fig 10A), while the individual cells in the two treatments showed similar diameters during incubation (Fig 11A). On the other hand, the morphology of suspensor cells was affected by the addition of Mps1 inhibitor, showing changes in the area (Fig 10B) as well as the length (Fig 11B) and width (Fig 11C). Beginning on the 6th day of incubation, the addition of Mps1 inhibitor reduced the area (Fig 10B) and length (Fig 11B) of suspensor cells in comparison to control cells. However, suspensor cells showed a significant increase in width from the 6th to the 21st day of incubation (Fig 11C).

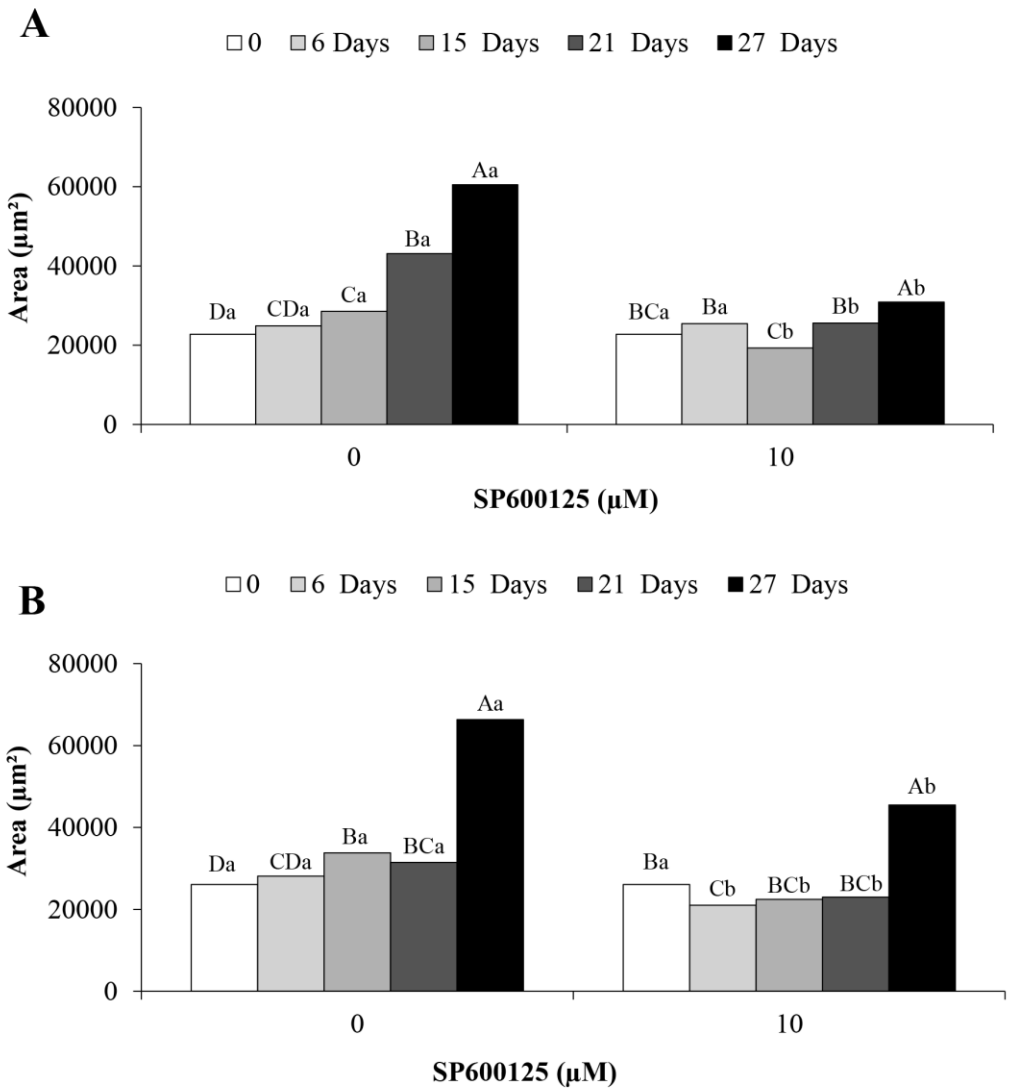

Fig 10. Analyses of PEM area. The group of embryogenic cells from the embryonal head of PEMs (A) and suspensor-type cells (B) from embryogenic suspension culture of *A. angustifolia* before (0) and after 6, 15, 21, and 27 days of incubation in MSG basic culture medium with (10 µM) or without the Mps1 inhibitor SP600125. Lowercase letters denote significant differences ($P < 0.01$) between treatments for each day of incubation. Capital letters denote significant differences ($P < 0.01$) in the same treatment during incubation. Means followed by different letters are significantly different ($P < 0.01$) according to Tukey's test. CV = coefficient of variation (n = 10; CV embryonal head = 13%; CV suspensor cells = 12%).

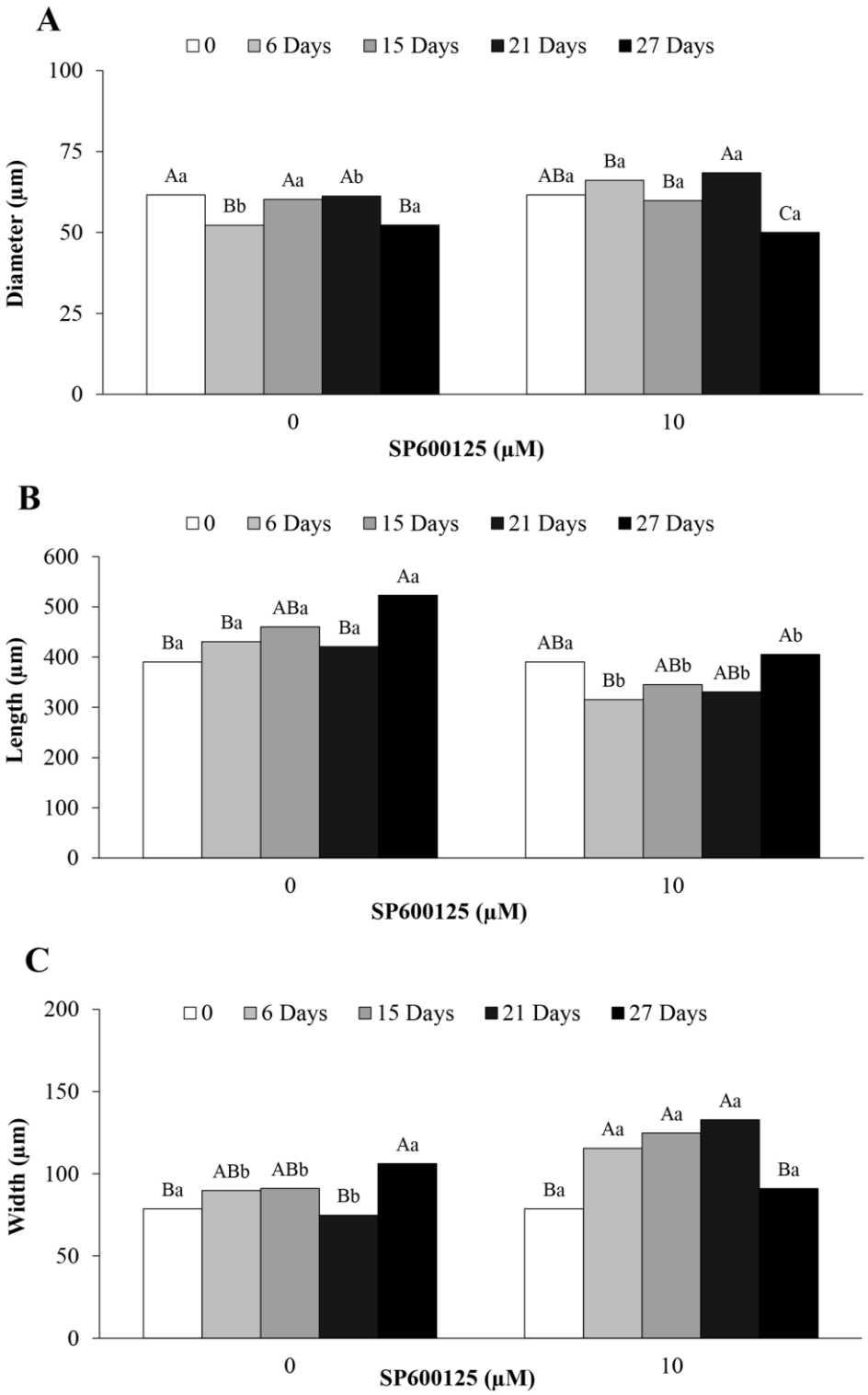

Fig 11. Analyses of cell size. Diameter of embryogenic cells (A) and length (B) and width (C) of suspensor cells from embryogenic suspension cultures of *A. angustifolia* before (0) and after 6, 15, 21, and 27 days of incubation in MSG basic culture medium with (10 µM) or without the Mps1 inhibitor SP600125. Lowercase letters denote significant differences ($P < 0.01$) between treatments for each day of incubation. Capital letters denote significant differences ($P < 0.01$) in the same treatment during incubation. Means followed by different letters are significantly different ($P < 0.01$) according to Tukey's test. CV = coefficient of variation (n = 50; CV diameter of embryogenic cells = 22.7%; CV length of suspensor cells = 35.2%; CV width of suspensor cells = 45.3%).

4.1.3.4 Identification and Quantification of the AaMps1 Protein

Mass spectrometry analyses compared the AaMps1 protein obtained by in silico analyses with the Araucaria transcriptome database [22, 23], resulting in 81.66% sequence coverage. These results confirm the presence of the Mps1 protein in *A. angustifolia* embryogenic suspension cultures (Table 3). Furthermore, the AaMps1 protein was highly similar to the AtMps1 protein (gi | 28416703), with 78.76% sequence coverage, indicating a strong homology between the AaMps1 and AtMps1 proteins (Table 3).

Table 3. AaMps1 protein identification.

	AaMps1	**AtMps1**
Score	191.25	226.92
Coverage (%)	81.6602	78.6358
mW (Da)	113944	86323
pI (pH)	**6.7**	**6.44**

AaMps1 protein identification by $HDMS^E$ (data-independent acquisition, with ion mobility) mass spectrometry in embryogenic suspension cultures of *A. angustifolia* incubated without Mps1 inhibitor SP600125, compared with transcriptomic sequences of AaMps1 and AtMps1 protein.

In addition, embryogenic suspension cultures at 15 days of incubation without Mps1 inhibitor (control) demonstrated a significant increase in the amount of AaMps1 compared with those analyzed before incubation (time 0). Furthermore, treatment with the Mps1 inhibitor (10 µM) induced a decrease in the amount of AaMps1 protein at 15 days of incubation compared with the control at 15 days of incubation and with embryogenic cultures before incubation (Fig 12).

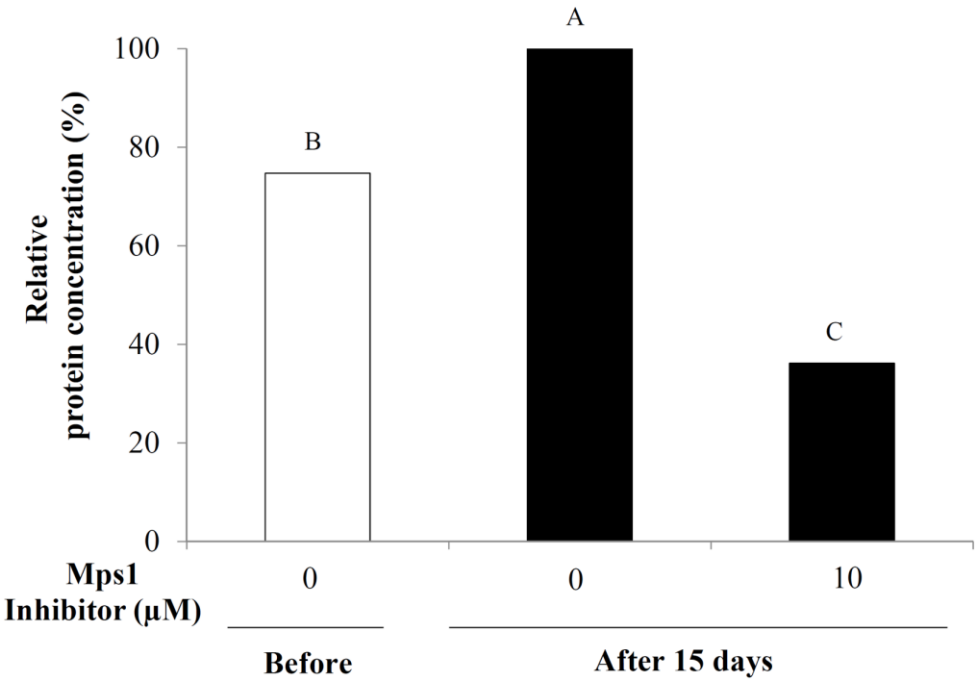

Fig 12. Quantification of the AaMps1 protein. Relative concentration (%) of AaMps1 protein by HDMSE (data-independent acquisition, with ion mobility) mass spectrometry analysis in embryogenic suspension cultures of A. angustifolia before (0) and after 15 days of incubation in MSG basic culture medium with (10 µM) or without Mps1 inhibitor SP600125. Means followed by different letters are significantly different ($P < 0.01$) according to Tukey's test. ($n = 3$; Coefficient of variation = 14.1%).

4.1.4 Discussion

Our results show the presence of the Mps1 protein in the gymnosperm species *A. angustifolia*, designated AaMps1. AaMps1 is homologous with the Mps1 proteins of other species, including the kinase domain that is highly conserved in eukaryotes. Our work confirmed the existence of the AaMps1 protein in embryogenic cultures by mass spectrometry analysis, demonstrating high coverage of the in silico predicted protein sequence of AaMps1 and with the AtMps1 (*A. thaliana)* protein.

Among the analyzed species, *A. trichopoda* (AbMps1) presented more similarities to AaMps1 in terms of residue number (Figs 1 and 2). This result may be related to the origin of *A. trichopoda*; this species is a member of an ancient lineage and is a unique and valuable reference that facilitates the interpretation of major genomic events in the evolution of flowering plants [41]. In addition, the AaMps1 protein shows similarities with AtMps1, the recently described Mps1 protein in plants [18] as well as other plants, such as *E. grandis*, *C. papaya*, and *M. truncatula* (Fig 2). However, the numbers of residues from the Mps1 protein of these species are lower compared with that of *A. angustifolia* (AaMps1) and *A. trichopoda* (AbMps1). This result could explain the larger size of the AaMps1 protein in relation to AtMps1, given that AaMps1 presented more similarities with AbMps1 from *A. trichopoda* in comparison with *A. thaliana. A. trichopoda* is an ancestral angiosperm species for which the genome has been published, making this species a pivotal reference for understanding genome and gene family evolution throughout angiosperm history [41].

Furthermore, AaMps1 has several structural features present in the Mps1 of all analyzed species, such as phosphorylation sites, DFG motifs, and the threonine triad (Figs 2, 3 and 6; Table 2). Events such as the phosphorylation and autophosphorylation of Mps1 by other proteins and Mps1-mediated phosphorylation are crucial for the correct location and activity of Mps1 in cell cycle control [42–44]. Autophosphorylation on three fundamental threonine residues (the threonine triad) in the Mps1 loop is necessary to activate this protein in humans (hMps1). Studies related to phosphorylation site mapping and mutation analysis in hMps1 indicate that three residues—T675, T676, and

T686—may be modified by autophosphorylation, given that the phosphorylation of T676 within the hMps1 activation loop is important for full kinase activity [43]. These three important residues in hMps1 are present in *A. thaliana* as T579, T580 and T590 [18], and they were shown to be conserved in *A. angustifolia* as T870, T871 and T881.

Other characteristic features of Mps1 were also observed in AaMps1 in terms of interaction regions with other proteins (Fig 6). Some motifs observed in AaMps1, such as DOC_CYCLIN_1, DOC_MAPK_1, LIG_MAD2, TRG_NES_CRM1_1, TRG_NLS_MonoExtC, DOC_PP1_RVXF_1, andMOD_PIKK_1 (Fig 3A), could potentially mediate interactions with cyclins, MAD2, the anaphase-promoting complex/cyclosome (APC/C), and MAPK-cell cycle regulators [44,45]. These motifs were similar to those of the other analyzed species, and some of the motifs have also been reported in Mps1 proteins in other plants, such as *A. thaliana* (AtMps1), *Populus trichocarpa* (PtMps1), *Ricinus communis* (RcMps1), *Oryza sativa* (OsMps1), *Sorghum bicolor* (SbMps1), and *Zea mays* (ZmMps1) [18]. These regions interact through short amino acid modules (linear motifs), which are frequently identified as regulatory protein parts that provide interactions and bind with other proteins, modifying their structures and activities [29].

In addition, some interactions between Mps1 and other proteins that were observed through the predicted motifs have been shown in previous studies related to Mps1, such as the presence of the LIG_MAD2 motif, thus suggesting an interaction between Mps1 and MAD2 proteins in *A. angustifolia* (Fig 6). Experiments using human HeLa cells verified that Mps1 kinase promotes C-MAD2 production and subsequently leads the mitotic checkpoint

complex (MCC) to activate the SAC; additionally, impaired inhibition of the Mps1, BubR1-MAD2 interaction has been shown, as well as the incorporation of MCC into MAD2 [44]. During the cell cycle, the increased phosphorylation of Mps1 at M phase is dependent on MAPK. MAPK is required for the SAC, and the phosphorylation of cell division control protein 20 (Cdc20) by MAPK is required for Cdc20 to associate with spindle-checkpoint proteins [45]. Herein, we identify the DOC_MAPK_1 motif in AaMps1, which may be another target for MAPK in the spindle checkpoint [45]. Therefore, the sequence of the AaMps1 protein shows some motifs and phosphorylation sites with higher similarities to those of other species, confirming the identity of this protein in *A. angustifolia*.

Our results showed that the inhibition of AaMps1 affects the cellular growth (Figs 7 and 8) and PEM morphology of embryogenic suspension cultures in *A. angustifolia* (Figs 9, 10 and 11). These results suggest that the Mps1 protein is present in this species and that the inhibition of this protein with the Mps1 inhibitor can arrest the cell cycle. In addition, a decrease in the amount of AaMps1 protein, which was induced by the inhibitor, showed a strong correlation with the cellular growth reduction observed in *A. angustifolia* embryogenic suspension cultures (Fig 12). SP600125 competes for the ATP binding site on Mps1 and thus prevents the activity of this protein kinase during cell cycle control in plants [18]. The inhibition of AaMps1 in *A. angustifolia* embryogenic suspension cultures reduces cellular growth, and it may be useful for understanding cell cycle control in gymnosperm somatic embryogenesis as well as for further studies on improving somatic embryo development.

4.1.5 Conclusions

This work has demonstrated the identification of Mps1 protein in *A. angustifolia* (AaMps1), showing that inhibition by the Mps1 inhibitor SP600125 affects the development of embryogenic cultures, reducing cellular growth, PEM morphology, and the amount of AaMps1 protein. Mass spectrometry analysis showed high homology with the AaMps1 predicted protein, obtained by in silico analyses with the Araucaria transcriptome database, and with the AtMps1 protein.

4.1.6 References

1. Fehér A. Somatic embryogenesis—Stress-induced remodeling of plant cell fate. **Biochim Biophys Acta**. 2015; 1849: 385–402. doi: 10.1016/j.bbagrm.2014.07.005 PMID: 25038583

2. Carrier DJ, Kendall EJ, Bock CA, Cunningham JE, Dunstan DI. Water content, lipid deposition, and (+)-abscisic acid content in developing white spruce seeds. **J Exp Bot**. 1999; 50: 1359–1364.

3. Ötvös K, Pasternak TP, Miskolczi P, Domoki M, Dorjgotov D, Szucs A, et al. Nitric oxide is required for and promotes auxin-mediated activation of, cell division and embryogenic cell formation but does not influence cell cycle progression in alfalfa cell cultures. **Plant Journal**. 2005; 43: 849–860.

4. Osti RZ, Andrade JBR, Souza JP, Silveira V, Balbuena TS, Guerra MP, et al. Nitrosyl ethylenediaminetetraacetate ruthenium(II) complex promotes cellular growth and could be used as nitric oxide donor in plants. **Plant Sci**. 2010; 178: 448–453

5. Attree SM, Fowke LC. Embryogeny of gymnosperms—advances in synthetic seed technology of conifers. **Plant Cell Tiss Org**. 1993; 35: 1–35.

6. Silveira V, Santa-Catarina C, Tun NN, Scherer GFE, Handro W, Guerra MP, et al. Polyamine effects on the endogenous polyamine contents, nitric oxide release, growth and differentiation of embryogenic suspension cultures of *Araucaria angustifolia* (Bert.) O. Ktze. **Plant Sci**. 2006; 171: 91–98.

7. Santa-Catarina C, Silveira V, Scherer GFE, Floh EIS. Polyamine and nitric oxide levels relate with morphogenetic evolution in somatic embryogenesis of *Ocotea catharinensis*. **Plant Cell Tiss Org**. 2007; 90: 93–101.

8. Vieira LDN, Santa-Catarina C, De Freitas Fraga HP, Wendt Dos Santos AL, Steinmacher DA, Schlogl PS, et al. Glutathione improves early somatic embryogenesis in *Araucaria angustifolia* (Bert) O. Kuntze by alteration in nitric oxide emission. **Plant Sci**. 2012; 195: 80–87.

9. Santa-Catarina C, Silveira V, Balbuena TS, Viana AM, Estelita MEM, Handro W, et al. IAA, ABA, polyamines and free amino acids associated with zygotic embryo development of *Ocotea catharinensis*. **Plant Growth Regul**. 2006; 49: 237–247.

10. Farias-Soares FL, Steiner N, Schmidt EC, Pereira MLT, Rogge-Renner GD, Bouzon ZL, et al. The transition of proembryogenic masses to somatic embryos in *Araucaria angustifolia* (Bertol.) Kuntze is related to the endogenous contents of IAA, ABA and polyamines. **Acta Physiol Plant**. 2014; 36: 1853–1865.

11. Planchais S, Glab N, Inzé D, Bergounioux C. Chemical inhibitors: a tool for plant cell cycle studies. **Febs Lett**. 2000; 476: 78–83.

12. Pasternak T, Asard H, Potters G, Jansen MA. The thiol compounds glutathione and homoglutathione differentially affect cell development in alfalfa (*Medicago sativa* L.). **Plant Physiol Biochem**. 2014; 74:16–23.

13. Inzé D, De Veylder L. Cell cycle regulation in plant development. **Annu Rev Genet**. 2006; 40: 77–105.

14. Dewitte W, Murray JA. The plant cell cycle**. Annu Rev Plant Biol**. 2003; 54: 235–264.

15. Liu X, Winey M. The MPS1 family of protein kinases. **Annu Rev Biochem**. 2012; 81: 561–585.

16. Musacchio A, Salmon ED. The spindle-assembly checkpoint in space and time. **Nat Rev Mol Cell Bio**. 2007; 8: 379–393.

17. Bennett BL, Sasaki DT, Murray BW, O'leary EC, Sakata ST, Xu W, et al. SP600125, an anthrapyrazoloneinhibitor of Jun N-terminal kinase. **Proc Natl Acad Sci USA**. 2001; 98: 13681–13686.

18. De Oliveira EAG, Romeiro NC, Da Silva Ribeiro E, Santa-Catarina C, Oliveira AEA, Silveira V, et al.Structural and functional characterization of the protein kinase Mps1 in *Arabidopsis thaliana*. **PloS One**. 2012; 7: e45707.

19. Steiner N, Vieira FDN, Maldonado S, Guerra MP. Effect of carbon source on morphology and histodifferentiation of *Araucaria angustifolia* embryogenic cultures. **Braz Arch Biol Techn**. 2005; 48: 895–903.

20. Steiner N, Farias-Soares F, Schmidt É, Pereira MT, Scheid B, Rogge-Renner G, et al. Toward establishing a morphological and ultrastructural

characterization of proembryogenic masses and early somatic embryos of *Araucaria angustifolia* (Bert.) O. Kuntze. **Protoplasma**. 2015: 1–15.

21. Altschul SF, Gish W, Miller W, Myers EW, Lipman DJ. Basic local alignment search tool. **J Mol Biol**. 1990; 215: 403–410.

22. Elbl P, Lira BS, Andrade SCS, Jo L, Dos Santos ALW, Coutinho LL, et al. Comparative transcriptome analysis of early somatic embryo formation and seed development in Brazilian pine, *Araucaria angustifolia* (Bertol.) Kuntze. **Plant Cell Tiss Org**. 2015; 120: 903–915.

23. Elbl P, Campos R, Lira B, Andrade S, Jo L, Dos Santos A, et al. Erratum to: comparative transcriptome analysis of early somatic embryo formation and seed development in Brazilian pine, *Araucaria angustifolia* (Bertol.) Kuntze. **Plant Cell Tiss Org**. 2015; 120: 917.

24. Tamura K, Stecher G, Peterson D, Filipski A, Kumar S. MEGA6: molecular evolutionary genetics analysis version 6.0. **Mol Biol Evol**. 2013; 30: 2725–2729.

25. Guindon S, Gascuel O. A simple, fast, and accurate algorithm to estimate large phylogenies by maximum likelihood. **Syst Biol**. 2003; 52: 696–704.

26. Arnold K, Bordoli L, Kopp J, Schwede T. The SWISS-MODEL workspace: a web-based environment for protein structure homology modelling. Bioinformatics. 2006; 22: 195–201.

27. Biasini M, Bienert S, Waterhouse A, Arnold K, Studer G, Schmidt T, et al. SWISS-MODEL: modelling protein tertiary and quaternary structure using evolutionary information. **Nucleic Acids Res**. 2014; 42: W252–W258.

28. Kiefer F, Arnold K, Künzli M, Bordoli L, Schwede T. The SWISS-MODEL repository and associated resources. **Nucleic Acids Res**. 2009; 37: D387–D392.

29. Dinkel H, Van Roey K, Michael S, Davey NE, Weatheritt RJ, Born D, et al. The eukaryotic linear motif resource ELM: 10 years and counting. **Nucleic Acids Res**. 2013; 42: gkt1047.

30. Fiser A, Sali A. ModLoop: automated modeling of loops in protein structures. **Bioinformatics**. 2003; 19: 2500–2501.

31. Šali A, Blundell TL. Comparative protein modelling by satisfaction of spatial restraints. **J Mol Biol**. 1993; 234: 779–815.

32. Chu ML, Chavas LM, Douglas KT, Eyers PA, Tabernero L. Crystal structure of the catalytic domain of the mitotic checkpoint kinase Mps1 in complex with SP600125. **J Biol Chem**. 2008; 283: 21495–21500.

33. Wang W, Yang Y, Gao Y, Xu Q, Wang F, Zhu S, et al. Structural and mechanistic insights into Mps1 kinase activation. **J Cell Mol Med**. 2009; 13: 1679–1694.

34. Chu ML, Lang Z, Chavas LM, Neres J, Fedorova OS, Tabernero L, et al. Biophysical and X-ray crystallographic analysis of Mps1 kinase inhibitor complexes. **Biochemistry**. 2010; 49: 1689–1701.

35. Morris GM, Huey R, Lindstrom W, Sanner MF, Belew RK, Goodsell DS, et al. AutoDock4 and Auto-DockTools4: automated docking with selective receptor flexibility. **J Comput Chem**. 2009; 30: 2785–2791.

36. Seeliger D, De Groot BL. Ligand docking and binding site analysis with PyMOL and Autodock/Vina. **JComput Aid Mol Des**. 2010; 24: 417–422.

37. Lee T-Y, Bretaña NA, Lu C-T. PlantPhos: using maximal dependence decomposition to identify plant phosphorylation sites with substrate site specificity. **BMC bioinformatics**. 2011; 12: 261.

38. Becwar MR, Noland TL, Wyckoff JL. Maturation, germination, and conversion of Norway spruce (*Picea abies* L.) somatic embryos to plants. **In Vitro Cel Dev Biol Plant**. 1989; 25: 575–580.

39. Balbuena TS, Silveira V, Junqueira M, Dias LLC, Santa-Catarina C, Shevchenko A, et al. Changes in the 2-DE protein profile during zygotic embryogenesis in the Brazilian Pine (*Araucaria angustifolia*). **J Proteomics**. 2009; 72: 337–352.

40. Reis RS, Vale EDM, Heringer AS, Santa-Catarina C, Silveira V. Putrescine induces somatic embryo development and proteomic changes in embryogenic callus of sugarcane. **J Proteomics**. 2016; 130:170–179.

41. Amborella Genome Project. The Amborella genome and the evolution of flowering plants. **Science**. 2013; 342: 1241089.

42. London N, Biggins S. Signalling dynamics in the spindle checkpoint response. **Nat Rev Mol Cell Bio**. 2014; 15: 736–748.

43. Mattison CP, Old WM, Steiner E, Huneycutt BJ, Resing KA, Ahn NG, et al. Mps1 activation loop autophosphorylation enhances kinase activity. **J Biol Chem**. 2007; 282: 30553–30561.

44. Tipton AR, Ji W, Sturt-Gillespie B, Bekier ME, Wang K, Taylor WR, et al. Monopolar spindle 1 (MPS1) kinase promotes production of closed MAD2 (C-MAD2) conformer and assembly of the mitotic checkpoint complex. **J Biol Chem**. 2013; 288: 35149–35158.

45. Zhao Y, Chen R-H. Mps1 phosphorylation by MAP kinase is required for kinetochore localization of spindle-checkpoint proteins. **Curr Biol**. 2006; 16: 1764–1769.

4.2 Capítulo 2

Mps1 protein inhibition induces changes on proteomic profile in somatic embryogenesis of *Araucaria angustifolia* (Bertol.) Kuntze

Abstract

Mps1 protein is a dual-specificity kinase and an important component for the assembly of the spindle checkpoint (SAC), which plays a critical role in the progression of the cell cycle. Recently, it was observed that the inhibition of AaMps1 affects cellular growth and pro-embryogenic mass (PEM) differentiation during *Araucaria angustifolia* somatic embryogenesis. Several studies show that the expression of certain proteins may be associated with embryogenic competence and somatic embryo development. In this work, a comparative proteomic approach was used to identify proteins differentially abundant in embryogenic cultures of *A. angustifolia* treated or not with the inhibitor of Mps1 during the multiplication phase of the cultures. A total of 1977 proteins were identified. From these, 2 proteins were unique and 227 proteins were up-regulated in cells treated with the Mps1 inhibitor, whereas 218 were down-regulated. Proteins related to cell cycle and proliferation, and abundant in the intense cell division phase were down-regulated using the Mps1 inhibitor. Developmental process related proteins were up-regulated and proteins involved in folding and oxidation-reduction process were also modulated by the inhibition of Mps1. This work contributed to the further elucidation of the mechanisms related with the inhibition of proliferation and differentiation of embryogenic cultures aiming at the formation of somatic embryos.

4.2.1 Introduction

In many vascular plants, embryos can also develop from induced somatic cells through the process of somatic embryogenesis (Leljak-Levanić et al., 2015). During somatic embryogenesis, somatic cells are induced to form totipotent embryogenic cells capable of regenerating into complete plants (Yang and Zhang, 2010). Although somatic and zygotic embryogenesis are not fully correlated, common features are similar, showing physiological and morphological characteristic stages of the somatic embryo that resemble to zygotic embryo development (Leljak-Levanić et al., 2015). Somatic embryogenesis is as a model system for the study of morphological, cellular, physiological, and molecular events that occur during embryonic development in plants (Santa-Catarina et al., 2013; Steiner et al., 2015) and may be considered as an important strategy of technological development when used together with conventional genetic improvement programs (Santa-Catarina et al., 2013).

Embryogenic cultures of *A. angustifolia* has been studied in order to elucidate what are the factors involved in the success of the somatic embryos formation (Silveira et al., 2006; Dutra et al., 2013; Farias-Soares et al., 2014; Elbl et al., 2015; Steiner et al., 2016). Several works were also carried out in order to relate the profile of differentially abundant proteins with embryogenic potential of cultures (Jo et al., 2014; Dos Santos et al., 2016) and to understand the changes in the proteome profiles that may be affected by plant growth regulators supplementation (Fraga et al., 2016).

Recently, it was observed that the inhibition of AaMps1 protein affects cellular growth and pro-embryogenic mass (PEM) differentiation during *A. angustifolia* somatic embryogenesis (Douetts-Peres et al., 2016). Mps1 protein is a dual-specificity kinase and an important component for the assembly of the spindle checkpoint (SAC), which plays a critical role in the progression of the cell cycle (Musacchio and Salmon, 2007). The inhibition of Mps1 protein in plants was observed by using a kinase protein inhibitor (SP600125 - Sigma-Aldrich) in *Arabidopsis thaliana* L. (De Oliveira et al., 2012) and *A. angustifolia* (Douetts-Peres et al., 2016). However, metabolic pathways affected by inhibition of AaMps1 during somatic embryogenesis of *A. angustifolia* remain unclear. Studies at protein levels are essential to reveal the molecular mechanisms of plant growth, development, and interactions with the environment (Chen and Harmon 2006). Therefore, analysis of the protein profile may help elucidate changes that occur during growth and development of somatic embryos.

In somatic embryogenesis of several plant species, proteomic approaches have been used to identify proteins differentially abundant that may have significant roles in molecular events during this complex process. For instance, in some species, such as *Vitis vinifera* (Zhang et al., 2009), *Crocus sativus* (Sharifi et al., 2012), *Zea mays* (Sun et al., 2013), and *Saccharum spp* (Heringer et al., 2015), differentially abundant proteins were associated with different embryogenic potentials of cultures. In somatic embryogenesis, proteomic analysis were also important to assess the effects of treatments in the increase of somatic embryo numbers (Rode et al., 2012; Vale et al., 2014; Reis et al., 2016). The disclosure of molecular markers to allow early detection

of embryogenic cultures responsive to factors that promote maturation is therefore highly desirable, and it would be of a great value in the optimization of the protocols for obtaining somatic embryos (Dos Santos et al., 2016).

In this sense, the objective of this work was to study the effects of AaMps1 protein inhibition on proteomic profiles of embryogenic suspension cultures of *A. angustifolia.*

4.2.2 Materials and methods

4.2.2.1 Plant Material

Embryogenic cellular suspension cultures of *A. angustifolia* was used in the experiment, induced according to the methodology established by Steiner et al. (2005).

4.2.2.2 Embryogenic Cell Suspension Culture Conditions

To obtain the cellular suspensions, somatic embryogenic cultures were multiplied and subcultured every 15 days in a liquid MSG culture medium (Becwar et al., 1989). Ten milliliters of the suspension culture were transferred to 60 mL of fresh liquid MSG culture medium, supplemented with 30 g L^{-1} sucrose, 1.4 g L^{-1} L-glutamine (Sigma-Aldrich, St. Louis, USA), and 0.1 g L^{-1} myo-inositol (Merck KGaA, Darmstadt, Germany), and the pH of the culture medium was adjusted to 5.7 before autoclaving at 121°C, for 20 min, 1.5 atm. The embryogenic cell suspension cultures were kept on an orbital shaker (Cientec, Minas Gerais, Brazil) at 100 rpm in the dark, at 25 ± 2°C.

4.2.2.3 Effets of AaMps1 inhibition on proteomic profile

To analyze the effect of AaMps1 inhibition on differential abundance of proteins, the embryogenic cell suspension cultures were subcultured by adding 1.2 g of the fresh matter into 60 mL of the liquid MSG culture medium as mentioned above, supplemented with (10 µM) or without Mps1 inhibitor SP600125 (Sigma-Aldrich). The Mps1 inhibitor was previously filter-sterilized through a 0.2 µm PVDF membrane (Millipore, São Paulo, Brazil) before addition into culture medium. After inoculation, embryogenic cultures were maintained on an orbital shaker at 100 rpm in the dark, at 25 ± 2°C during 15 days. Samples were collected after 15 days of incubation in the treatments, frozen in liquid Nitrogen, and stored at -70 ºC until the proteomic analysis.

4.2.2.3 Protein Extraction

The extraction of total protein was performed according to Balbuena et al. (2009). Three biological samples (300 mg fresh matter – FM, each sample) were firstly macerated with liquid nitrogen until obtaining a powder. Following, 1 mL of extraction buffer, consisting of 7 M urea, 2 M thiourea, 2% triton X-100, 1% dithiothreitol (DTT), 1 mM phenylmethanesulfonyl fluoride (PMSF), and 5 µM pepstatin, was added to the samples. Then, samples were vortexed and incubated on ice for 30 min, followed by centrifugation at 16,000 g for 20 min, at 4 °C. The supernatants were collected, and the protein concentration was measured using a 2-D Quant Kit (GE Healthcare, Piscataway, NJ, USA).

4.2.2.4 Protein Digestion

For protein digestion, three biological replicates of 100 µg of proteins were used for each treatment. Before digestion step with trypsin, samples were precipitated using the methanol/chloroform methodology to remove any MS interfering compound (Nanjo et al., 2011). After that, samples were desalted on Amicon Ultra-0.5 3 kDa centrifugal filters (Merck Millipore, Germany) using 50 mM ammonium bicarbonate (Sigma-Aldrich) pH 8.5, as washing buffer. This procedure was repeated at least three times, resulting in approximately 50 µL per sample.

The protein digestion was performed according to methodology described by (Calderan-Rodrigues et al., 2014). For each biological sample, 25 µL of 0.2% (v/v) RapiGest® (Waters, Milford, CT, USA) was added, and samples were briefly vortexed and incubated in an Eppendorf Thermomixer® at 80 °C for 15 min. Then, 2.5 µL of 100 mM DTT (Bio-Rad Laboratories, Hercules, CA, USA) was added, and the tubes were vortexed and incubated at 60 °C for 30 min under agitation in the thermomixer. Next, 2.5 µL of 300 mM iodoacetamide (GE Healthcare) was added, the samples were vortexed and incubated in the dark for 30 min at room temperature. The digestion was performed by adding 20 µL of trypsin solution (50 ng/µL; V5111, Promega, Madison, WI, USA) prepared in 50 mM ammonium bicarbonate, and samples were incubated at 37 °C overnight. For RapiGest® precipitation, 10 µL of 5% (v/v) trifluoroacetic acid (TFA, Sigma-Aldrich) was added and incubated at 37 °C for 90 min, followed by a centrifugation step of 30 min at 16,000 x g. Samples were transferred to Total Recovery Vials (Waters).

4.2.2.5 Mass spectrometry analysis

A nanoAcquity UPLC connected to a Synapt G2-Si HDMS mass spectrometer (Waters, Manchester, UK) was used for ESI-LC-MS/MS analysis. The chromatography step was performed by injecting 1 µL of digested samples to normalize them before the relative quantification of proteins. To ensure standardized molar values for all conditions, normalization among samples was based on stoichiometric measurements of total ion counts of MS^E scouting runs prior to analyses. Runs consisted of three biological replicates. During separation, samples were loaded onto the nanoAcquity UPLC 5 µm C18 trap column (180 µm × 20 mm) at 5 µL min^{-1} during 3 min and then, on the nanoAcquity HSS T3 1.8 µm analytical reversed phase column (75 µm × 150 mm) at 350 nL/min, with a column temperature of 60 °C. For peptide elution, a binary gradient was used, with mobile phase A consisting of water (Tedia, Fairfield, Ohio, USA) and 0.1% formic acid (Sigma-Aldrich) and mobile phase B consisting of acetonitrile (SigmaAldrich) and 0.1% formic acid. Gradient elution started at 7% phase B and was held for 3 min, then ramped from 7 to 40% phase B up to 90.09 min, and from 40 to 85% phase B until 94.09 min, being maintained at 85 until 98.09 min, then decreasing to 7% phase B until 100.09 min and kept 7% phase B until the end of experiment at 108.09 min. Mass spectrometry was performed in positive and resolution mode (V mode), 35,000 FWHM, with ion mobility, and in data-independent acquisition (DIA) mode; IMS wave velocity was set to 600 m/s; the transfer collision energy ramped from 19 V to 45 V in high-energy mode; cone and capillary voltages of 30 V and 2800 V, respectively; and a source temperature of 70 °C. In TOF parameters, the scan time was set to 0.5 s in continuum mode with a mass range of 50 to 2000 Da.

The human [Glu1]-fibrinopeptide B (Sigma-Aldrich) at 100 fmol μL^{-1} was used as an external calibrant and lock mass acquisition was performed every 30 s.

4.2.2.6 Bioinformatics

Spectra processing and database searching conditions were performed by Progenesis QI for Proteomics Software V.2.0 (Nonlinear Dynamics, Newcastle, UK). The analysis used the following parameters: one missed cleavage, minimum fragment ion per peptide equal to two, minimum fragment ion per protein equal to five, minimum peptide per protein equal to two, fixed modifications of carbamidomethyl (C) and variable modifications of oxidation (M) and phosphoryl (STY), and a default false discovery rate (FDR) value at a 4% maximum, score greater than five, and maximum mass errors of 10 ppm. For protein identification we use the *A. angustifolia* transcriptome database (Elbl et al., 2015). Label-free relative quantitative analyses were performed based on the ratio of protein ion counts among contrasting samples. After data processing and to ensure the quality of results, the following protein refinement parameters were used: only proteins present in 3 of 3 runs. Furthermore, differentially abundant proteins were selected based on a max fold change of at least 1.5 and ANOVA ($P < 0.05$). Functional annotation was performed using Blast2Go software v. 3.2 PRO (Conesa et al., 2005).

4.2.3 Results

In this study we identified 1977 non-redundant proteins in the embryogenic cultures of *A. angustifolia* treated or not with 10 µM of Mps1 inhibitor after 15 days of culture, being two of them unique for cells treated with

Mps1 inhibitor. Moreover, 227 proteins were up-regulated, and 218 were down-regulated when the AaMps1 was inhibited (Figure 1).

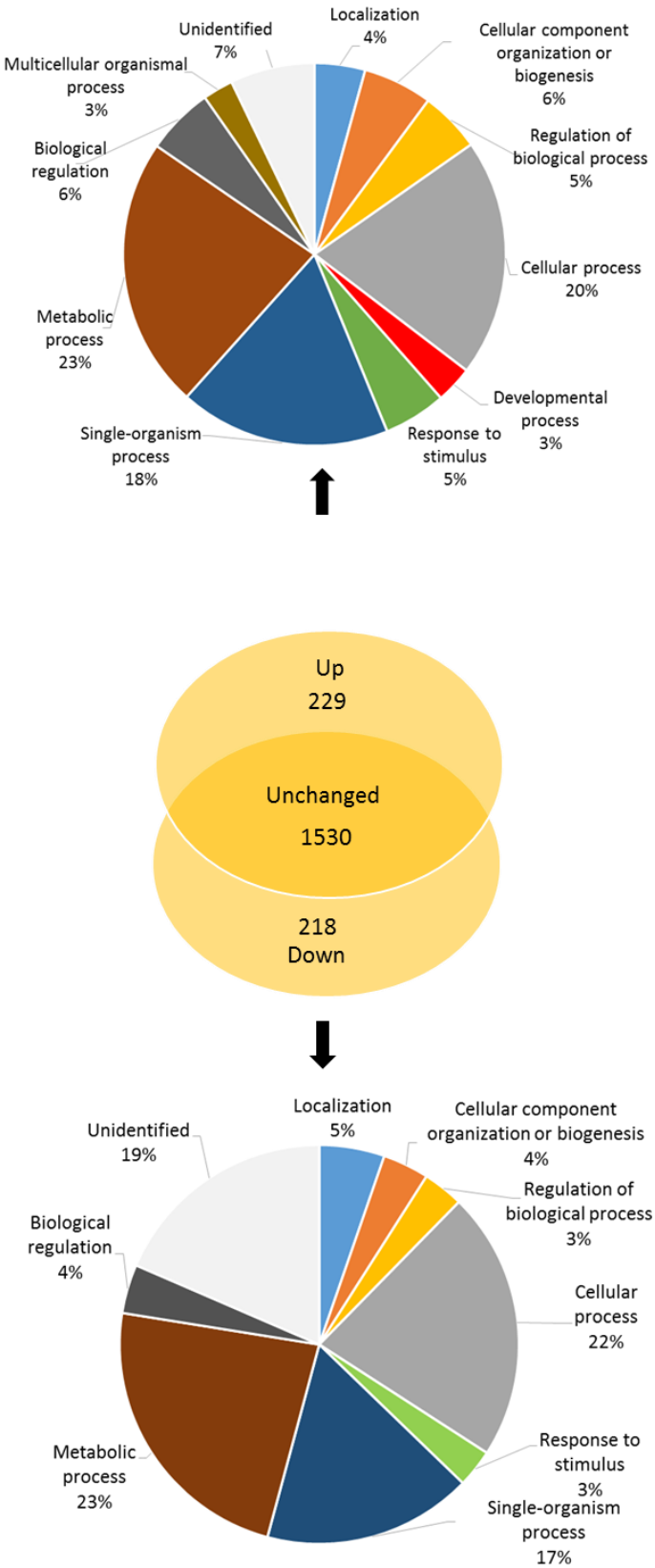

Figure 1. Functional classification of proteins Up- and Down-regulated in embryogenic cell suspension cultures of *A. angustifolia* treated with Mps1 inhibitor (below) compared to the control (above).

The functional classification of proteins showed differences in the percentage of abundant proteins according to the treatment (control and Mps1 inhibition). Using the classification by biological process, and considering the regulation of proteins in up- or down-regulated in terms of abundance of the ratio Mps1 inhibition/control, proteins were divided into 11 classes (Figures 1 and 2). However, 2 classes of proteins, the “Developmental process” and “Multicellular organismal process” showed only up-regulated proteins.

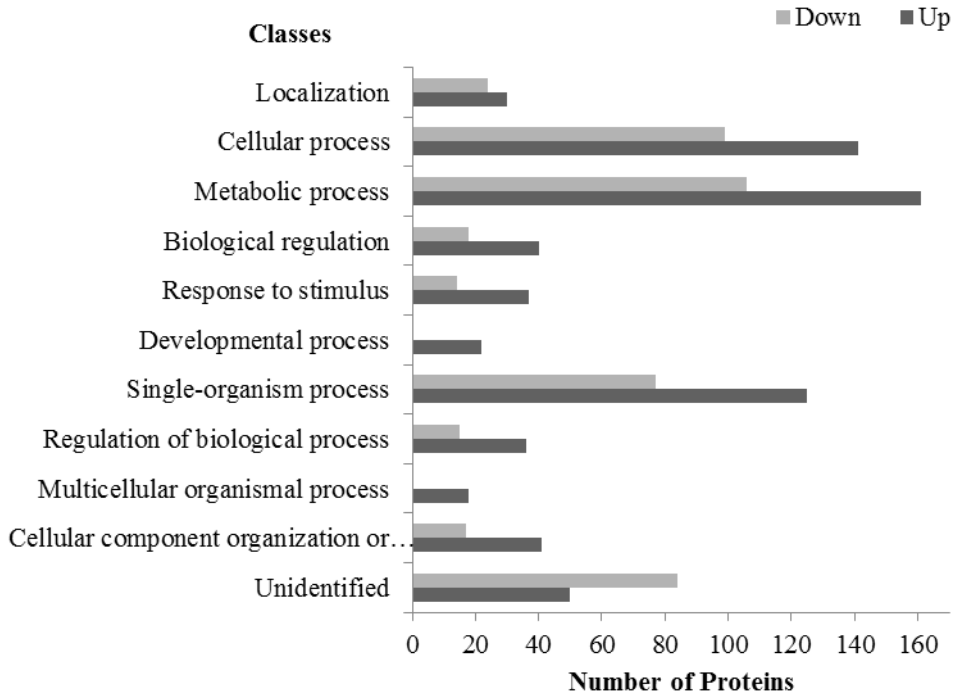

Figure 2. Number of proteins Up- and Down-regulated in each class with Mps1 inhibitor treatment (below) compared to in control (above) and in suspension cellular embryogenic cultures of *A. angustifolia*.

Most of the proteins identified in “Developmental process” and “Multicellular organismal process” are common to both classes. In these classes (Table 1), there are three L-ascorbate oxidase homolog proteins that were up-

regulated 101.53, 3.41, and 4.05 times in the Mps1 inhibition treatment in relation to the control. In the “Developmental process” class, were also identified the glutamate-cysteine ligase (Up - 1.55 times), late embryogenesis abundant (LEA - Up - 12.31 times), and malate dehydrogenase (Up - 1.78 times).

The “Cellular process” and “Metabolic process” classes present several common proteins. One protein, the casein kinase, was unique in the Mps1 inhibition treatment. In these classes, proteins involved in cell division processes, such as DNA replication licensing factors MCM4 (2.91 times) and MCM7 (3.49 times), DNA polymerase alpha (2.43 times), ethylene metabolism 1-aminociclopropano-1-carboxilato oxidase (2.92 times), LL-diaminopimelate aminotransferase (1.57 times), and UBP1-associated 2A-like (1.57 times), were down-regulated in the Mps1 inhibition treatment. In addition, a total of 51 proteins related with the oxidation-reduction process were identified, in which 17 were down- and 34 up-regulated (Table 1). Folding proteins, such as the probable prefoldin subunit 3 (4.92 times), grpE homolog (2.69 time), and one heat shock 83-like (1.68 time), were up-regulated. On the other hand, thioredoxin m isoform 2 (1.58 times), peptidyl-prolyl cis-trans isomerase (PPIase) (1.58 times), two heat shock cognate 70 kDa (2.07 and 2.74 times), and two heat shock 83-like (1.56 and 1.58 times) were down-regulated. In the class “Regulation of biological process” were identified two proteins related to proliferating cell nuclear antigen (PCNA), one up (5.30 times) and other down-regulated (1.93 times).

Table 1 – Identified proteins differentially abundant in embryogenic cultures of *A. angustifolia* at 15 days of incubation on control and 10 µM of Mps1 inhibitor (SP600125).

SeqName (blat go)	Description (blast go)	Peptide count	Score	Fold change	Biological process	Control 10 µM
Multicellular organismal process / Developmental process						
comp50340_c0_seq1|m.39757	glutamate-cysteine ligase, chloroplastic	8	53.07	1.55	glutathione biosynthetic Process; response to heat	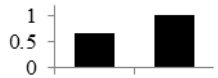
comp26674_c0_seq1|m.4799	L-ascorbate oxidase homolog	4	35.29	101.53	multidimensional cell growth; oxidation-reduction Process; cell wall organization	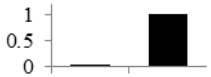
comp46904_c0_seq1|m.28034	L-ascorbate oxidase homolog	23	212.33	3.41	multidimensional cell growth; L-ascorbic acid metabolic Process; oxidation-reduction Process	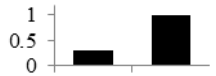
comp56334_c0_seq1|m.72391	L-ascorbate oxidase homolog	10	82.44	4.05	developmental Process; oxidation-reduction Process; cell growth	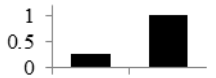
comp39962_c0_seq1|m.14266	Late embryogenesis abundant , group 2 isoform 1	21	174.95	2.31	cell growth	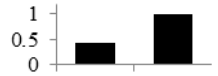
comp28819_c0_seq1|m.6038	malate dehydrogenase, glyoxysomal	11	96.20	1.78	MAPK cascade; regulation of fatty acid beta-oxidation; reductive tricarboxylic acid cycle; regulation of hydrogen Peroxide metabolic Process; malate metabolic Process; cell differentiation.	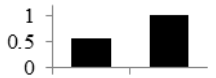
Developmental process						

comp49407_c0_seq1|m.35882	E3 ubiquitin- ligase UPL3	4	32.92	1.72	single-organism developmental Process	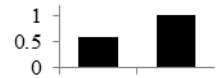
comp45078_c0_seq1|m.23567	endoglucanase 18-like	19	148.29	2.27	fruit ripening; starch metabolic Process	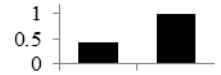
comp50340_c0_seq1|m.39757	glutamate--cysteine ligase, chloroplastic	8	53.07	1.55	response to salt stress; glutathione biosynthetic Process; response to heat	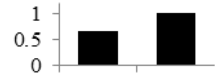
comp26674_c0_seq1|m.4799	L-ascorbate oxidase homolog	4	35.29	101.53	multidimensional cell growth; oxidation-reduction Process	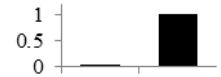
comp46904_c0_seq1|m.28034	L-ascorbate oxidase homolog	23	212.33	3.41	multidimensional cell growth; oxidation-reduction Process	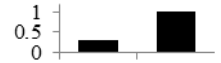
comp56334_c0_seq1|m.72391	L-ascorbate oxidase homolog	10	82.44	4.05	cellular developmental Process; plant organ development; oxidation-reduction Process; cell growth	
comp39962_c0_seq1|m.14266	Late embryogenesis abundant , group 2 isoform 1	21	174.95	2.31	cell morphogenesis; response to desiccation; cell growth	
comp28819_c0_seq1|m.6038	malate dehydrogenase, glyoxysomal	11	96.20	1.78	MAPK cascade; regulation of fatty acid beta-oxidation; reductive tricarboxylic acid cycle; glyoxylate cycle; cell differentiation	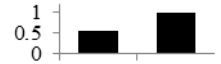
comp40185_c0_seq1|m.14616	peroxisomal fatty acid beta-oxidation multifunctional AIM1	27	207.27	2.76	fatty acid biosynthetic Process; fatty acid beta-oxidation	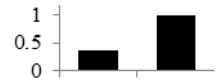

comp36513_c0_seq1|m.10876	tropinone reductase-like 3	10	70.88	2.11	oxidation-reduction Process; response to indolebutyric acid	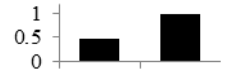
comp46657_c0_seq1|m.27393	tubulin-folding cofactor D	3	21.88	1.75	tubulin complex assembly; post-embryonic development; post-chaperonin tubulin folding Pathway; microtubule cytoskeleton organization	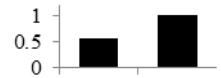
Cellular process / Metabolic process						
comp51260_c0_seq1|m.44319	casein kinase I isoform delta-like	2	11.95	unique	serine family amino acid metabolic Process; peptidyl-serine Phosphorylation	
comp44486_c0_seq1|m.22419	peptidyl-prolyl cis-trans isomerase	15	137.30	1.58	response to oxidative stress; response to cold; unsaturated fatty acid biosynthetic Process; protein folding; oxidoreduction coenzyme metabolic Process; coenzyme biosynthetic Process; cell differentiation	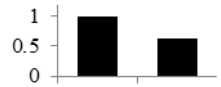
comp55344_c0_seq1|m.72250	DNA replication licensing factor MCM4	5	35.77	2.91	cell Proliferation; DNA replication initiation; nucleolus organization; cytokinesis by cell Plate formation; regulation of DNA replication; chromatin silencing; DNA methylation; nuclear division; regulation of cell cycle	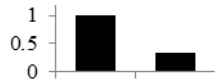
comp47434_c0_seq1|m.29749	DNA replication licensing factor MCM7	10	57.14	3.49	cell Proliferation; DNA replication initiation; cell cycle; DNA methylation	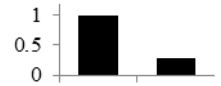

comp48685_c0_seq1|m.33425	DNA polymerase alpha catalytic subunit	3	15.95	2.43	DNA replication initiation; DNA biosynthetic Process	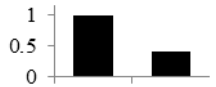
comp49150_c0_seq1|m.34839	arginine N-methyltransferase	7	38.75	1.61	embryo development ending in seed dormancy; embryo sac egg cell differentiation	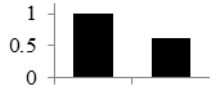
comp24690_c0_seq1|m.3973	1-aminocyclopropane-1-carboxylate oxidase	9	66.46	2.92	oxidation-reduction Process	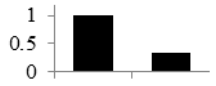
comp46686_c0_seq1|m.27442	LL-diaminopimelate aminotransferase, chloroplastic isoform X1	16	109.87	1.57	ethylene biosynthetic Process	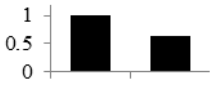
comp44933_c0_seq3|m.23224	UBP1-associated 2A-like	17	161.18	1.57	cell death; ethylene biosynthetic Process; defense response	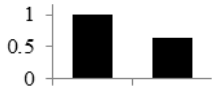
comp48796_c0_seq1|m.33788	glutathione S-transferase	10	101.27	2.63	obsolete glutathione conjugation reaction; glutathione metabolic Process;	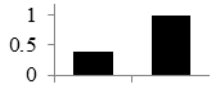
comp49942_c0_seq2|m.37916	glutathione S-transferase GSTU6, , expressed	5	27.59	2.11	obsolete glutathione conjugation reaction; toxin catabolic Process; glutathione metabolic Process;	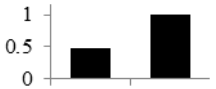
comp17146_c0_seq1|m.2331	dehydroascorbate reductase	13	115.63	1.67	obsolete glutathione conjugation reaction; obsolete electron transport; glutathione metabolic Process; cellular oxidant detoxification; L-ascorbic acid metabolic Process; oxidation-reduction Process	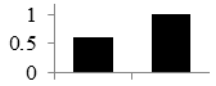

comp47283_c0_seq1|m.29253	monodehydroascorbate reductase	30	316.67	1.60	cell redox homeostasis; oxidation-reduction Process	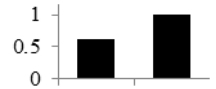
comp24493_c0_seq1|m.3929	non-functional NADPH-dependent codeinone reductase 2	2	11.71	1.73	oxidation-reduction Process	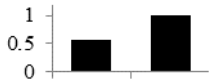
comp56334_c0_seq1|m.72391	L-ascorbate oxidase homolog	10	82.44	4.05	developmental growth involved in morphogenesis; cellular developmental Process; plant organ development; cellular component organization; oxidation-reduction Process; cell growth	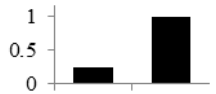
comp56412_c0_seq1|m.72398	L-ascorbate oxidase homolog	4	58.34	5.31	oxidation-reduction Process;	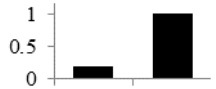
comp46904_c0_seq1|m.28034	L-ascorbate oxidase homolog	23	212.33	3.41	regulation of meristem growth; regulation of hormone levels; multidimensional cell growth; L-ascorbic acid metabolic Process; oxidation-reduction Process	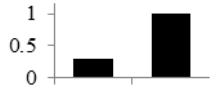
comp26674_c0_seq1|m.4799	L-ascorbate oxidase homolog	4	35.29	101.53	regulation of meristem growth; ; cell tip growth; regulation of hormone levels; multidimensional cell growth; oxidation-reduction Process	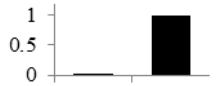
comp28668_c0_seq1|m.5942	probable NAD(P)H dehydrogenase (quinone) FQR1-like 1	6	46.35	1.91	negative oxidation-reduction Process	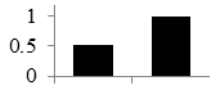

comp28863_c0_seq1|m.6071	aldehyde dehydrogenase family 2 member B7, mitochondrial-like	23	187.64	1.85	L-ascorbic acid metabolic Process; oxidation-reduction Process	
comp29445_c0_seq1|m.6443	GDP-L-fucose synthase 2	11	64.77	2.03	oxidation-reduction Process;	
comp36120_c0_seq2|m.10145	guanosine nucleotide diphosphate dissociation inhibitor 2	21	167.70	1.80	regulation of catalytic activity; oxidation-reduction Process	
comp36385_c0_seq1|m.10624	delta-1-pyrroline-5-carboxylate synthase	5	28.79	1.84	oxidation-reduction Process	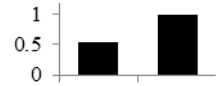
comp36513_c0_seq1|m.10876	tropinone reductase-like 3	10	70.88	2.11	oxidation-reduction Process	
comp36546_c0_seq1|m.10921	glutaredoxin C4	5	55.99	1.65	oxidation-reduction Process	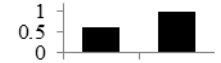
comp36772_c0_seq1|m.11361	minor allergen Alt a 7-like	7	83.22	1.95	negative oxidation-reduction Process;	
comp36851_c0_seq2|m.11510	urate oxidase	8	49.31	1.76	oxidation-reduction Process	
comp39681_c0_seq1|m.13859	aldo-keto reductase family 4 member C9-like	6	34.52	2.42	oxidation-reduction Process	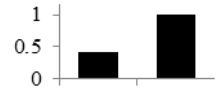

comp39830_c1_seq1|m.14090	glyoxysomal fatty acid beta-oxidation multifunctional MFP-a	8	53.14	1.66	fatty acid catabolic Process; fatty acid biosynthetic Process; oxidation-reduction Process	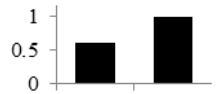
comp40783_c0_seq1|m.15817	NAD-dependent dyhydrogenase, Gfo Idh family	5	34.44	1.88	oxidation-reduction Process	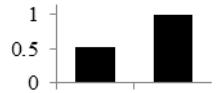
comp41537_c0_seq2|m.17206	PREDICTED: uncharacterized protein At1g32220, chloroplastic-like	2	13.05	3.63	oxidation-reduction Process	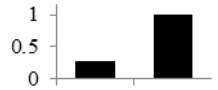
comp46602_c0_seq6|m.27273	D-2-hydroxyglutarate dehydrogenase, mitochondrial	6	33.30	2.54	oxidation-reduction Process	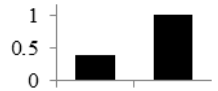
comp47017_c0_seq1|m.28363	UDP-glucose 6-dehydrogenase 5	21	193.66	1.71	oxidation-reduction Process	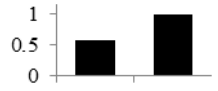
comp47283_c0_seq1|m.29253	monodehydroascorbate reductase	30	316.67	1.60	oxidation-reduction Process	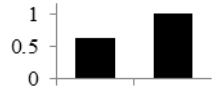
comp49827_c0_seq1|m.37482	peroxiredoxin-2B	11	86.02	2.65	response to oxidative stress; cellular oxidant detoxification; oxidation-reduction Process	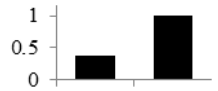
comp50810_c0_seq2|m.41945	UDP-glucose 6-dehydrogenase 1	12	125.89	1.53	oxidation-reduction Process	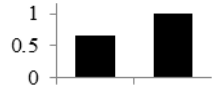
comp51057_c0_seq1|m.43141	12-oxophytodienoate reductase 11	12	74.11	2.92	oxidation-reduction Process	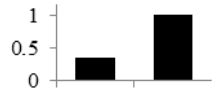

comp52561_c0_seq1|m.52713	2-alkenal reductase (NADP(+)-dependent)-like	13	88.95	2.80	oxidation-reduction Process	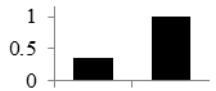
comp52921_c0_seq1|m.55068	quinone oxidoreductase PIG3	3	23.45	1.94	oxidation-reduction Process	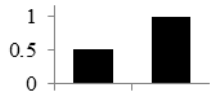
comp52968_c0_seq1|m.55367	glyceraldehyde-3-phosphate dehydrogenase, cytosolic	34	478.89	2.46	oxidation-reduction Process	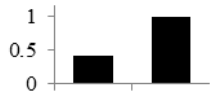
comp52968_c0_seq2|m.55369	glyceraldehyde-3-phosphate dehydrogenase, cytosolic	35	496.61	3.95	oxidation-reduction Process;	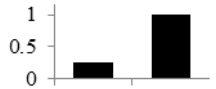
comp53056_c0_seq1|m.56209	catalase isozyme 1	22	163.25	1.60	oxidation-reduction Process	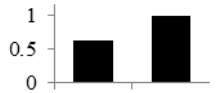
comp53555_c0_seq2|m.60188	4-hydroxyphenylpyruvate dioxygenase	9	59.37	2.63	oxidation-reduction Process	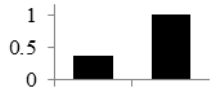
comp53731_c0_seq2|m.62522	delta-1-pyrroline-5-carboxylate synthase	9	61.80	3.42	oxidation-reduction Process	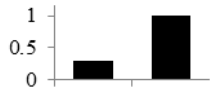
comp54000_c0_seq3|m.66011	probable nucleoredoxin 1	28	204.69	1.74	oxidation-reduction Process;	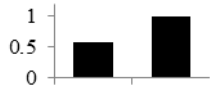
comp54449_c0_seq1|m.71872	cinnamyl alcohol dehydrogenase	25	252.60	1.51	oxidation-reduction Process	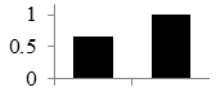

comp24690_c0_seq1|m.3973	1-aminocyclopropane-1-carboxylate oxidase	9	66.46	2.92	oxidation-reduction Process	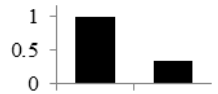
comp50443_c1_seq2|m.40220	2-oxoisovalerate dehydrogenase subunit beta 1, mitochondrial	3	17.50	1.64	oxidation-reduction Process	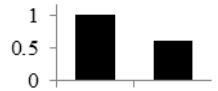
comp50410_c0_seq2|m.40107	alcohol dehydrogenase	25	256.40	1.54	oxidation-reduction Process;	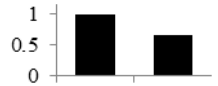
comp50410_c0_seq1|m.40106	alcohol dehydrogenase, partial	7	69.84	3.38	oxidation-reduction Process;	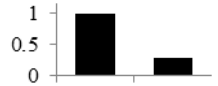
comp52462_c0_seq1|m.52080	cationic peroxidase 1-like	5	32.67	17.79	obsolete Peroxidase reaction; cellular oxidant detoxification; oxidation-reduction Process	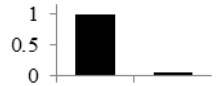
comp36583_c0_seq1|m.10990	cytochrome c	8	85.68	2.72	oxidation-reduction Process;	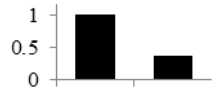
comp54354_c0_seq1|m.71799	dihydropyrimidine dehydrogenase [NADP(+)]	25	198.72	1.59	oxidation-reduction Process;	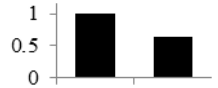
comp36614_c0_seq1|m.11055	enoyl-[acyl-carrier-] reductase [NADH], chloroplastic-like	15	109.70	1.61	oxidation-reduction Process	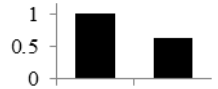
comp46943_c0_seq1|m.28158	heat shock cognate 70 kDa 2	46	503.77	2.07	protein folding; oxidation-reduction Process	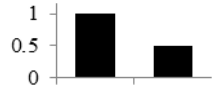

comp53509_c1_seq3|m.59848	L-ascorbate oxidase homolog	10	57.49	1.61	cell tip growth; regulation of hormone levels; multidimensional cell growth; L-ascorbic acid metabolic Process; oxidation-reduction Process; cell wall organization	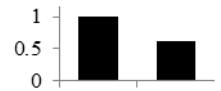
comp52365_c0_seq1|m.51400	NADH dehydrogenase subunit 7 (mitochondrion)	11	77.08	1.54	oxidation-reduction Process;	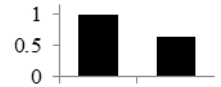
comp34706_c0_seq1|m.8679	peroxidase 57-like	7	38.83	1.80	response to oxidative stress; obsolete Peroxidase reaction; oxidation-reduction Process	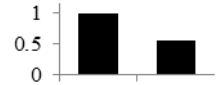
comp47377_c0_seq3|m.29563	PREDICTED: uncharacterized protein LOC103720589 isoform X3	2	17.40	3.54	oxidation-reduction Process	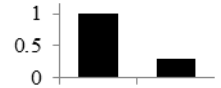
comp49954_c0_seq2|m.37956	protoporphyrinogen oxidase 1, chloroplastic	3	16.77	2.60	; oxidation-reduction Process	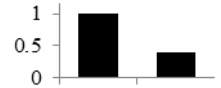
comp46549_c0_seq1|m.27105	thioredoxin F-type, chloroplastic	3	19.38	2.22	cell redox homeostasis; oxidation-reduction Process	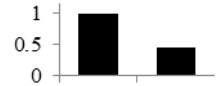
comp21015_c0_seq1|m.3200	Thioredoxin m, isoform 2	4	28.06	2.25	cellular response to oxidative stress; cell redox homeostasis; oxidation-reduction Process; protein folding	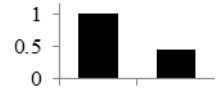
comp52280_c0_seq2|m.50866	Unknown	4	27.16	4.71	cellular oxidant detoxification; oxidation-reduction Process	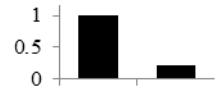
comp51720_c0_seq2|m.46817	heat shock 83-like	36	250.02	1.58	protein folding	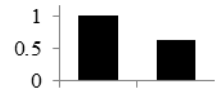

comp50903_c0_seq1|m.42354	heat shock 83-like	11	105.08	1.56	protein folding	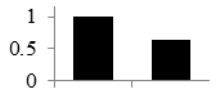
comp46943_c0_seq1|m.28158	heat shock cognate 70 kDa 2	46	503.77	2.07	protein folding; oxidation-reduction Process	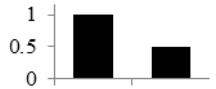
comp46943_c0_seq2|m.28160	heat shock cognate 70 kDa 2	21	197.44	2.74		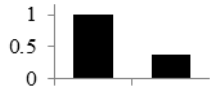
comp21015_c0_seq1|m.3200	Thioredoxin m, isoform 2	4	28.06	2.25	cellular response to oxidative stress; cell redox homeostasis; oxidation-reduction Process; protein folding	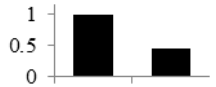
comp49589_c0_seq1|m.36503	grpE homolog, mitochondrial	13	79.65	2.69	embryo development ending in seed dormancy; protein folding	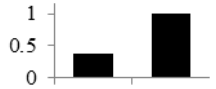
comp50903_c0_seq2|m.42355	heat shock 83-like	13	126.10	1.68	protein folding	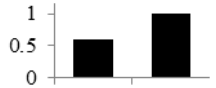
comp30021_c0_seq1|m.6821	probable prefoldin subunit 3	3	26.49	4.92	tubulin complex assembly; protein folding; microtubule-based Process	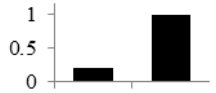
Regulation of biological process						
comp36201_c0_seq1|m.10286	elongation factor 2	8	91.27	1.65	regulation of translational elongation;	
comp37151_c0_seq1|m.11974	proliferating cell nuclear antigen	8	65.35	5.30	leading strand elongation; regulation of DNA replication; mismatch repair; translesion synthesis	

comp44392_c0_seq1|m.22235	probable serine threonine-kinase mps1 isoform X1	135	828.30	2.76	mitotic cell cycle checkpoint; chromatin silencing; protein Phosphorylation; chromosome separation	
comp52605_c0_seq1|m.52938	proliferating cell nuclear antigen	15	112.87	1.93	leading strand elongation; regulation of DNA replication; mismatch repair; translesion synthesis	
Single-organism process						
comp21044_c0_seq1|m.3207	AUGMIN subunit 5	7	46.94	2.87	spindle assembly;	
comp27882_c0_seq1|m.5427	NADH dehydrogenase [ubiquinone] flavo 1, mitochondrial	14	114.46	1.87	proteasome core complex assembly; cell growth	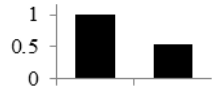
comp39874_c0_seq3|m.14161	NADH dehydrogenase [ubiquinone] 1 alpha subcomplex subunit 6	4	25.91	1.89	generation of Precursor metabolites and energy; response to chemical;	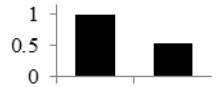
comp41516_c0_seq1|m.17158	nuclear-pore anchor	2	11.87	10.21	mitotic spindle assembly checkpoint; protein import into nucleus;	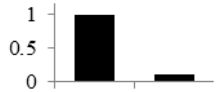
comp49942_c0_seq2|m.37916	glutathione S-transferase GSTU6, , expressed	5	27.59	2.11	toxin catabolic Process; glutathione metabolic Process;	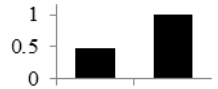
comp52365_c0_seq1|m.51400	NADH dehydrogenase subunit 7 (mitochondrion)	11	77.08	1.54	oxidation-reduction Process;	

comp56412_c0_seq1|m.72398	L-ascorbate oxidase homolog	4	58.34	5.31	oxidation-reduction Process;	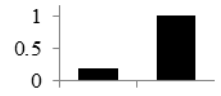

4.2.4 Discussion

The inhibition of Mps1affected significantly the abundance of proteins identified in embryogenic cultures of *A. angustifolia* after 15 days of incubation. In previous work, we have already reported that the inhibition of AaMps1 may affect significantly the growth and morphology of PEMs that compose the embryogenic cultures of *A. angustifolia* (Douetts-Peres et al., 2016). In somatic embryogenesis, during the transition of somatic cells into somatic embryos, the cells need to be restructured and sustain division, which increase the enzyme activity (mainly kinases), the conversion of ATP to ADP, and the rate of oxygen uptake (Mahdavi-Darvari et al., 2015). The AaMps1 inhibition affected mostly the classes of proteins related to the developmental, cellular, metabolic, and regulation of biological process. In this sense, the proteins from these classes were evaluated.

4.2.4.1 Developmental Process

Increased abundance of proteins involved in developmental processes indicates that the inhibition of AaMps1 can promote cellular development. Three proteins Ascorbate oxidase (AO) were up-regulated (Table 1). The activity of AO at high levels is related to young and growing tissues (Lin and Varner, 1991; Kato and Esaka, 1996) and its expression is correlated to cell expansion and/or elongation (Lin and Varner, 1991; Esaka et al., 1992; Al-Madhoun et al., 2003). In tobacco studies, protoplasts prepared from transgenic tobacco cells over-expressing pumpkin AO elongated more rapidly than those from wild type cells, showing a direct relation for the participation of AO in cell expansion (Kato and Esaka, 2000). The monodehydroascorbate reductase (MDHAR) and dehydroascorbate reductase (DHAR) are components of the ascorbate-glutathione

cycle (Saruhan et al., 2009) and were up-regulated in embryogenic cultures of *A. angustifolia* grown in AaMps1 inhibition treatment. DHAR is essential for recycling of monodehydroascorbate (MDHA), which may then accomplish the ascorbate regeneration (Chen and Gallie, 2006). The MDHA is a radical that can accept electrons from the plasma membrane redox system. This reduction of the MDHA back to ascorbate, then, results in the acidification of the apoplast, hyperpolarization of the plasma membrane, and the activation of the ion transport that leads to vacuole and cell enlargement (Gonzalez-Reyes et al., 1994; Al-Madhoun et al., 2003). Increasing the abundance of AO, DHAR, and MDHAR in the AaMps1 inhibition treatment indicates that these proteins may be responsible for the increase in the width of the suspensor cells-type in *A. angustifolia* when compared to the untreated cells (Douetts-Peres et al., 2016).

In the AaMps1 Inhibition treatment, proteins related to cell differentiation were up-regulated such as the malate dehydrogenase and the LEAs proteins. The malate dehydrogenase belongs to the tricarboxylic acid cycle (TCA), and was reported in somatic embryos of *Theobroma cacao* L. (Noah et al., 2013), as well as participating in the processes of seed germination in the cotyledons of *Vigna radiata* L. Wilczek (Ghosh and Pal, 2012). The LEAs are hydrophilic members of a class of highly conserved proteins, and are known to play protective roles under environmental stresses and to be up-regulation stress-responsive. Their expression is an important mechanism for stress tolerance to desiccation preventing protein aggregation and preserving enzymatic activity during dehydration (Huang et al., 2012). These proteins are usually present in seeds, for example, in seeds of *Amaranthus cruentus* L. (Maldonado-Cervantes et al., 2014) and during the seed desiccation in *Gossypium hirsutum* L. (Dure et al., 1981). In zygotic embryos of maize (*Zea mays* L.), there was a greater abundance of LEA

proteins in embryos that were tolerant to desiccation (Huang et al., 2012). These desiccation protection mechanisms may usually confer a better condition to the development of embryogenic cultures, as suggested in callus cultures of sugarcane, in which LEA proteins were up-regulated in the maturation treatment, resulting in a greater number of somatic embryos formed (Reis et al., 2016). The increased abundance of these proteins indicates that the inhibition of AaMps1 and hence the cell cycle arrest, may cause cells to synthesize more proteins involved in cellular development.

4.2.4.2 Cellular process / Metabolic process

Casein kinase I is a protein associated with the cell cycle and was found to be unique in the treatment with Mps1 inhibitor (Table 1). This protein plays an important role in the formation of the cytoskeleton. In human ameloblastoma cell lines, Casein kinase I regulates the organization of the keratin cytoskeleton and maintains the formation of desmosomes. In mouse, mutants of this protein disrupt the keratin cytoskeleton and subsequently impair the formation of desmosomes (Kuga et al., 2016).

In our work, the Mps1 inhibition treatment reduced the abundance of proteins related to proliferation, cell growth, spindle assembly, and the regulation of DNA. (Table 1). The decrease in the abundance of this protein provides us a positive evidence that inhibition of Mps1 affects cell cycle progression in embryogenic cultures of *A. angustifolia.* This may help us to clarify the mechanisms related to the inhibition of the proliferation and beginning of the differentiation until the formation of somatic embryo. In some species, such as *Quercus suber* L., proteins involved in cell division during the proliferative phase are more abundant (Guan et al., 2016). In eukaryotes, the MCM proteins are conserved from yeast to mammals and include six subunits MCM2–7 that participate in DNA replication (Forsburg, 2004; Rizvi et al., 2016). In this work, two

proteins are part of the heterohexamer MCM complex, the DNA replication licensing factors MCM4 and MCM7, which were more abundant in the cells during the proliferative phase (control) and down-regulated in cells with inhibited Mps1 (Table 1). The MCM complex is a component of the helicase that unwinds DNA during replication and there exist evidences that indicate that the MCMs recruit or anchor checkpoint proteins at the stalled replication forks (Forsburg, 2004). In Arabidopsis, heterozygous mutation gene (PROLIFERA) that expresses MCM7, leads to improper cytokinesis due to defects in S-phase progression (Holding and Springer, 2002).

In tobacco, in the Cyclic cAMP deficiency cells, MCM7 is significantly reduced and low levels of free cAMP delay cell cycle progression and negatively affects cell growth, enhancing the stress-related responses (Sabetta et al., 2016). Additionally, the expression of the gene PROLIFERA in *A. thaliana* is related to tissue in the phase of active cell division, then decreasing its expression as the cells stop the division and begin to differentiate and expand (Holding and Springer, 2002). In eukaryotes, a complex composed of the small and large subunits of DNA primase, and the catalytic and non-catalytic subunits of DNA polymerase initiate nuclear DNA replication. After DNA replication initiation, the DNA polymerase E and D replace the DNA polymerase A to continue synthesizing the leading and lagging strands, respectively (Perera et al., 2013; Micol-Ponce et al., 2015). The use of the Mps1 inhibitor reduced the abundance of DNA polymerase Alpha protein (Table 1), which is responsible (together with DNA primase) by the nuclear DNA replication. This indicates less DNA replication according to the lower cell division rate of *A. angustifolia* embryogenic cultures.

During induction and development of somatic embryos, the conjugation of glutathione by glutathione S-transferase (GSTs) influences the signaling pathways related to the hormones auxin and ethylene (Stasolla, 2010; Noah et al., 2013). In our

work, the protein 1-aminociclopropano-1-carboxilato oxidase (ACC oxidase), which is a key enzyme in the ethylene biosynthesis, were more abundant in proliferating cells (control treatment) and down-regulated in the AaMps1 inhibition treatment (Table 1). Ethylene is usually correlated with the development of somatic embryos in *Picea mariana* (Mill.) BSP (Meskaoui and Tremblay, 2001), *Pinus sylvestris* L. (Lu et al., 2011), and *A. angustifolia*. The latter, embryogenic cultures produce higher amounts of ethylene during the proliferative phase when compared with non-embryogenic cultures (Jo et al., 2014). Another three proteins involved in ethylene biosynthesis, the LL-diaminopimelate aminotransferase, the chloroplastic isoform X1, and the UBP1-associated 2A-like, were down-regulated in the AaMps1 inhibition treatment (Table 1). The decrease in the abundance of these proteins in embryogenic cultures of *A. angustifolia* indicates that inhibition of cell cycle affects ethylene biosynthesis, whereas an increased GST may be correlated with increased oxidative stress.

4.2.4.3 Oxidation-reduction process

In this study, we identified 34 proteins up-regulated and 17 down-regulated that were involved in the oxidation-reduction process in the AaMps1 inhibition treatment (Table 1). The oxidative burst may represent a key factor for obtaining embryogenic competence (Sun et al., 2013), since the initial stages of embryogenesis in plants are characterized by intense metabolic activity, high cell division rates, and increased production of reactive oxygen species (ROS) (Dos Santos et al., 2016). In *A. angustifolia* it has been observed that the cell lines with higher potential to generate somatic embryos produce higher levels of endogenous ROS compared with other cell lines (Jo et al., 2014).

The ROS-scavenging system is responsible for removing the excessive ROS and protecting the embryogenic cell cultures from its toxicity (Sun et al., 2013). The GST protein conjugates glutathione to a variety of substrates. The protein is associated with 'response to ROS' and acts by ensuring the correct development of the somatic embryo and protecting it against the oxidative stress caused by byproducts of the cellular metabolism (Galland et al., 2007; Dos Santos et al., 2016). Additionally, GST together with AO and DHAR makes part of an integrated network that interacts strongly with ROS (Maldonado-Cervantes et al., 2014). In *A. thaliana,* changes in the endogenous ascorbate redox status accelerate cell proliferation during the induction phase and improve the maturation of somatic embryos (Becker et al., 2014). In *A. angustifolia,* the presence of DHAR was more abundant and was related to cell cultures with more embryogenic potential (Jo et al., 2014; Dos Santos et al., 2016). In our work, a larger amount of proteins with oxidation-reduction process function were up-regulated with AaMps1 inhibition (Table 1). Thus, differently of less embryogenic cells, the increasing abundance of these proteins in embryogenic cultures may be associated with a more efficient enzymatic apparatus that regulates the cellular redox homeostasis and the ROS-induced signal transduction (Dos Santos et al., 2016).

4.2.4.4 Folding Proteins

The alterations caused by the AaMps1 inhibition treatment also affected the abundance of proteins with folding function. The probable prefoldin subunit 3, grpE homolog, and one heat shock 83-like proteins were up-regulated in the presence of the Mps1 inhibitor (Table 1). Others, such as thioredoxin m isoform 2, peptidyl-prolyl cis-trans isomerase, two heat shock cognate 70 kDa 2, and two heat shock 83-like, were more abundant in proliferating cells (control) (Table 1).

Heat shock proteins (HSPs) are molecular chaperones that regulate the folding, localization, accumulation, and degradation of proteins, thus playing a broad role in many cellular processes and helping cells to cope with multiple environmental stresses (Feder and Hofmann, 1999). These proteins have essential functions in preventing aggregation, by binding to denatured proteins, forcing their refolding to a native conformation, and assisting refolding of non-native proteins under stress conditions (Bechtold et al., 2008) (Feder and Hofmann, 1999). In maize, the HSP70 protein, one of many families of these proteins, showed variation in the expression levels at different developmental stages in different organs of maize plants. Differently, the HSP83 protein was not detected in specific organs and in any developmental stage, but in other species it was detected during a biotic stress response to an infection (Horst et al., 2010). This suggests that the HSP83 transcription is activated as a specific signal response to this type of stress (Pegoraro et al., 2011).

In conjunction with chaperones, the activity of PPIases also assists in folding of newly synthesized proteins. These proteins bind to isomerization peptidyl prolyl, ensuring a proper folding of the proteins. This occurs because the cis to trans isomerization of peptide bonds is essential, since cis-proline introduces bends within a protein, decreasing its stability. PPIases are the only enzymes known for stabilizing this cis-trans transition, lowering the activation energy of the stabilized product and accelerating the isomerization process (Fischer et al., 1989; Kaur et al., 2015). In addition, the activity of PPIases ensure the rescue of denatured proteins during stress conditions (Mainali et al., 2014). These proteins were down-regulated in embryogenic cells with Mps1 inhibited (Table 1), suggesting that the inhibition of cell division reduces the abundance of this protein, which means it must not be necessary when the cultures of *A. angustifolia* is not in proliferative phase. Modulation of this protein shows that a

folding and refolding apparatus are necessary for newly synthesized proteins during cell division. Even when the cells are not in active proliferative stage, these proteins are important mainly for preventing aggregation and denaturation of proteins.

4.2.4.5 Regulation of biological process

In this study, two proteins of PCNA were identified, being one up- and other dow-regulated (Table 1). The PCNA is a recognized master coordinator protein of cellular responses to DNA damage, and interacts with numerous DNA repair, cell-cycle control, and DNA replication proteins (Kimura et al., 2001; Strzalka et al., 2010; Yu et al., 2015). In eukaryotes, PCNA performs its function directly by interacting with several proteins involved in DNA repair. And although DNA polymerases are engaged in DNA synthesis during DNA replication and repair, these interactions may also occur between factors required in the steps prior to DNA synthesis(Strzalka and Ziemienowicz, 2011). PCNA can positively or negatively control the progression of the cell cycle, because the interaction with other factors that prevents inappropriate homologous recombination, allows for sister-chromatid cohesion (Strzalka and Ziemienowicz, 2011). In cell cultures of rice, the use of inhibitors holding the cells in S phase prevent DNA elongation, which causes an increase in the abundance of PCNA, while the M phase arrested cells showed no differences in the abundance of this protein (Kimura et al., 2001). The difference in the abundance of this protein in the treatment with the Mps1 inhibitor in *A. angustifolia* (Table 1) may be associated with the presence of more than one PCNA gene in plants. Duplicated PCNA genes seem to have slightly different functions. One gene encodes the main PCNA protein and shows all, or nearly all, the features that are characteristic to the PCNA protein, whereas a second gene is most likely to be involved in some aspects of the cell response to DNA-damaging factors. However, the exact

function of the second PCNA gene in both animal and plant cells remains to be discovered (Strzalka and Ziemienowicz, 2011).

In conclusion, the inhibition of AaMps1 in the embryogenic cultures of *A. angustifolia* had an effect in modulating the abundance of important proteins for the development of somatic embryogenesis, such as LEAs proteins. Proteins related to cell development process were up-regulated in the AaMps1 inhibition treatment, whereas those related to proliferating and DNA synthesis proteins were down-regulated. Proteins involved in folding and oxidation-reduction process was also modulated, indicating that they may be the key mechanisms influencing the embryogenic potential of the cultures.

4.2.5 References

Al-Madhoun, A. S.; Sanmartin, M. and Kanellis, A. K. 2003. Expression of ascorbate oxidase isoenzymes in cucurbits and during development and ripening of melon fruit. **Postharvest Biology and Technology**, v. 27, n. 2, p. 137-146.

Balbuena, T. S.; Silveira, V.; Junqueira, M.; Dias, L. L. C.; Santa-Catarina, C.; Shevchenko, A. and Floh, E. I. S. 2009. Changes in the 2-DE protein profile during zygotic embryogenesis in the Brazilian Pine (*Araucaria angustifolia*). **Journal of Proteomics**, v. 72, n. 3, p. 337-352.

Bechtold, U.; Richard, O.; Zamboni, A.; Gapper, C.; Geisler, M.; Pogson, B.; Karpinski, S. and Mullineaux, P. M. 2008. Impact of chloroplastic-and extracellular-sourced ROS on high light-responsive gene expression in Arabidopsis. **Journal of Experimental Botany**, v. 59, n. 2, p. 121-133.

Becker, M. G.; Chan, A.; Mao, X.; Girard, I. J.; Lee, S.; Mohamed, E.; Stasolla, C. and Belmonte, M. F. 2014. Vitamin C deficiency improves somatic embryo development through distinct gene regulatory networks in Arabidopsis. **Journal of Experimental Botany**, p. eru330.

Becwar, M. R.; Noland, T. L. and Wyckoff, J. L. 1989. Maturation, germination, and conversion of Norway spruce (*Picea abies L.*) somatic embryos to plants. **In vitro cellular & developmental biology**, v. 25, n. 6, p. 575-580.

Calderan-Rodrigues, M. J.; Jamet, E.; Bonassi, M. B. C. R.; Guidetti-Gonzalez, S.; Begossi, A. C.; Setem, L. V.; Franceschini, L. M.; Fonseca, J. G. and Labate, C. A. 2014. Cell wall proteomics of sugarcane cell suspension cultures. **Proteomics**, v. 14, n. 6, p. 738-749.

Chen, Z. and Gallie, D. R. 2006. Dehydroascorbate reductase affects leaf growth, development, and function. **Plant Physiology**, v. 142, n. 2, p. 775-787.

Conesa, A.; Götz, S.; García-Gómez, J. M.; Terol, J.; Talón, M. and Robles, M. 2005. Blast2GO: a universal tool for annotation, visualization and analysis in functional genomics research. **Bioinformatics**, v. 21, n. 18, p. 3674-3676.

De Oliveira, E. A.; Romeiro, N. C.; Ribeiro Eda, S.; Santa-Catarina, C.; Oliveira, A. E.; Silveira, V.; De Souza Filho, G. A.; Venancio, T. M. and Cruz, M. A. 2012. Structural and functional characterization of the protein kinase Mps1 in *Arabidopsis thaliana*. **PloS ONE**, v. 7, n. 9, p. 45707.

Dos Santos, A. L. W.; Elbl, P.; Navarro, B. V.; De Oliveira, L. F.; Salvato, F.; Balbuena, T. S. and Floh, E. I. S. 2016. Quantitative proteomic analysis of *Araucaria angustifolia* (Bertol.) Kuntze cell lines with contrasting embryogenic potential. **Journal of Proteomics**, v. 130, p. 180-189.

Douetts-Peres, J. C.; Cruz, M. A.; Reis, R. S.; Heringer, A. S.; De Oliveira, E. A.; Elbl, P. M.; Floh, E. I.; Silveira, V. and Santa-Catarina, C. 2016. Mps1 (Monopolar Spindle 1) Protein Inhibition Affects Cellular Growth and Pro-Embryogenic Masses Morphology in Embryogenic Cultures of *Araucaria angustifolia* (Araucariaceae). **PloS ONE**, v. 11, n. 4.

Dure, L.; Greenway, S. C. and Galau, G. A. 1981. Developmental biochemistry of cottonseed embryogenesis and germination - changing messenger ribonucleic-acid populations as shown by invitro and in vivo protein-synthesis. **Biochemistry**, v. 20, n. 14, p. 4162-4168.

Dutra, N. T.; Silveira, V.; De Azevedo, I. G.; Gomes-Neto, L. R.; Facanha, A. R.; Steiner, N.; Guerra, M. P.; Floh, E. I. S.; Santa-Catarina, C. Polyamines affect the cellular growth and structure of pro-embryogenic masses in Araucaria angustifolia embryogenic cultures through the modulation of proton pump activities and endogenous levels of polyamines. 2013. **Physiologia Plantarum**, v. 148, n. 1, p. 121-132.

Elbl, P.; Lira, B. S.; Andrade, S. C. S.; Jo, L.; Dos Santos, A. L. W.; Coutinho, L. L.; Floh, E. I. S. and Rossi, M. 2015. Comparative transcriptome analysis of early somatic embryo formation and seed development in Brazilian pine, *Araucaria angustifolia* (Bertol.) Kuntze. **Plant Cell, Tissue and Organ Culture**, v. 120, n. 3, p. 903-915.

Esaka, M.; Fujisawa, K.; Goto, M. and Kisu, Y. 1992. Regulation of ascorbate oxidase expression in pumpkin by auxin and copper. **Plant Physiology**, v. 100, n. 1, p. 231-237.

Farias-Soares, F. L.; Steiner, N.; Schmidt, E. C.; Pereira, M. L. T.; Rogge-Renner, G. D.; Bouzon, Z. L.; Floh, E. S. I.; Guerra, M. P. 2014. The transition of proembryogenic masses to somatic embryos in *Araucaria angustifolia* (Bertol.) Kuntze is related to the endogenous contents of IAA, ABA and polyamines. **Acta Physiologiae Plantarum**, v. 36, n. 7, p. 1853-1865.

Feder, M. E. and Hofmann, G. E. 1999. Heat-shock proteins, molecular chaperones, and the stress response: evolutionary and ecological physiology. **Annual Review of Physiology**, v. 61, n. 1, p. 243-282.

Fischer, G.; Wittmann-Liebold, B.; Lang, K.; Kiefhaber, T. and Schmid, F. X. 1989. Cyclophilin and peptidyl-prolyl cis-trans isomerase are probably identical proteins. p. 476-478.

Forsburg, S. L. 2004. Eukaryotic MCM proteins: beyond replication initiation. **Microbiology and Molecular Biology Reviews**, v. 68, n. 1, p. 109-131.

Fraga, H. P.; Vieira, L. N.; Heringer, A. S.; Puttkammer, C. C.; Silveira, V. and Guerra, M. P. 2016. DNA methylation and proteome profiles of *Araucaria angustifolia* (Bertol.) Kuntze embryogenic cultures as affected by plant growth regulators supplementation. **Plant Cell, Tissue and Organ Culture (PCTOC)**, v. 125, n. 2, p. 353-374.

Galland, R.; Blervacq, A.-S.; Blassiau, C.; Smagghe, B.; Decottignies, J.-P. and Hilbert, J.-L. 2007. Glutathione-S-transferase is detected during somatic embryogenesis in chicory. **Plant Signal Behav**, v. 2, n. 5, p. 343-348.

Ghosh, S. and Pal, A. 2012. Identification of differential proteins of mungbean cotyledons during seed germination: a proteomic approach. **Acta Physiologiae Plantarum**, v. 34, n. 6, p. 2379-2391.

Gonzalez-Reyes, J. A.; Hidalgo, A.; Caler, J. A.; Palos, R. and Navas, P. 1994. Nutrient uptake changes in ascorbate free radical-stimulated onion roots. **Plant Physiology**, v. 104, n. 1, p. 271-276.

Guan, Y.; Li, S.-G.; Fan, X.-F. and Su, Z.-H. 2016. Application of Somatic Embryogenesis in Woody Plants. **Frontiers in Plant Science**, v. 7.

Heringer, A. S.; Barroso, T.; Macedo, A. F.; Santa-Catarina, C.; Souza, G. H. M. F.; Floh, E. I. S.; De Souza-Filho, G. A. and Silveira, V. 2015. Label-Free Quantitative Proteomics of Embryogenic and Non-Embryogenic Callus during Sugarcane Somatic Embryogenesis. **PloS ONE**, v. 10, n. 6, p. e0127803.

Holding, D. R. and Springer, P. S. 2002. The Arabidopsis gene PROLIFERA is required for proper cytokinesis during seed development. **Planta**, v. 214, n. 3, p. 373-382.

Horst, R. J.; Doehlemann, G.; Wahl, R.; Hofmann, J.; Schmiedl, A.; Kahmann, R.; Kämper, J.; Sonnewald, U. and Voll, L. M. 2010. Ustilago maydis infection strongly alters organic nitrogen allocation in maize and stimulates productivity of systemic source leaves. **Plant Physiology**, v. 152, n. 1, p. 293-308.

Huang, H.; Møller, I. M. and Song, S.-Q. 2012. Proteomics of desiccation tolerance during development and germination of maize embryos. **Journal of Proteomics**, v. 75, n. 4, p. 1247-1262.

Jo, L.; Dos Santos, A. L.; Bueno, C. A.; Barbosa, H. R. and Floh, E. I. 2014. Proteomic analysis and polyamines, ethylene and reactive oxygen species levels of *Araucaria angustifolia* (Brazilian pine) embryogenic cultures with different embryogenic potential. **Tree Physiology**, v. 34, n. 1, p. 94-104.

Kato, N. and Esaka, M. 1996. cDNA cloning and gene expression of ascorbate oxidase in tobacco. **Plant Molecular Biology**, v. 30, n. 4, p. 833-837.

Kato, N. and Esaka, M. 2000. Expansion of transgenic tobacco protoplasts expressing pumpkin ascorbate oxidase is more rapid than that of wild-type protoplasts. **Planta**, v. 210, n. 6, p. 1018-1022.

Kaur, G.; Singh, S.; Singh, H.; Chawla, M.; Dutta, T.; Kaur, H.; Bender, K.; Snedden, W.; Kapoor, S. and Pareek, A. 2015. Characterization of Peptidyl-Prolyl Cis-Trans

Isomerase-and Calmodulin-Binding Activity of a Cytosolic *Arabidopsis thaliana* Cyclophilin AtCyp19-3. **PloS ONE**, v. 10, n. 8, p. e0136692.

Kimura, S.; Suzuki, T.; Yanagawa, Y.; Yamamoto, T.; Nakagawa, H.; Tanaka, I.; Hashimoto, J. and Sakaguchi, K. 2001. Characterization of plant proliferating cell nuclear antigen (PCNA) and flap endonuclease-1 (FEN-1), and their distribution in mitotic and meiotic cell cycles. **The Plant Journal**, v. 28, n. 6, p. 643-653.

Kuga, T.; Sasaki, M.; Mikami, T.; Miake, Y.; Adachi, J.; Shimizu, M.; Saito, Y.; Koura, M.; Takeda, Y. and Matsuda, J. 2016. FAM83H and casein kinase I regulate the organization of the keratin cytoskeleton and formation of desmosomes. **Scientific Reports**, v. 6.

Leljak-Levanić, D.; Mihaljević, S. and Bauer, N. 2015. Somatic and zygotic embryos share common developmental features at the onset of plant embryogenesis. **Acta Physiologiae Plantarum**, v. 37, n. 7, p. 1-14.

Lin, L.-S. and Varner, J. E. 1991. Expression of ascorbic acid oxidase in zucchini squash (*Cucurbita pepo* L.). **Plant Physiology**, v. 96, n. 1, p. 159-165.

Lu, J.; Vahala, J. and Pappinen, A. 2011. Involvement of ethylene in somatic embryogenesis in Scots pine (*Pinus sylvestris* L.). **Plant Cell, Tissue and Organ Culture (PCTOC)**, v. 107, n. 1, p. 25-33.

Mahdavi-Darvari, F.; Noor, N. M. and Ismanizan, I. 2015. Epigenetic regulation and gene markers as signals of early somatic embryogenesis. **Plant Cell, Tissue and Organ Culture**, v. 120, n. 2, p. 407-422.

Mainali, H. R.; Chapman, P. and Dhaubhadel, S. 2014. Genome-wide analysis of Cyclophilin gene family in soybean (*Glycine max*). **Bmc Plant Biology**, v. 14, n. 1, p. 1.

Maldonado-Cervantes, E.; Huerta-Ocampo, J. A.; Montero-Morán, G. M.; Barrera-Pacheco, A.; Espitia-Rangel, E. and De La Rosa, A. P. B. 2014. Characterization of *Amaranthus cruentus* L. seed proteins by 2-DE and LC/MS–MS: Identification and cloning of a novel late embryogenesis-abundant protein. **Journal of Cereal Science**, v. 60, n. 1, p. 172-178.

Meskaoui, A. E. and Tremblay, F. M. 2001. Involvement of ethylene in the maturation of black spruce embryogenic cell lines with different maturation capacities. **Journal of Experimental Botany**, v. 52, n. 357, p. 761-769.

Micol-Ponce, R.; Sánchez-García, A. B.; Xu, Q.; Barrero, J. M.; Micol, J. L. and Ponce, M. R. 2015. Arabidopsis INCURVATA2 regulates salicylic acid and abscisic acid signaling, and oxidative stress responses. **Plant and Cell Physiology**, v. 56, n. 11, p. 2207-2219.

Musacchio, A. and Salmon, E. D. 2007. The spindle-assembly checkpoint in space and time. **Nature reviews Molecular cell biology**, v. 8, n. 5, p. 379-393.

Nanjo, Y.; Skultety, L.; UváČKová, L. U.; Klubicová, K. N.; Hajduch, M. and Komatsu, S. 2011. Mass spectrometry-based analysis of proteomic changes in the root tips of flooded soybean seedlings. **Journal of Proteome Research**, v. 11, n. 1, p. 372-385.

Noah, A. M.; Niemenak, N.; Sunderhaus, S.; Haase, C.; Omokolo, D. N.; Winkelmann, T. and Braun, H.-P. 2013. Comparative proteomic analysis of early somatic and zygotic embryogenesis in *Theobroma cacao* L. **Journal of Proteomics**, v. 78, p. 123-133.

Pegoraro, C.; Mertz, L.; Maia, L.; Rombaldi, C. and Oliveira, A. 2011. Importance of heat shock proteins in maize. **Journal of Crop Science and Biotechnology**, v. 14, n. 2, p. 85-95.

Perera, R. L.; Torella, R.; Klinge, S.; Kilkenny, M. L.; Maman, J. D. and Pellegrini, L. 2013. Mechanism for priming DNA synthesis by yeast DNA Polymerase α. **Elife**, v. 2, p. e00482.

Reis, R. S.; De Moura Vale, E.; Heringer, A. S.; Santa-Catarina, C. and Silveira, V. 2016. Putrescine induces somatic embryo development and proteomic changes in embryogenic callus of sugarcane. **Journal of Proteomics**, v. 130, p. 170-179.

Rizvi, I.; Choudhury, N. R. and Tuteja, N. 2016. *Arabidopsis thaliana* MCM3 single subunit of MCM2–7 complex functions as 3′ to 5′ DNA helicase. **Protoplasma**, v. 253, n. 2, p. 467-475.

Rode, C.; Lindhorst, K.; Braun, H.-P. and Winkelmann, T. 2012. From callus to embryo: a proteomic view on the development and maturation of somatic embryos in *Cyclamen persicum*. **Planta**, v. 235, n. 5, p. 995-1011.

Sabetta, W.; Vannini, C.; Sgobba, A.; Marsoni, M.; Paradiso, A.; Ortolani, F.; Bracale, M.; Viggiano, L.; Blanco, E. and De Pinto, M. C. 2016. Cyclic AMP deficiency negatively affects cell growth and enhances stress-related responses in tobacco Bright Yellow-2 cells. **Plant Molecular Biology**, v. 90, n. 4-5, p. 467-483.

Santa-Catarina, C.; Silveira, V.; Guerra, M. P.; Steiner, N.; Macedo, A. F.; Floh, E. I. S. and Dos Santos, A. L. W. 2013. The use of somatic embryogenesis for mass clonal propagation and biochemical and physiological studies in woody plants. **Plant Biology**, v. 13, p. 103-119.

Saruhan, N.; Terzi, R.; Saglam, A. and Kadioglu, A. 2009. The relationship between leaf rolling and ascorbate-glutathione cycle enzymes in apoplastic and symplastic areas of *Ctenanthe setosa* subjected to drought stress. **Biological research**, v. 42, n. 3, p. 315-326.

Sharifi, G.; Ebrahimzadeh, H.; Ghareyazie, B.; Gharechahi, J. and Vatankhah, E. 2012. Identification of differentially accumulated proteins associated with embryogenic and non-embryogenic calli in saffron (*Crocus sativus* L.). **Proteome Science**, v. 10, n. 1, p. 1.

Silveira, V.; Santa-Catarina, C.; Tun, N. N.; Scherer, G. F. E.; Handro, W.; Guerra, M. P.; Floh, E. I. S. 2006. Polyamine effects on the endogenous polyamine contents, nitric oxide release, growth and differentiation of embryogenic suspension cultures of Araucaria angustifolia (Bert.) O. Ktze. **Plant Science,** v. 171, n. 1, p. 91-98.

Stasolla, C. 2010. Glutathione redox regulation of in vitro embryogenesis. **Plant Physiology and Biochemistry**, v. 48, n. 5, p. 319-327.

Steiner, N.; Farias-Soares, F. L.; Schmidt, É. C.; Pereira, M. L.; Scheid, B.; Rogge-Renner, G. D.; Bouzon, Z. L.; Schmidt, D.; Maldonado, S. and Guerra, M. P. 2015. Toward

establishing a morphological and ultrastructural characterization of proembryogenic masses and early somatic embryos of *Araucaria angustifolia* (Bert.) O. Kuntze. **Protoplasma**, p. 1-15.

Steiner, N.; Vieira, F. D. N.; Maldonado, S. and Guerra, M. P. 2005. Effect of carbon source on morphology and histodifferentiation of *Araucaria angustifolia* embryogenic cultures. **Brazilian Archives of Biology and Technology**, v. 48, n. 6, p. 895-903.

Strzalka, W.; Kaczmarek, A.; Naganowska, B. and Ziemienowicz, A. 2010. Identification and functional analysis of PCNA1 and PCNA-like1 genes of Phaseolus coccineus. **Journal of Experimental Botany**, v. 61, n. 3, p. 873-888.

Strzalka, W. and Ziemienowicz, A. 2011. Proliferating cell nuclear antigen (PCNA): a key factor in DNA replication and cell cycle regulation. **Annals of Botany**, v. 107, n. 7, p. 1127-1140.

Sun, L.; Wu, Y.; Zou, H.; Su, S.; Li, S.; Shan, X.; Xi, J. and Yuan, Y. 2013. Comparative proteomic analysis of the H99 inbred maize (*Zea mays* L.) line in embryogenic and non-embryogenic callus during somatic embryogenesis. **Plant Cell, Tissue and Organ Culture**, v. 113, n. 1, p. 103-119.

Vale, E. M.; Heringer, A. S.; Barroso, T.; Ferreira, A. T.; Da Costa, M. N.; Perales, J. E. A.; Santa-Catarina, C. and Silveira, V. 2014. Comparative proteomic analysis of somatic embryo maturation in Carica papaya L. **Proteome Science**, v. 12, n. 1, p. 37.

Yang, X. and Zhang, X. 2010. Regulation of somatic embryogenesis in higher plants. **Critical Reviews in Plant Science**, v. 29, n. 1, p. 36-57.

Yu, Y.; Zhang, G.; Zhang, J.; Ju, L.; Zhu, Q.; Song, Y.; Wang, J.; Niu, N. and Ma, S. 2015. Molecular cloning and characterization of a proliferating cell nuclear antigen gene by chemically induced male sterility in wheat (*Triticum aestivum* L.). **Genetics and molecular research: GMR**, v. 14, n. 4, p. 12030-12042.

Zhang, J.; Ma, H.; Chen, S.; Ji, M.; Perl, A.; Kovacs, L. and Chen, S. 2009. Stress response proteins' differential expression in embryogenic and non-embryogenic callus of *Vitis vinifera* L. cv. Cabernet Sauvignon - a proteomic approach. **Plant Science**, v. 177, n. 2, p. 103-113.

5 CONSIDERAÇÕES GERAIS

A partir deste estudo foi possível identificar e caracterizar a proteína Mps1 de células embriogênicas de *A. angustifolia* mantidas em suspensão, descritas no Capítulo 1. A Mps1 de *A. angustifolia* (AaMps1) possui homologia com a Mps1 de humanos e com a Mps1 de várias espécies vegetais (Figuras 1, 2, 3, 4 e 5, capítulo 1). Embora a AaMps1 possua uma maior semelhança com a Mps1 de uma espécie angiosperma ancestral (*A. Trichopoda*) (Figura 2, capítulo 1), esta proteína quinase possui características como sitio catalítico, sítios de fosforilação, regiões de interação e ligação com outras proteínas altamente conservadas entre várias espécies vegetais (Figura 3). Este resultado é inédito e importante, por ter sido a primeira vez reportado esta proteína em uma gimnosperma, mostrando a importância evolutiva da mesma. Ademais, a identificação a partir do banco de dados de transcriptoma de Araucaria (Elbl et al., 2015a; Elbl et al., 2015b) foi fundamental para a caracterização da AaMps1.

Uma vez identificada, objetivou-se verificar o efeito da inibição desta proteína sobre o crescimento (Figuras 7 e 8, capítulo 1) e morfologia (Figuras 9 e 10, capítulo 1) das culturas embriogênicas de *A. angustifolia*. Durante o ciclo de multiplicação das culturas embriogênicas, sem o tratamento com o inibidor, verificou-se que a abundância da proteína AaMps1 aumentou na fase de crescimento exponencial (Figura 12, capítulo 1). Por outro lado, nas culturas embriogênicas tratadas com o inibidor da Mps1, ocorreu a inibição do crescimento das culturas embriogênicas (Figuras 7 e 8, capítulo 1) e alteração na morfologia das PEMs (Figura 9, capítulo 1). A abundância da AaMps1 (Figura 12, capítulo 1) foi menor comparativamente ao controle. Desta forma, estes resultados mostram que a inibição da AaMps1 provocou uma redução no crescimento celular das culturas embriogênicas, demostrando a influência desta

proteína na proliferação celular. A morfologia das PEMs também foi afetada pela inibição da AaMps1, a área da cabeça embriogênica e das células do suspensor foram reduzidas (Figura 10, capítulo 1), porém quando avaliadas separadamente, somente o comprimento das células do suspensor foi reduzido (Figura 10, capítulo 1) pela presença do inibidor. Desta forma, é evidente que a proteína AaMps1 é importante para a progressão do ciclo celular em culturas embriogênicas de *A. angustifolia,* e alterações na abundancia desta proteína causadas pelo inibidor da Mps1 sugerem que, nas culturas tratadas, o ciclo celular esteja bloqueado influenciando assim o desenvolvimento das culturas embriogênicas.

Posteriormente, objetivou-se verificar a influência da inibição desta proteína sobre a abundância de proteínas em culturas embriogênicas de *A. angustifolia* não tratadas (controle) e tratadas com inibidor da Msp1, cujos resultados foram descritos no capítulo 2. Neste sentido, procedeu-se a análise das proteínas afetadas pela inibição da AaMps1 (Figuras 1 e 2, capítulo 2), sendo identificadas, por espectrometria de massas via *Shotgun*, um total de 1977 proteínas, sendo destas 229 up- e 218 down-reguladas (Figura 1, capítulo 2).

Das proteínas com abundância diferencial entre os tratamentos, verificou-se que classes de proteínas relacionadas com processos de desenvolvimento, organização do citoesqueleto, expansão celular e proteção contra dessecação (como as proteínas LEAs) foram up-reguladas nas culturas embriogênicas com a AaMps1 inibida, no tratamento com inibidor da Mps1 (Tabela 1, capítulo 2). Estas classes de proteínas estão relacionadas com células embriogênicas que apresentam maior competência para formação de embriões, conforme demonstrado em estudos com calos de cana de açúcar (Reis et al., 2016). Desta forma, é sugerido que a inibição do crescimento das culturas embriogênicas quando submetidas à fase de maturação pode ser uma etapa

crucial para aquisição da competência, pela expressão de proteínas importantes, que promovem o desenvolvimento das PEMs em embriões somáticos. Em contra partida, proteínas envolvidas com a fase de multiplicação das culturas embriogênicas, e abundantes na fase de intensa divisão (no controle) foram down-reguladas com a utilização do inibidor da Mps1 (Tabela 1, capítulo 2). As proteínas envolvidas no processo de enovelamento e de oxidação-redução, também foram moduladas, indicando que estes podem ser os principais mecanismos que influenciam o potencial embriogênico nestas culturas.

Dentre as proteínas identificadas, e com padrão de abundancia diferencial, duas proteínas apresentaram grande diferença de abundância entre os tratamentos. A proteína caseina quinase I foi identificada somente nas culturas embriogênicas com a Mps1 inibida e a proteína ascorbato oxidase foi identificada up-regulada 101 vezes nestas células. A caseina quinase I mantem a formação dos desmossomos e tem um papel importante na formação do citoesqueleto, regulando a organização da queratina, enquanto que a ascorbato oxidase está correlacionada com a elongação e/ou expansão celular, estas funções podem ser importantes para a etapa de diferenciação das células na conversão de embriões somáticos.

A partir deste estudo pode-se perceber que a manipulação do ciclo celular, como a inibição da AaMps1, pode ser utilizada como ferramenta para auxiliar o entendimento do metabolismo e sinalização celular que atuam no desenvolvimento de embriões somáticos em *A. angustifolia*, bem como em sistemas de embriogênese somática em outras espécies.

6 CONCLUSÕES

A partir dos resultados obtidos neste estudo pode-se concluir que:

- ✓ A proteína Mps1 está presente em culturas embriogênicas de *A. angustifolia* (AaMps1), sendo a primeira vez que esta proteína foi identificada em uma espécie gimnosperma.
- ✓ A AaMps1 apresentou domínio quinase, sítios de interação com outras proteínas, sítios de fosforilação e resíduos de aminoácidos importantes para a sua função quinase.
- ✓ A AaMps1 é homóloga a proteínas Mps1 de outras espécies, incluindo o domínio quinase, altamente conservado nos eucariotos.
- ✓ A utilização do inibidor da Mps1 reduz a quantidade relativa da proteína AaMps1 após 15 dias de incubação em culturas embriogênicas de *A. angustifolia* mantidas em suspensão.
- ✓ O crescimento de culturas embriogênicas mantidas em suspensão, assim como, a morfologia das PEMs destas culturas, foram afetados pela inibição da AaMps1.
- ✓ A inibição da AaMps1 influenciou a abundancia das proteínas identificadas na fase de multiplicação das culturas embriogênicas de *A. angustifolia*.
- ✓ Proteínas que tem funções relacionadas com proliferação celular, progressão do ciclo celular e metabolismo de etileno foram Down-reguladas com a inibição da AaMps1.
- ✓ Proteínas que tem funções relacionadas com organização do citoesqueleto, ciclo ascorbato-glutationa, expansão celular e proteção contra a dessecação foram Up-reguladas com a inibição da AaMps1.

- ✓ Proteínas que tem funções relacionadas com enovelamento e processos de oxidação/redução foram moduladas com a inibição da AaMps1, sendo algumas Up-reguladas e outras Down-reguladas.

7 REFERÊNCIAS

Almeida, A. M.; Parreira, J. R.; Santos, R.; Duque, A. S.; Francisco, R.; Tomé, D. F.; Ricardo, C. P.; Coelho, A. V. and Fevereiro, P. 2012. A proteomics study of the induction of somatic embryogenesis in *Medicago truncatula* using 2DE and MALDI- TOF/TOF. **Physiologia Plantarum**, v. 146, n. 2, p. 236-249.

Andrade, J. B. D. R. 2010. Efeito dos agentes de maturação, ABA, PEG e maltose, na produção de óxido nítrico e de espécies reativas de oxigênio em culturas embriogênicas de *Araucaria angustifolia*. Dissertação (Mestrado). Departamento de Botânica, Universidade de São Paulo, São Paulo, 74p.

Aquila, M. E. A. and Ferreira, A. G. 1984. Germinação de sementes escarificadas de *Araucaria angustifolia* em solo. **Ciência e Cultura**, v. 36, n. 9, p. 1583-1590.

Astarita, L. V. 2000. Aspectos bioquímicos e fisiológicos da embriogênese zigótica e culturas celulares embriogênicas de *Araucaria angustifolia* (Bert.) O. KTZE. Tese (Doutorado). Instituto de Biociências, Universidade de São Paulo, São Paulo, 112p.

Balbuena, T. S. 2009. Proteômica do desenvolvimento da semente de *Araucaria angustifolia*. Tese (Doutorado). Departamento de Botânica, Universidade de São Paulo, São Paulo, 102p.

Balbuena, T. S.; Jo, L.; Pieruzzi, F. P.; Dias, L. L. C.; Silveira, V.; Santa-Catarina, C.; Junqueira, M.; Thelen, J. J.; Shevchenko, A. and Floh, E. I. S. 2011. Differential proteome analysis of mature and germinated embryos of *Araucaria angustifolia*. **Phytochemistry**, v. 72, n. 4-5, p. 302-311.

Bennett, B. L.; Sasaki, D. T.; Murray, B. W.; O'leary, E. C.; Sakata, S. T.; Xu, W.; Leisten, J. C.; Motiwala, A.; Pierce, S. and Satoh, Y. 2001. SP600125, an anthrapyrazolone inhibitor of Jun N-terminal kinase. **Proceedings of the National Academy of Sciences**, v. 98, n. 24, p. 13681-13686.

Binarová, P.; Doležel, J.; Draber, P.; Heberle-Bors, E.; Strnad, M. and Bögre, L. 1998. Treatment of *Vicia faba* root tip cells with specific inhibitors to cyclin- dependent kinases leads to abnormal spindle formation. **The Plant Journal**, v. 16, n. 6, p. 697-707.

Bunn, E.; Turner, S. R. and Dixon, K. W. 2011. Biotechnology for saving rare and threatened flora in a biodiversity hotspot. **In Vitro Cellular & Developmental Biology-Plant**, v. 47, n. 1, p. 188-200.

Campalans, A.; Pagès, M. and Messeguer, R. 2000. Protein analysis during almond embryo development. Identification and characterization of a late embryogenesis abundant protein. **Plant Physiology and Biochemistry**, v. 38, n. 6, p. 449-457.

Carvalho, P. E. R. 1994. **Espécies florestais brasileiras: Recomendações silviculturais, potencialidades e uso da madeira**. Colombo: EMBRAPA-CNPF/SPI, 639

Chu, M. L.; Chavas, L. M.; Douglas, K. T.; Eyers, P. A. and Tabernero, L. 2008. Crystal structure of the catalytic domain of the mitotic checkpoint kinase Mps1 in complex with SP600125. **Journal of Biological Chemistry**, v. 283, n. 31, p. 21495-21500.

Correia, S. I.; Alves, A. C.; Veríssimo, P. and Canhoto, J. M. 2016. Somatic Embryogenesis in Broad-Leaf Woody Plants: What We Can Learn from Proteomics. **In Vitro Embryogenesis in Higher Plants**, p. 117-129.

De Oliveira, E. a. G.; Romeiro, N. C.; Da Silva Ribeiro, E.; Santa-Catarina, C.; Oliveira, A. E. A.; Silveira, V.; De Souza Filho, G. A.; Venancio, T. M. and Cruz, M. a. L. 2012. Structural and functional characterization of the protein kinase Mps1 in *Arabidopsis thaliana*. **Plos One**, v. 7, n. 9, p. e45707.

Dewitte, W. and Murray, J. A. 2003. The plant cell cycle. **Annual review of plant biology**, v. 54, n. 1, p. 235-264.

Dos Santos, A. L. W.; Elbl, P.; Navarro, B. V.; De Oliveira, L. F.; Salvato, F.; Balbuena, T. S. and Floh, E. I. S. 2016. Quantitative proteomic analysis of *Araucaria angustifolia* (Bertol.) Kuntze cell lines with contrasting embryogenic potential. **Journal of Proteomics**, v. 130, p. 180-189.

Douétts-Peres, J. C. 2013. Aspectos morfológicos e bioquímicos durante o controle do ciclo celular na embriogênese somática em *Araucaria angustifólia* (Bert.) O. Ktze. Dissertação de Mestrado Centro de Biociências e Biotecnologia, Universidade Estadual do Norte Fluminense - Darcy Ribeiro, Rio de Janeiro, 74p.

Elbl, P.; Campos, R.; Lira, B.; Andrade, S.; Jo, L.; Dos Santos, A.; Coutinho, L.; Floh, E. and Rossi, M. 2015a. Erratum to: Comparative transcriptome analysis of early somatic embryo formation and seed development in Brazilian pine, Araucaria angustifolia (Bertol.) Kuntze. **Plant Cell, Tissue and Organ Culture**, v. 120, n. 3, p. 917-917.

Elbl, P.; Lira, B. S.; Andrade, S. C. S.; Jo, L.; Dos Santos, A. L. W.; Coutinho, L. L.; Floh, E. I. S. and Rossi, M. 2015b. Comparative transcriptome analysis of early somatic embryo formation and seed development in Brazilian pine, *Araucaria angustifolia* (Bertol.) Kuntze. **Plant Cell, Tissue and Organ Culture**, v. 120, n. 3, p. 903-915.

FAO. 1986. Food And Agriculture Organization. Databook on endangered tree and shrub species and provenances. Rome. V. 77, p. 524.

Farias-Soares, F. L.; Burrieza, H. P.; Steiner, N.; Maldonado, S. and Guerra, M. P. 2013. Immunoanalysis of dehydrins in *Araucaria angustifolia* embryos. **Protoplasma**, v. 250, n. 4, p. 911-918.

Farias-Soares, F. L.; Steiner, N.; Schmidt, E. C.; Pereira, M. L. T.; Rogge-Renner, G. D.; Bouzon, Z. L.; Floh, E. S. I. and Guerra, M. P. 2014. The transition of proembryogenic masses to somatic embryos in *Araucaria angustifolia* (Bertol.) Kuntze is related to the endogenous contents of IAA, ABA and polyamines. **Acta Physiologiae Plantarum**, v. 36, n. 7, p. 1853-1865.

Farrant, J.; Pammenter, N. and Berjak, P. 1989. Germination-associated events and the desiccation sensitivity of recalcitrant seeds—a study on three unrelated species. **Planta**, v. 178, n. 2, p. 189-198.

Fisk, H. A. and Winey, M. 2004. Spindle regulation: Mps1 flies into new areas. **Current Biology**, v. 14, n. 24, p. R1058-R1060.

Fraga, H. P.; Vieira, L. N.; Heringer, A. S.; Puttkammer, C. C.; Silveira, V. and Guerra, M. P. 2016. DNA methylation and proteome profiles of *Araucaria angustifolia* (Bertol.) Kuntze embryogenic cultures as affected by plant growth regulators supplementation. **Plant Cell, Tissue and Organ Culture (PCTOC)**, v. 125, n. 2, p. 353-374.

Guan, Y.; Li, S.-G.; Fan, X.-F. and Su, Z.-H. 2016. Application of Somatic Embryogenesis in Woody Plants. **Frontiers in plant science**, v. 7.

Guerra, M. P.; Silveira, V.; Dos Santos, A. L. W.; Astarita, L. V. and Nodari, R. O. 2000. Somatic embryogenesis in *Araucaria angustifolia*. In: JAIN, S.;P, G.*, et al* (Ed.). **Somatic Embryogenesis in Woody Plants**. 1. Dordrecht: Kluwer Academics Publishers, v.6 p.457-478.

Guerra, M. P.; Steiner, N.; Mantovani, A.; Nodari, R. O.; Dos Reis, M. S. and Dos Santos, K. L. 2008. **Origem e Evolução de Plantas Cultivadas.** Brasília: Embrapa Informação Tecnológica, 149-184

IBAMA. 1992. Lista oficial de espécies da flora brasileira ameaçadas de extinção. Instituto Brasileiro do Meio Ambiente e dos Recursos Naturais Renováveis. Diário Oficial da União. Portaria IBAMA n.06 N. Brasília. p. 870-872.

Inze, D. and De Veylder, L. 2006. Cell cycle regulation in plant development. **Annu Rev Genet**, v. 40, p. 77-105.

IUCN. 2015. International Union for Conservation of Nature (IUCN) red list of threatened species. Version 2014.3. . Disponível em: < http://www.iucnredlist.org >. Acesso em: 02/09/2016.

Jelluma, N.; Brenkman, A. B.; Van Den Broek, N. J.; Cruijsen, C. W.; Van Osch, M. H.; Lens, S.; Medema, R. H. and Kops, G. J. 2008. Mps1 phosphorylates Borealin to control Aurora B activity and chromosome alignment. **Cell**, v. 132, n. 2, p. 233-246.

Jo, L.; Dos Santos, A. L.; Bueno, C. A.; Barbosa, H. R. and Floh, E. I. 2014. Proteomic analysis and polyamines, ethylene and reactive oxygen species levels of *Araucaria angustifolia* (Brazilian pine) embryogenic cultures with different embryogenic potential.**Tree Physiology**, v. 34, n. 1, p. 94-104.

Koch, Z. and Corrêa, M. S. 2002. **Araucária: a floresta do Brasil meridional**. Olhar brasileiro, 148

Lan, W. and Cleveland, D. W. 2010. A chemical tool box defines mitotic and interphase roles for Mps1 kinase. **The Journal of Cell Biology**, v. 190, n. 1, p. 21-24.

Lehninger, A. L.; Nelson, D. L. and Cox, M. M. 2002. **Princípios de bioquímica**. Omega, p. 1152

Leite, P. F. and Klein, R. M. 1990. Vegetação. **Geografia do Brasil: região sul**, v. 2, p. 113-150.

Liu, X. and Winey, M. 2012. The MPS1 family of protein kinases. **Annual Review of Biochemistry**, v. 81, p. 561-85.

Longhi, S. J. 1980. A estrutura de uma floresta natural de *Araucaria angustifoli*a (Bert.) O. Ktze, no sul do Brasil. Dissertação de Mestrado Ciências Florestais, Universidade Federal do Paraná, Curitiba, 198 p.

Merkle, S. A. and Dean, J. F. 2000. Forest tree biotechnology. **Current Opinion in Biotechnology**, v. 11, n. 3, p. 298-302.

Mills, G. B.; Schmandt, R.; Mcgill, M.; Amendola, A.; Hill, M.; Jacobs, K.; May, C.; Rodricks, A.-M.; Campbell, S. and Hogg, D. 1992. Expression of TTK, a novel human protein kinase, is associated with cell proliferation. **Journal of Biological Chemistry**, v. 267, n. 22, p. 16000-16006.

Mironov, V.; De Veylder, L.; Van Montagu, M. and Inzé, D. 1999. Cyclin-dependent kinases and cell division in plants—the nexus. **The Plant Cell Online**, v. 11, n. 4, p. 509-521.

Musacchio, A. and Salmon, E. D. 2007. The spindle-assembly checkpoint in space and time. **Nature Reviews Molecular Cell Biology**, v. 8, n. 5, p. 379-393.

Noah, A. M.; Niemenak, N.; Sunderhaus, S.; Haase, C.; Omokolo, D. N.; Winkelmann, T. and Braun, H.-P. 2013. Comparative proteomic analysis of early somatic and zygotic embryogenesis in *Theobroma cacao* L. **Journal of Proteomics**, v. 78, p. 123-133.

Osti, R. Z.; Andrade, J. B. R.; Souza, J. P.; Silveira, V.; Balbuena, T. S.; Guerra, M. P.; Franco, D. W.; Floh, E. I. S. and Santa-Catarina, C. 2010. Nitrosyl ethylenediaminetetraacetate ruthenium(II) complex promotes cellular growth and could be used as nitric oxide donor in plants. **Plant Science**, v. 178, n. 5, p. 448-453.

Park, Y.; Barrett, J. and Bonga, J. 1998. Application of somatic embryogenesis in high-value clonal forestry: deployment, genetic control, and stability of cryopreserved clones. **In Vitro Cellular & Developmental Biology-Plant**, v. 34, n. 3, p. 231-239.

Pinhal, H. F.; Anastácio, M. R.; Carneiro, P. a. P.; Silva, V. J. D.; Morais, T. P. D. and Luz, J. M. Q. 2011. Aplicações da cultura de tecidos vegetais em fruteiras do Cerrado. **Ciência Rural**, v. 41, n. 7, p. 1136-1142.

Planchais, S.; Glab, N.; Inzé, D. and Bergounioux, C. 2000. Chemical inhibitors: a tool for plant cell cycle studies. **FEBS Letters**, v. 476, n. 1, p. 78-83.

Schmidt, M.; Budirahardja, Y.; Klompmaker, R. and Medema, R. H. 2005. Ablation of the spindle assembly checkpoint by a compound targeting Mps1. **EMBO Reports**, v. 6, n. 9, p. 866-872.

Silveira, V.; Santa-Catarina, C.; Tun, N. N.; Scherer, G. F. E.; Handro, W.; Guerra, M. P. and Floh, E. I. S. 2006. Polyamine effects on the endogenous polyamine contents, nitric oxide release, growth and differentiation of embryogenic suspension cultures of *Araucaria angustifolia* (Bert.) O. Ktze. **Plant Science**, v. 171, n. 1, p. 91-98.

Silveira, V.; Steiner, N.; Santos, A.; Nodari, R. O. and Guerra, M. P. 2002. Biotechnology tolls in *Araucaria angustifolia* conservation and improvement: inductive factors affecting somatic embryogenesis. **Crop Breeding And Applied Biotechnology**, v. 2, p. 463-470.

Smertenko, A. and Bozhkov, P. V. 2014. Somatic embryogenesis: life and death processes during apical–basal patterning. **Journal of Experimental Botany**, p. eru005.

Steiner, N. 2005. Parâmetros fisiológicos e bioquímicos durante a embriogênese zigótica e somática de *Auracaria angustifolia* (BERT.) O. KUNTZE. Dissertação Genética e Melhoramento Vegetal, Universidade Federal de Santa Catarina, Santa Catarina, 129p.

Steiner, N.; Santa-Catarina, C.; Andrade, J. B. R.; Balbuena, T. S.; Guerra, M. P.; Handro, W.; Floh, E. I. S. and Silveira, V. 2008. *Araucaria angustifolia* biotechnology - review. **Functional Plant Science & Biotechnology**, v. 2, p. 20-28.

Steiner, N.; Santa-Catarina, C.; Silveira, V.; Floh, E. I. S. and Guerra, M. P. 2007. Polyamine effects on growth and endogenous hormones levels in *Araucaria angustifolia* embryogenic cultures. **Plant Cell, Tissue and Organ Culture**, v. 89, n. 1, p. 55-62.

Steiner, N.; Vieira, F. D. N.; Maldonado, S. and Guerra, M. P. 2005. Effect of carbon source on morphology and histodifferentiation of *Araucaria angustifolia* embryogenic cultures. **Brazilian Archives of Biology and Technology**, v. 48, n. 6, p. 895-903.

Tautorus, T. E.; Fowke, L. C. and Dunstan, D. I. 1991. Somatic embryogenesis in conifers. **Canadian Journal of Botany-Revue Canadienne De Botanique**, v. 69, n. 9, p. 1873-1899.

Termignoni, R. R. 2005. **Cultura de tecidos vegetais**. Porto Alegre: UFRGS, 182

Tompsett, P. 1984. Desiccation studies in relation to the storage of Araucaria seed. **Annals of Applied Biology**, v. 105, n. 3, p. 581-586.

Vantard, M.; Cowling, R. and Delichere, C. 2000. Cell cycle regulation of the microtubular cytoskeleton. In: (Ed.). **The Plant Cell Cycle**: Springer p.147-159.

Ventosa, M. a. L. D. L. 2010. Differential proteomics: a study in *Medicago truncatula* somatic embryogenesis. Dissertação de Mestrado Biologia Vegetal, Universidade de Lisboa45p.

Vieira, L. D. N.; Santa-Catarina, C.; De Freitas Fraga, H. P.; Wendt Dos Santos, A. L.; Steinmacher, D. A.; Schlogl, P. S.; Silveira, V.; Steinera, N.; Segal Floh, E. L. and Guerra, M. P. 2012. Glutathione improves early somatic embryogenesis in *Araucaria angustifolia* (Bert) O. Kuntze by alteration in nitric oxide emission. **Plant Science**, v. 195, p. 80-87.

Wasinger, V. C.; Cordwell, S. J.; Cerpapoljak, A.; Yan, J. X.; Gooley, A. A.; Wilkins, M. R.; Duncan, M. W.; Harris, R.; Williams, K. L. and Humpherysmith, I. 1995. Progress with gene-product mapping of the mollicutes - *Mycoplasma genitalium*. **Electrophoresis**, v. 16, n. 7, p. 1090-1094.

Winey, M.; Goetsch, L.; Baum, P. and Byers, B. 1991. MPS1 and MPS2: novel yeast genes defining distinct steps of spindle pole body duplication. **The Journal of cell biology**, v. 114, n. 4, p. 745-754.

Young, C. W. and Hodas, S. 1964. Hydroxyurea: inhibitory effect on DNA metabolism. **Science**, v. 146, n. 3648, p. 1172-1174.

Zhao, Y. and Chen, R.-H. 2006. Mps1 phosphorylation by MAP kinase is required for kinetochore localization of spindle-checkpoint proteins. **Current Biology**, v. 16, n. 17, p. 1764-1769.

Anexo 1

PLOS ONE

RESEARCH ARTICLE

Mps1 (Monopolar Spindle 1) Protein Inhibition Affects Cellular Growth and Pro-Embryogenic Masses Morphology in Embryogenic Cultures of Araucaria angustifolia (Araucariaceae)

Jackellinne C. Douétts-Peres[1], Marco Antônio L. Cruz[2], Ricardo S. Reis[3,4], Angelo S. Heringer[3,4], Eduardo A. G. de Oliveira[2], Paula M. Elbl[5], Eny I. S. Floh[5], Vanildo Silveira[3,4], Claudete Santa-Catarina[1]*

2. Laboratório de Biologia Celular e Tecidual, Centro de Biociências e Biotecnologia (CBB), Universidade Estadual do Norte Fluminense Darcy Ribeiro (UENF), Campos dos Goytacazes, Rio de Janeiro, Brazil, 3. Laboratório de Biotecnologia Vegetal, Núcleo em Ecologia e Desenvolvimento Sócio-ambiental de Macaé, Universidade Federal do Rio de Janeiro, Macaé, Rio de Janeiro, Brazil, 3 Laboratório de Biotecnologia, CBB, UENF, Campos dos Goytacazes, Rio de Janeiro, Brazil, 4 Unidade de Biologia Integrativa, Setor de Proteômica, UENF, Campos dos Goytacazes, Rio de Janeiro, Brazil, 5 Laboratório de Biologia Celular de Plantas, Departamento de Botânica, Instituto de Biociências, Universidade de São Paulo, São Paulo, São Paulo, Brazil

* claudete@uenf.br

Abstract

Somatic embryogenesis has been shown to be an efficient tool for studying processes based on cell growth and development. The fine regulation of the cell cycle is essential for proper embryo formation during the process of somatic embryogenesis. The aims of the present work were to identify and perform a structural and functional characterization of Mps1 and to analyze the effects of the inhibition of this protein on cellular growth and pro-embryogenic mass (PEM) morphology in embryogenic cultures of A. angustifolia. A single-copy Mps1 gene named AaMps1 was retrieved from the A. angustifolia transcriptome data-base, and through a mass spectrometry approach, AaMps1 was identified and quantified in embryogenic cultures. The Mps1 inhibitor SP600125 (10 μM) inhibited cellular growth and changed PEMs, and these effects were accompanied by a reduction in AaMps1 protein lev-els in embryogenic cultures. Our work has identified the Mps1 protein in a gymnosperm spe-cies for the first time, and we have shown that inhibiting Mps1 affects cellular growth and PEM differentiation during A. angustifolia somatic embryogenesis. These data will be useful for better understanding cell cycle control during somatic embryogenesis in plants.

OPEN ACCESS

Citation: Douétts-Peres JC, Cruz MAL, Reis RS, Heringer AS, de Oliveira EAG, Elbl PM, et al. (2016) Mps1 (Monopolar Spindle 1) Protein Inhibition Affects Cellular Growth and Pro-Embryogenic Masses Morphology in Embryogenic Cultures of Araucaria angustifolia (Araucariaceae). PLoS ONE 11(4): e0153528. doi:10.1371/journal.pone.0153528

Editor: Michael Polymenis, Texas A&M University, UNITED STATES

Received: January 23, 2016

Accepted: March 30, 2016

Published: April 11, 2016

Data Availability Statement: All relevant data are within the paper and its Supporting Information files.

Funding: This work was supported by the National Council for Scientific and Technological Development (CNPq) (476465/2011-7 and 305645/2013-7) and the Carlos Chagas Filho Foundation for Research Support in the State of Rio de Janeiro (FAPERJ) (E26/112.055/2011, E26/110.390/2012, E26/111.389-2012, E26/102.989/2012, and E26/010.001507/ 2014).

Competing Interests: The authors have declared that no competing interests exist.

Introduction

The transition from a somatic cell into a somatic embryo, during somatic embryogenesis, is a complex event, consisting of the following crucial steps: induction, cell dedifferentiation, and competence acquisition; multiplication, with intense cell division; maturation, which deter-mines fate; and the germination of somatic embryos [1].

During somatic embryo formation, the correct performance of the cell cycle is crucial, and adequate levels of certain signaling molecules, such as polyamines, carbohydrates, and nitric oxide (NO), are required [2–4]. The maturation induction of somatic embryogenic cultures with maturation promoters, such as abscisic acid (ABA), or with osmotic agents, such as polyethylene glycol (PEG) and maltose, induce cell growth inhibition, preventing division and promoting the differentiation of cell cultures [5–8]. However, other compounds, such as auxins, NO, and putres-cine, promote cell division, thereby increasing growth and inhibiting cell differentiation into somatic embryos [4,6,7]. Embryogenic suspension culture systems have been developed for Arau-caria angustifolia, and they have been shown to be efficient systems for studying the effects of sig-naling molecules in gymnosperms [4,9,10]. Cell cycle regulation can be used as a tool for the elucidation of metabolism-related events, and it involves signaling compounds that are important for various processes in plant development [11], including somatic embryogenesis [12].

Cell division in eukaryotes is controlled by a complex mechanism that involves cyclin-dependent kinases (CDKs) as key regulators [13,14]. One of these kinases is Mps1 (monopolar spindle 1), which has been described in humans and is characterized as a cell cycle regulator that is evolutionarily conserved in eukaryotes [15]. Mps1 is a dual-specificity protein kinase that plays a critical role in monitoring the accuracy of chromosome segregation at the mitotic checkpoint, and it is an important component of the spindle assembly checkpoint (SAC) [16]. Among chemical inhibitors, SP600125 acts on Jun N-terminal kinase (JNK) proteins in humans [17] and has been valuable in validating the cellular functions of Mps1. In plants, a protein was found that was highly similar to human Mps1 in terms of structural characteristics, such as its catalytic site, and it was conserved relative to the Mps1 protein found in A. thaliana [18]. The inhibitor SP600125 blocks the G2-M transition in Arabidopsis by specifically inhibit-ing the activity of AtMps1 [18]. However, the role of Mps1 in gymnosperm species, such as A. angustifolia, has not yet been shown.

The aims of the present work were to identify and perform a structural and functional characterization of Mps1 and to analyze the effects of the inhibition of this protein on cellular growth and pro-embryogenic mass (PEM) morphology in embryogenic cultures of A. angustifolia.

Materials and Methods

Plant Material

Embryogenic suspension cultures of A. angustifolia were induced according to the methodol-ogy established by Steiner et al. [19] and then used for these experiments. Embryogenic cell suspension cultures are formed by PEMs made of embryogenic cells (which are rounded, with a dense cytoplasm) and suspensor cells (which are highly vacuolated and elongated) [6,20].

Mps1 Sequence Identification and Structural Analyses

To identify a putative Mps1 from A. angustifolia, we performed a tBLASTn search [21] by using the Mps1 protein sequence of A. thaliana (AT1G77720) as a query against the A. angusti-folia transcriptome database [22,23], with the following parameters: E-value > E^{-10} and a mini-mum coverage threshold of 30% (query and hit). The complete sequence is available at GenBank under accession number KU600448. Other sequences that were homologous to their

A. thaliana counterpart were identified by searching the Phytozome 10.2 database (http://www.phytozome.net/), NCBI (http://www.ncbi.nlm.nih.gov/), TAIR (https://www.arabidopsis.org), and SustainPineDB (http://www.scbi.uma.es/sustainpinedb) using BLAST. All the sequences obtained here and the putative AaMps1 were aligned with MEGA software, version 6.0 [24] using MUSCLE/CLUSTALW with default parameters. The alignment was analyzed using the Neighbor-Joining method, and the distances were calculated according to the best model identified by the program. The model parameter and tree estimates were performed with PhyML [25], and the tree topology was evaluated with 1500 bootstrap replications. Detailed information on all the sequences used for analysis is available in S1 Table.

A template identification using the Mps1 sequence from A. angustifolia was performed using the template identification tool from SWISS-MODEL [26–28] to find the most accurate templates (by considering the sequence identity, coverage, and crystal resolution). Additionally, we performed a motif search analysis with the aid of the Eukaryotic Linear Motif (ELM) server [29] to find interaction sites with other cell cycle regulation elements.

Molecular modeling was performed using MODELLER v9.14 [30,31] with the following struc-tures as templates: 2ZMD [32], 3DBQ [33], 3HMN [34], and 3VQU (http://dx.doi.org/10.2210/pdb3vqu/pdb). All four crystals are representations of the human Mps1 protein. Molecular dock-ing experiments with the A. angustifolia Mps1 3D model were performed with Autodock v4.6.2 [35]. Experimental conditions were set using the oxygen atom (position 838) from the GLU-790 residue inside a 45x45x45 (XYZ dimensions) grid box centered at approximately 0.9460/-32.2960/-9.4240 (x/y/z coordinates). The molecular docking and modeling solutions were visual-ized and registered with PyMOL v1.3 (Schrödinger, LCC), using the Autodock plugin [36].

Linear protein interaction motifs were detected with the ELM Database (http://elm.eu.org/) [29]. The Mps1 proteins analyzed here were from the species A. angustifolia (AaMps1), Ambor-ella trichopoda (AbMps1 –gi | 586646077), Eucalyptus grandis (EgMps1 –gi | 702379945), Car-ica papaya (CpMps1 -| evm.TU.supercontig_36.11), and Medicago truncatula (MtMps1 gi | 357461629). Phosphorylation sites were predicted with PlantPhos, a tool that was developed to predict phosphorylation sites in plant proteins [37].

Suspension Culture Conditions

To obtain cell suspensions, embryogenic cultures were multiplied and maintained in the basic liq-uid culture medium MSG [38] supplemented with 30 g l^{-1} sucrose, 1.4 g l^{-1} L-glutamine (Sigma-Aldrich, St. Louis, USA), and 0.1 g l^{-1} myo-inositol (Merck KGaA, Darmstadt, Germany), and the pH of the culture medium was adjusted to 5.7 before autoclaving at 121°C for 20 min, 1.5 atm. The embryogenic cell suspension cultures were subcultured every 15 days by adding 10 ml of the old suspension culture to 60 ml of fresh liquid medium. Embryogenic cell suspension cultures were kept on an orbital shaker (Cientec, Minas Gerais, Brazil) at 100 rpm in the dark, at 25 ± 2°C.

To analyze the effect of Mps1 inhibition on cellular growth and the PEM morphology, embryogenic cell suspension cultures were grown in basic MSG culture medium supplemented with 30 g l^{-1} sucrose, 1.4 g l^{-1} L-glutamine, and 0.1 g l^{-1} myo-inositol, and with or without Mps1 inhibitor SP600125 (Sigma-Aldrich). The Mps1 inhibitor was filter-sterilized through a 0.2-μm PVDF membrane (Millipore, São Paulo, Brazil) before being added to the culture medium. After the inoculation of embryogenic cell culture with 15-day-old cell suspensions, the flasks were maintained on an orbital shaker at 100 rpm in the dark, at 25 ± 2°C.

Effects of Mps1 Inhibition on Cellular Growth

The cellular growth in suspension cultures was measured using settled cell volume (SCV) according to Osti et al. [4] to establish the growth curve for different concentrations (0, 1 and

10 μM) of Mps1 inhibitor. The SCV was determined by cell sedimentation in the side arm of the adapted flasks and was evaluated every three days until day 30 of the culture. Each treat-ment was performed in triplicate. From the resulting growth curve, the initial time, lag phase, early exponential phase, exponential phase, and stationary phase were established as days 0, 6, 15, 21, and 27, respectively, of the incubation.
To analyze cellular growth based on increases in fresh matter (FM) and dry matter (DM), 60 mg aliquots of 15-day-old embryogenic suspension cultures were inoculated into 12-well tissue culture plates (TPP[1]) containing 2 ml/well of basic MSG culture medium without (control) or with (10 μM) Mps1 inhibitor. The application of Mps1 inhibitor (10 μM) inhibited the cellular growth according to SCV analyses. Six samples (corresponding to six wells) from each treatment were obtained to measure the FM before (0) and after 6, 15, 21, and 27 days of incu-bation. The DM was obtained by drying the FM samples at 70°C for 48 h.

Effects of Mps1 Inhibition on PEM Morphology

The analyses of PEM morphology were performed by measuring the area and size of embryo-genic cells and suspensor cells. For both analyses, samples were collected before (0) and after 6, 15, 21, and 27 days of incubation without (control) or with (10 μM) Mps1 inhibitor, which showed cellular growth inhibition in the SCV analyses. Samples were collected and prepared on slides, followed by examination under an Axioplan light microscope (Carl Zeiss, Jena, Ger-many) equipped with an AxioCam MRC5 digital camera (Carl Zeiss). After the images were obtained, area and size were measured using AxioVision LE software, version 4.8 (Carl Zeiss).
The area measurements were performed from PEMs, from the group of embryogenic-type cells that form the embryonal head, and from the suspensor-type cells. For these analyses, for each treatment and each incubation time, three slides were prepared, and at least ten images of PEMs were obtained.
For the cell size analyses, the PEMs were treated with cellulase (Fluka Analytical, Buchs, Switzerland) 0.1% for 3 h to dissociate the embryogenic and suspensor cells of PEM. As embryogenic-type cells are isodiametric, the size was measured based on the diameter, and as suspensor-type cells are elliptic and elongated, the size was measured using the length and width (at the middle of the cell). For these analyses, for each treatment and each incubation time, three slides were prepared, and fifty images from each cell type (embryogenic or suspen-sor) were obtained.

Identification and Quantification of the AaMps1 Protein

The AaMps1 protein was identified and quantified using embryogenic suspension cultures before (time 0) and after 15 days of incubation (the period of cellular growth) without (control) and with Mps1 inhibitor (10 μM), which inhibited cellular growth. This analysis was per-formed to confirm the presence of this protein in the embryogenic suspension cultures and to observe the effect of the inhibitor on the protein concentration in the two treatments.
Protein extractions were performed according to Balbuena et al. [39] with some modifica-tions. Samples containing 300 mg FM were ground in liquid nitrogen and transferred into clear 2 ml microtubes containing 1.0 ml of extraction buffer made of 7 M urea (GE Healthcare, Freiburg, Germany), 2 M thiourea (GE Healthcare), 1% dithiothreitol (DTT; GE Healthcare), 2% Triton X-100 (GE Healthcare), 0.5% pharmalyte (GE Healthcare), 1 mM phenylmethane-sulfonyl fluoride (PMSF; Sigma-Aldrich), and 5 μM pepstatin (Sigma-Aldrich). All extracts were vortexed for 2 min and kept in the extraction buffer on ice for 30 min, followed by centri-fugation at 12,000 x g for 10 min at 4°C. The supernatants were transferred to clear microtubes; then, the proteins were precipitated in ice for 30 min in 10% trichloroacetic acid (TCA; Sigma-

Aldrich) and were washed three times with cold acetone (Merck). Finally, the proteins were re-suspended and concentrated in 1 ml of the same extraction buffer. The protein concentration was estimated using a 2-D Quant Kit (GE Healthcare). Sample preparation and HDMS^E (data-independent acquisition, with ion mobility) mass spectrometry analyses were performed according to Reis et al. [40].

MS data processing and database searching were performed using Progenesis QI for Proteomics Software V. 2.0 (Nonlinear Dynamics, Newcastle, UK). The analysis used the following parameters: 1 missed cleavage; minimum fragment ion per peptide equal to 1; minimum fragment ion per protein equal to 3; minimum peptide per protein equal to 1; variable modifications by carbamidomethyl (C), acetyl N-terminal, and oxidation (M); a default false discovery rate (FDR) value with a 4% maximum; a score greater than 5; and a maximum of 10 ppm for mass errors. This program compares the AtMps1 (A. thaliana) sequence—gi | 28416703 and the AaMps1 (A. angustifolia) predicted protein sequence obtained by BLAST with the A. angustifolia transcriptome database [22,23] for protein identification.

Data Analysis

The data presented here were statistically analyzed using analysis of variance (ANOVA) ($P< 0.01$) followed by Tukey's test using R software (Foundation for Statistical Computing, version 3.0.3, 2014, Vienna, Austria). Nucleotide sequence data from this article can be found in the GenBank under accession number KU600448.

Results

Mps1 Sequence Identification and Structural Analyses

Using AtMps1 as a query, we identified a single-copy gene in A. angustifolia, and its protein was designated AaMps1 (Fig 1 and S1 Table). This sequence presented higher homology with AbMps1 protein in Amborella trichopoda, EgMps1 in Eucalyptus grandis, CpMps1 in Carica papaya, and MtMps1 in Medicago truncatula (S1 Fig).

A kinase domain with 293 amino acid residues could be identified, with approximately 91% of these amino acids being common between the different species, thus showing that this kinase domain is conserved among the analyzed species (S1 Fig). Tridimensional modeling of the AaMps1 kinase domain (Fig 2A) presents two subdomains that are connected by a flexible loop. The larger subdomain is composed of five α-helices and four β-sheets, and the smaller subdomain contains one α-helix and five β-sheets (Fig 2A). The alignment of the AaMps1 kinase domain reveals a structure that is similar to that of hMps1 (S2 Fig) and AtMps1 (S3 Fig). A tridimensional analysis of the AaMps1 kinase domain also showed that an Asp-Phe-Gly (DFG) motif (Fig 2B) and a threonine triad (T870, T871 and T881) related to autopho-sphorylation (Fig 2C) were highly conserved in other analyzed plant species (S1 Fig).

The phosphorylation sites in the kinase domain of the Mps1 protein were predicted (Table 1) using the AtMps1 sequence in PlantPhos, leading to the identification of 18 sites in AaMps1 that are analogous to the phosphorylation sites observed in AtMps1. In comparison with the AaMps1 sequence, 16 phosphorylation sites were predicted in EgMps1, 18 in CpMps1, and 17 in MtMps1.

The AaMps1 sequence revealed 1036 residues, and the proteins AbMps1, EgMps1, CpMps1 and MtMps1 contained 950, 851, 821 and 742 residues, respectively (Fig 3A). The linear pro-tein interaction motifs of Mps1 were analyzed with ELM prediction tool motifs to compare AaMps1 with Mps1 proteins from other species. AaMps1 had the characteristic motifs of the Mps1 protein kinase (Fig 3A), which were observed in A. trichopoda, E. grandis, C. papaya, and M. truncatula. The motifs that were found to be conserved in these species include the

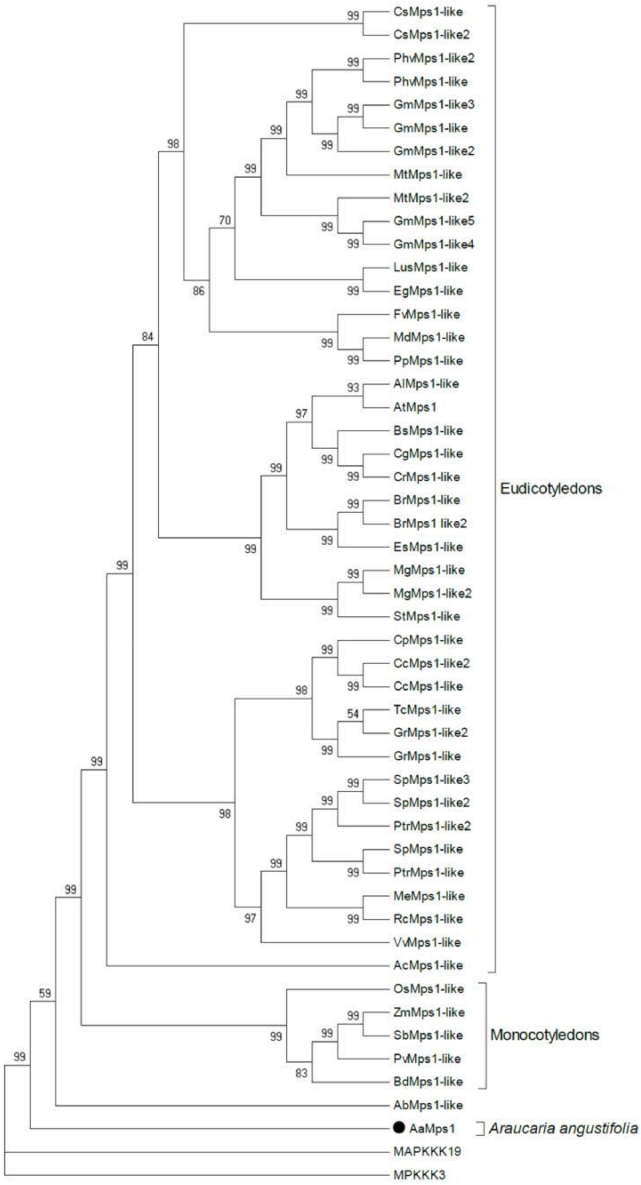

Fig 1. Phenogram of Mps1. Sequence data details are listed in S1 Table. The topology of the tree was consistent with the phylogenetic distribution of the species. Mps1 is encoded by a single-copy gene in monocotyledons and Araucaria angustifolia. Paralogs were found in some species inside the Eudicotyledons clade, indicating species-specific duplications. The bootstrap values are shown on the branches. The tree was rooted with MAPKs of Arabidopsis thaliana as the outgroup. Amborella trichopoda (Ab), Aquilegia coerulea (Ac), Arabidopsis lyrata (Al), Arabidopsis thaliana (At), Araucaria angustifolia (Aa), Boechera stricta (Bs), Brachypodium distachyon (Bd), Brassica rapa (Br), Capsella grandiflora (Cg), Capsella rubella (Cr), Carica papaya (Cp), Citrus clementina (Cc), Cucumis sativus (Cs), Eucalyptus grandis (Eg), Eutrema salsugineum (Es), Fragaria vesca (Fv), Glycine max (Gm), Gossypium raimondii (Gr), Linum usitatissimum (Lu), Malus domestica (Md), Manihot esculenta (Me), Medicago trunculata (Mt), Mimulus guttatus (Mg), Oryza sativa (Os), Panicum virgatum (Pv), Phaseolus vulgaris (Phv), Pinus pinaster (Ppi), Populus trichocarpa (Pt), Prunus persica (Pp), Ricinus communis (Rc), Salix purpurea (Sp), Solanum tuberosum (St), Sorghum bicolor (Sb), Theobroma cacao (Tc), Vitis vinifera (Vv), and Zea mays (Zm).

doi:10.1371/journal.pone.0153528.g001

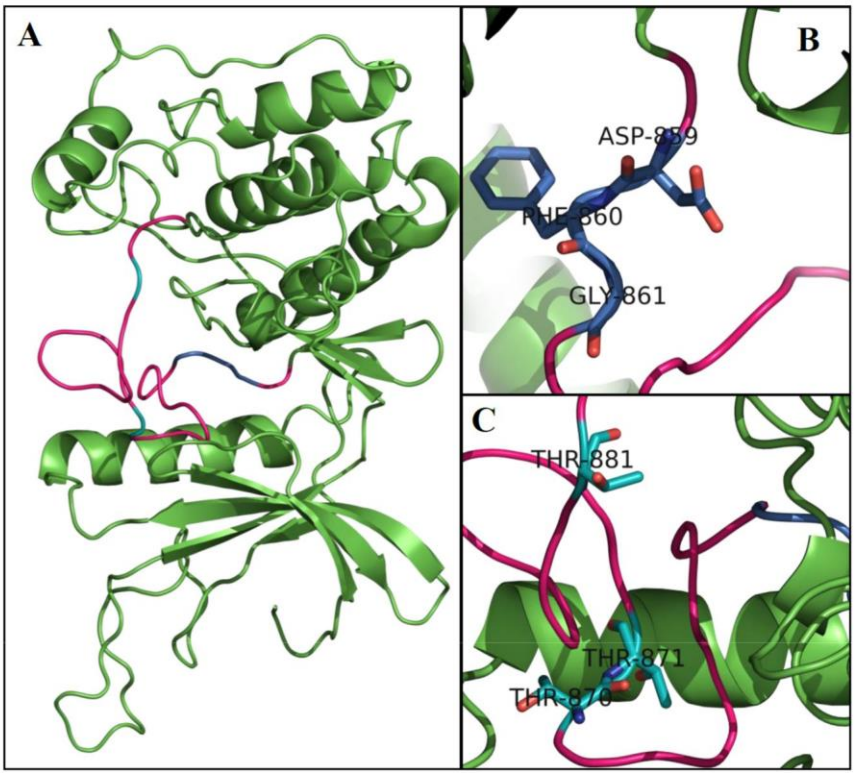

Fig 2. A 3D model of the AaMps1 kinase domain. (A) An overview of the kinase domain. Rose: activation loop; Blue: DFG motif; and Cyan: threonines. (B) A detailed view of the DFG motif. (C) A detailed view of the threonine residues (T870, T871, and T881) that are related to autophosphorylation.

doi:10.1371/journal.pone.0153528.g002

Mitotic arrest-deficient 2 (MAD2) binding motif LIG_MAD2, the Cyclin recognition site DOC_CYCLIN_1, the MAPK docking motif DOC_MAPK_1, the Nuclear Export Signal TRG_NES_CRM1_1, the Nuclear Localization Signal TRG_NLS_MonoExtC_3, the Protein phosphatase-1 (PP1) regulation site DOC_PP1_RVXF_1, a motif phosphorylated by phosphoinositide-3-OH-kinase (PIKK) family members, MOD_PIKK_1, and a motif for the DFG structural conformation. These motifs were present in at least four species among those analyzed here (AaMps1, AbMps1, EgMps1, CpMps1, and MtMps1). The structures of the DOC_CYCLIN_1, DOC_MAPK_1, and LIG_MAD2 motifs in AaMps1 were observed by tridimensional model analyses (Fig 3B).

Effects of Mps1 Inhibition on Cellular Growth of Embryogenic Suspension Cultures

Through SCV analysis (Fig 4), it was possible to observe the inhibition of cellular growth in *A. angustifolia* embryogenic suspension cultures treated with the Mps1 inhibitor at 10 μM, without significant differences in the incubation times. However, the cellular growth of embryogenic suspension cultures incubated in the control and 1 μM Mps1 inhibitor treatments increased during the incubation times, enabling the identification of the lagging (until the 12th day), exponential (from the 15th day), and stationary (27 days) phases (Fig 4).

Cellular growth, in terms of the FM and DM increments in embryogenic suspension cultures during incubation, was affected by the Mps1 inhibitor. Beginning at 15 days of incubation, growth inhibition according to FM (Fig 5A) and DM (Fig 5B) analysis was observed in

Table 1. Phosphorylation sites of the kinase domain.

Residue Position	Residue Substrate	A. angustifolia	A. thaliana	E. grandis	C. papaya	M. truncatula
691	Y	X	X	X	X	X
699	S	X	X	-	X	X
702	S	X	X	X	X	X
703	S	X	X	X	X	X
710	S	X	X	X	X	X
711	S	X	X	X	X	X
714	T/S	X	X	X	X	-
716	Y	X	X	X	X	X
728	Y	X	X	X	X	X
732	Y	X	X	X	X	-
756	Y	X	X	-	X	-
786	Y	X	X	X	-	X
870	T	-	-	-	-	X
871	T	X	X	X	X	X
881	T	X	X	X	X	X
884	Y	X	X	X	X	X
922	Y	X	X	X	X	X
941	T	X	-	X	X	X
949	Y	X	X	-	X	X
953	S	X	X	X	X	X

Phosphorylation sites of the kinase domain in A. angustifolia AaMps1 analyzed by PlantPhos and compared with A. thaliana (AtMps1), E. grandis (EgMps1), C. papaya (CpMps1), and M. truncatula (MtMps1). Arrows indicate conserved threonine triads in the species. Y = tyrosine; S = serine; T = threonine; X = presence; and − = absence.

doi:10.1371/journal.pone.0153528.t001

the presence of the Mps1 inhibitor. In addition, embryogenic suspension cultures showed a sig-nificant increase in the FM increment beginning on the 15th day of incubation in the control treatment (Fig 5A). The DM increment in the control treatment was significant and progres-
sive from the 6th day until the end of incubation (Fig 5B).

Effects of Mps1 Inhibition on PEM Morphology

The morphology of PEMs was affected by the addition of 10 μM Mps1 inhibitor compared to the control treatment (Fig 6). These PEMs contain two types of cells: embryogenic cells (EC), which are grouped to form the embryonal head (HC), and the suspensor cells (SC). Embryo-genic cells are isodiametric, with an evident nucleus, while suspensor cells are elliptic, being elongated and oblong (Fig 6).

The embryogenic cells from the embryonal head of PEMs had significantly greater area from the 15th to 27th day in the control compared with those treated with 10 μM Mps1 inhibi-tor (Fig 7A), while the individual cells in the two treatments showed similar diameters during incubation (Fig 8A). On the other hand, the morphology of suspensor cells was affected by the addition of Mps1 inhibitor, showing changes in the area (Fig 7B) as well as the length (Fig 8B)
and width (Fig 8C). Beginning on the 6th day of incubation, the addition of Mps1 inhibitor reduced the area (Fig 7B) and length (Fig 8B) of suspensor cells in comparison to control cells.
However, suspensor cells showed a significant increase in width from the 6th to the 21st day of incubation (Fig 8C).

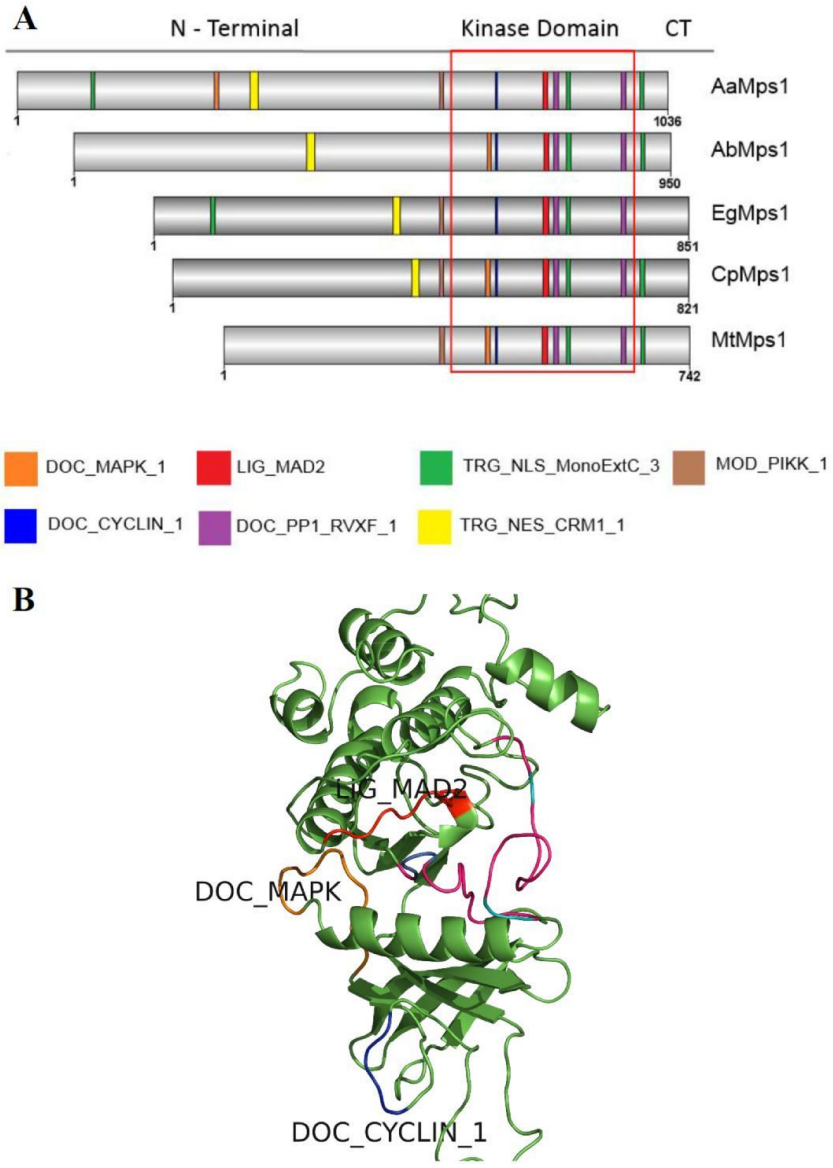

Fig 3. Mps1 motifs related to the cell cycle in plants. (A) Linear motifs of several Mps1 orthologs that were observed in A. angustifolia (AaMps1), A. thicopoda (AbMps1), E. grandis (EgMps1), C. papaya (CpMps1), and M. truncatula (MtMps1). (B) The 3D model of relevant interaction motifs DOC_CYCLIN_1, DOC_MAPK and LIG_MAD2 in AaMps1.

doi:10.1371/journal.pone.0153528.g003

Identification and Quantification of the AaMps1 Protein

Mass spectrometry analyses compared the AaMps1 protein obtained by *in silico* analyses with the Araucaria transcriptome database [22,23], resulting in 81.66% sequence coverage. These results confirm the presence of the Mps1 protein in A. angustifolia embryogenic suspension cultures (Table 2). Furthermore, the AaMps1 protein was highly similar to the AtMps1 protein (gi | 28416703), with 78.76% sequence coverage, indicating a strong homology between the AaMps1 and AtMps1 proteins (Table 2).

In addition, embryogenic suspension cultures at 15 days of incubation without Mps1 inhibi-tor (control) demonstrated a significant increase in the amount of AaMps1 compared with

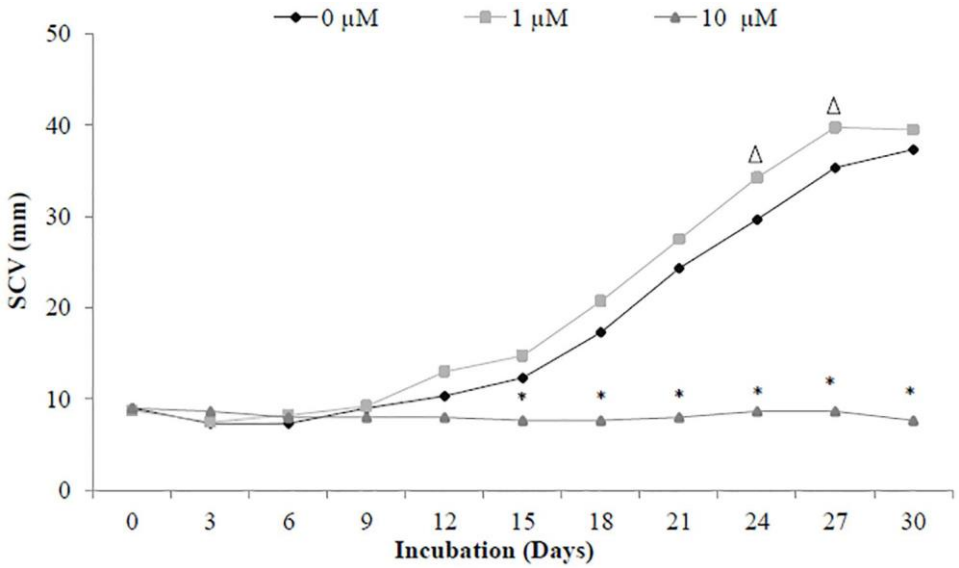

Fig 4. Cellular growth curve. Growth curve by settled cell volume (SCV) analyzes in embryogenic suspension cultures of A. angustifolia incubated with different concentrations (0, 1, and 10 µM) of Mps1 inhibitor SP600125, during 30 days of incubation. Triangles denote significant differences ($P < 0.01$) between control and 1 µM Mps1 inhibitor, and asterisks denote significant differences ($P < 0.01$) comparing 10 µM Mps1 inhibitor with the control and 1 µM Mps1 inhibitor treatments according to Tukey's test ($n = 3$; coefficient of variation = 14.5%).

doi:10.1371/journal.pone.0153528.g004

those analyzed before incubation (time 0). Furthermore, treatment with the Mps1 inhibitor (10 µM) induced a decrease in the amount of AaMps1 protein at 15 days of incubation com-pared with the control at 15 days of incubation and with embryogenic cultures before incuba-tion (Fig 9).

Discussion

Our results show the presence of the Mps1 protein in the gymnosperm species A. angustifolia, designated AaMps1. AaMps1 is homologous with the Mps1 proteins of other species, including the kinase domain that is highly conserved in eukaryotes. Our work confirmed the existence of the AaMps1 protein in embryogenic cultures by mass spectrometry analysis, demonstrating high coverage of the in silico predicted protein sequence of AaMps1 and with the AtMps1 (A. thaliana) protein.

Among the analyzed species, A. trichopoda (AbMps1) presented more similarities to AaMps1 in terms of residue number (Fig 1 and S1 Fig). This result may be related to the origin of A. trichopoda; this species is a member of an ancient lineage and is a unique and valuable reference that facilitates the interpretation of major genomic events in the evolution of flowering plants [41]. In addition, the AaMps1 protein shows similarities with AtMps1, the recently described Mps1 protein in plants [18] as well as other plants, such as E. grandis, C. papaya, and M. truncatula (S1 Fig). However, the numbers of residues from the Mps1 protein of these species are lower compared with that of A. angustifolia (AaMps1) and A. trichopoda (AbMps1). This result could explain the larger size of the AaMps1 protein in relation to AtMps1, given that AaMps1 presented more similarities with AbMps1 from A. trichopoda in comparison with A. thaliana. A. trichopoda is an ancestral angiosperm species for which the genome has been published, making this species a pivotal reference for understanding genome and gene family evolution throughout angiosperm history [41].

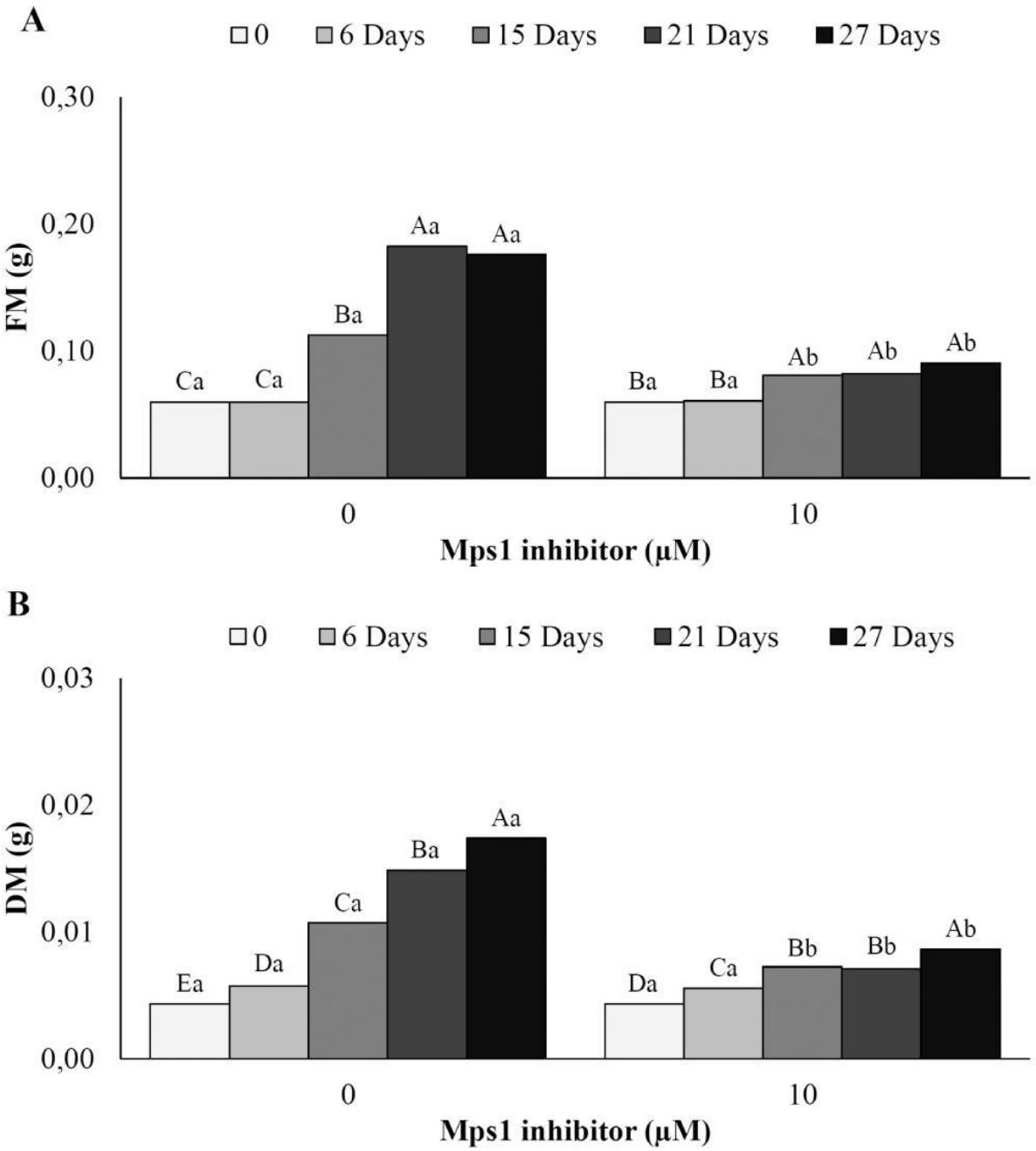

Fig 5. Mass increment (g) in A. angustifolia embryogenic suspension cultures. (A) FM and (B) DM values in embryogenic suspension cultures before (0) and after 6, 15, 21, and 27 days of incubation in MSG basic culture medium with (10 μM) or without Mps1 inhibitor SP600125. Lowercase letters denote significant differences ($P < 0.01$) between treatments for each day of incubation. Capital letters denote significant differences ($P < 0.01$) in the same treatment during incubation. Means followed by different letters are significantly different ($P < 0.01$) according to Tukey's test. CV = coefficient of variation (n = 6; CV FM = 10.3%; CV DM = 7.3%).

doi:10.1371/journal.pone.0153528.g005

Furthermore, AaMps1 has several structural features present in the Mps1 of all analyzed species, such as phosphorylation sites, DFG motifs, and the threonine triad (Figs 2 and 3; Table 1). Events such as the phosphorylation and autophosphorylation of Mps1 by other pro-teins and Mps1-mediated phosphorylation are crucial for the correct location and activity of

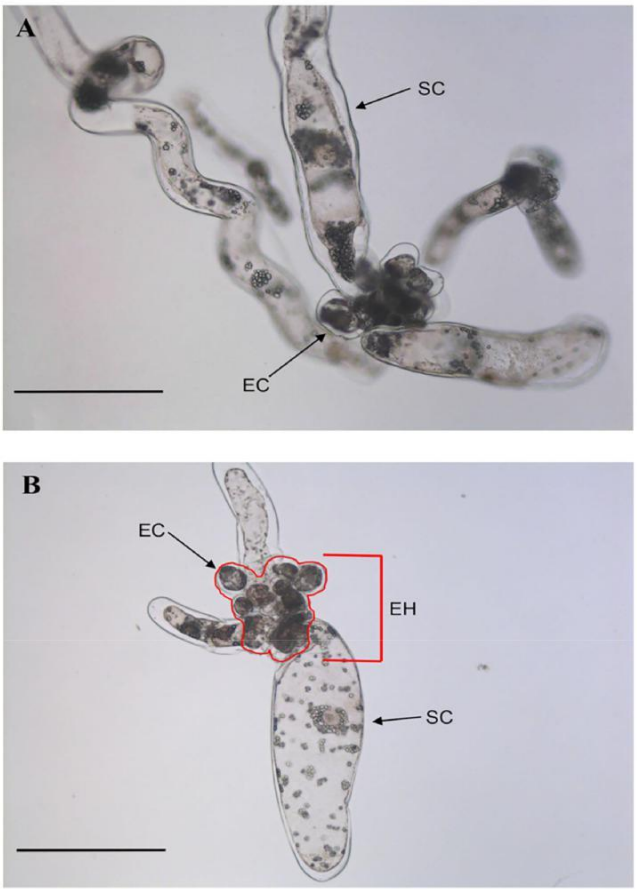

Fig 6. The morphology of A. angustifolia PEMs in cell suspension culture. Morphological features of PEMs after 15 days of incubation in MSG basic culture medium without (A) or with the Mps1 inhibitor SP600125 (10 μM) (B). EH = embryonal head; EC = embryogenic cells; SC = suspensor cells. Bars = 200 μm.

doi:10.1371/journal.pone.0153528.g006

Mps1 in cell cycle control [42–44]. Autophosphorylation on three fundamental threonine resi-dues (the threonine triad) in the Mps1 loop is necessary to activate this protein in humans (hMps1). Studies related to phosphorylation site mapping and mutation analysis in hMps1 indicate that three residues—T675, T676, and T686—may be modified by autophosphoryla-tion, given that the phosphorylation of T676 within the hMps1 activation loop is important for full kinase activity [43]. These three important residues in hMps1 are present in A. thaliana as T579, T580 and T590 [18], and they were shown to be conserved in A. angustifolia as T870, T871 and T881. Other characteristic features of Mps1 were also observed in AaMps1 in terms of interaction regions with other proteins (Fig 3). Some motifs observed in AaMps1, such as DOC_CYCLIN_1, DOC_MAPK_1, LIG_MAD2, TRG_NES_CRM1_1, TRG_NLS_MonoExtC, DOC_PP1_RVXF_1, and MOD_PIKK_1 (Fig 3A), could potentially mediate interactions with cyclins, MAD2, the ana-phase-promoting complex/cyclosome (APC/C), and MAPK-cell cycle regulators [44,45]. These motifs were similar to those of the other analyzed species, and some of the motifs have also been reported in Mps1 proteins in other plants, such as A. thaliana (AtMps1), Populus trichocarpa (PtMps1), Ricinus communis (RcMps1), Oryza sativa (OsMps1), Sorghum bicolor (SbMps1), and Zea mays (ZmMps1) [18]. These regions interact through short amino acid modules (linear

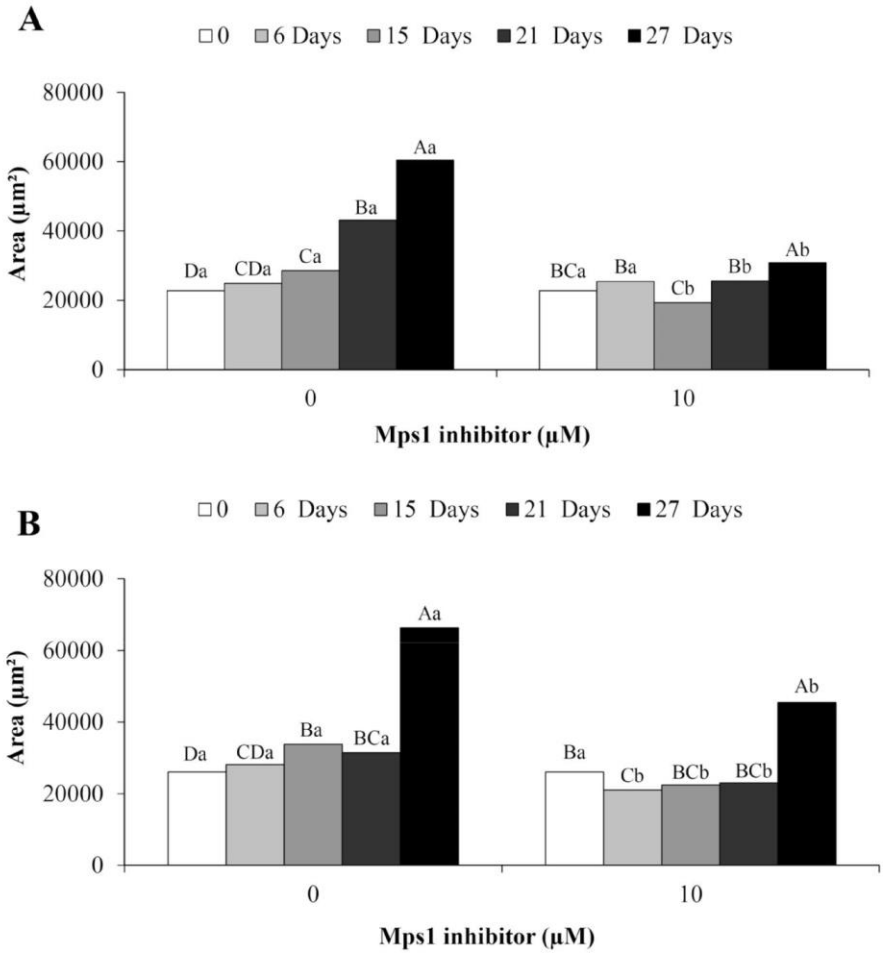

Fig 7. Analyses of PEM area. The group of embryogenic cells from the embryonal head of PEMs (A) and suspensor-type cells (B) from embryogenic suspension culture of A. angustifolia before (0) and after 6, 15, 21, and 27 days of incubation in MSG basic culture medium with (10 μM) or without the Mps1 inhibitor SP600125. Lowercase letters denote significant differences ($P < 0.01$) between treatments for each day of incubation. Capital letters denote significant differences ($P < 0.01$) in the same treatment during incubation. Means followed by different letters are significantly different ($P < 0.01$) according to Tukey's test.
CV = coefficient of variation (n = 10; CV embryonal head = 13%; CV suspensor cells = 12%).

doi:10.1371/journal.pone.0153528.g007

motifs), which are frequently identified as regulatory protein parts that provide interactions and bind with other proteins, modifying their structures and activities [29]. In addition, some interactions between Mps1 and other proteins that were observed through the predicted motifs have been shown in previous studies related to Mps1, such as the presence of the LIG_MAD2 motif, thus suggesting an interaction between Mps1 and MAD2 proteins in A. angustifolia (Fig 3). Experiments using human HeLa cells verified that Mps1 kinase pro-motes C-MAD2 production and subsequently leads the mitotic checkpoint complex (MCC) to activate the SAC; additionally, impaired inhibition of the Mps1, BubR1-MAD2 interaction has been shown, as well as the incorporation of MCC into MAD2 [44]. During the cell cycle, the increased phosphorylation of Mps1 at M phase is dependent on MAPK. MAPK is required for the SAC, and the phosphorylation of cell division control protein 20 (Cdc20) by MAPK is required for Cdc20 to associate with spindle-checkpoint proteins [45]. Herein, we identify the DOC_MAPK_1 motif in AaMps1, which may be another target for MAPK in the spindle

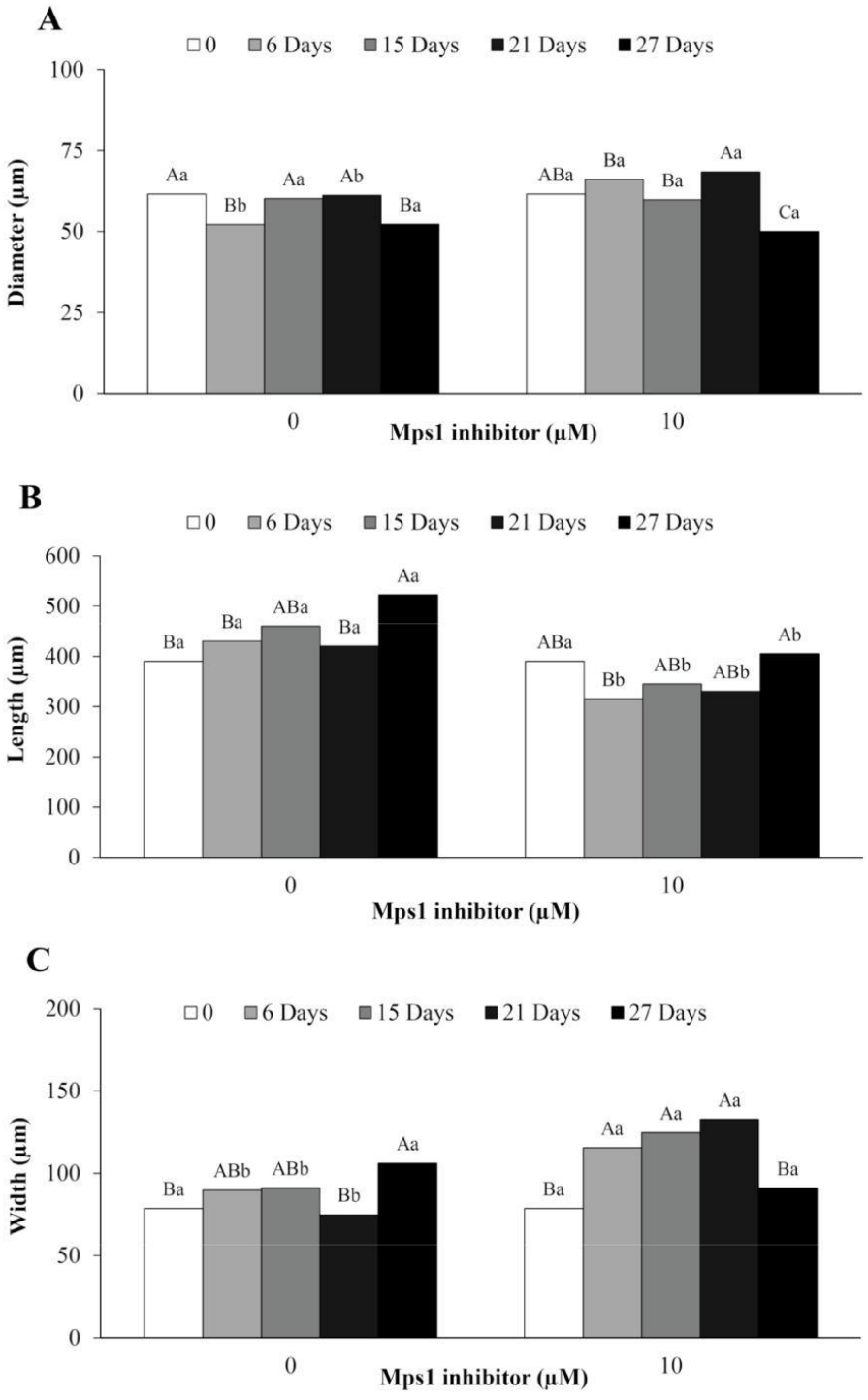

Fig 8. Analyses of cell size. Diameter of embryogenic cells (A) and length (B) and width (C) of suspensor cells from embryogenic suspension cultures of A. angustifolia before (0) and after 6, 15, 21, and 27 days of incubation in MSG basic culture medium with (10 µM) or without the Mps1 inhibitor SP600125. Lowercase letters denote significant differences ($P < 0.01$) between treatments for each day of incubation. Capital letters denote significant differences ($P < 0.01$) in the same treatment during incubation. Means followed by different letters are significantly different ($P < 0.01$) according to Tukey's test. CV = coefficient of variation (n = 50; CV diameter of embryogenic cells = 22.7%; CV length of suspensor cells = 35.2%; CV width of suspensor cells = 45.3%).

doi:10.1371/journal.pone.0153528.g008

Table 2. AaMps1 protein identification.

Parameters	AaMps1	AtMps1
Score	191.25	226.92
Coverage (%)	81.6602	78.6358
mW (Da)	113944	86323
pI (pH)	6.7	6.44

AaMps1 protein identification by HDMS^E (data-independent acquisition, with ion mobility) mass spectrometry in embryogenic suspension cultures of A. angustifolia incubated without Mps1 inhibitor SP600125, compared with in silico predicted protein sequence of AaMps1 (from A. angustifolia transcriptome database) and AtMps1 (A. thaliana) protein.

doi:10.1371/journal.pone.0153528.t002

checkpoint [45]. Therefore, the sequence of the AaMps1 protein shows some motifs and phos-phorylation sites with higher similarities to those of other species, confirming the identity of this protein in A. angustifolia.

Our results showed that the inhibition of AaMps1 affects the cellular growth (Figs 4 and 5) and PEM morphology of embryogenic suspension cultures in A. angustifolia (Figs 6, 7 and 8). These results suggest that the Mps1 protein is present in this species and that the inhibition of this protein with the Mps1 inhibitor can arrest the cell cycle. In addition, a decrease in the amount of AaMps1 protein, which was induced by the inhibitor, showed a strong correlation with the cellular growth reduction observed in A. angustifolia embryogenic suspension cultures (Fig 9). SP600125 competes for the ATP binding site on Mps1 and thus prevents the activity of

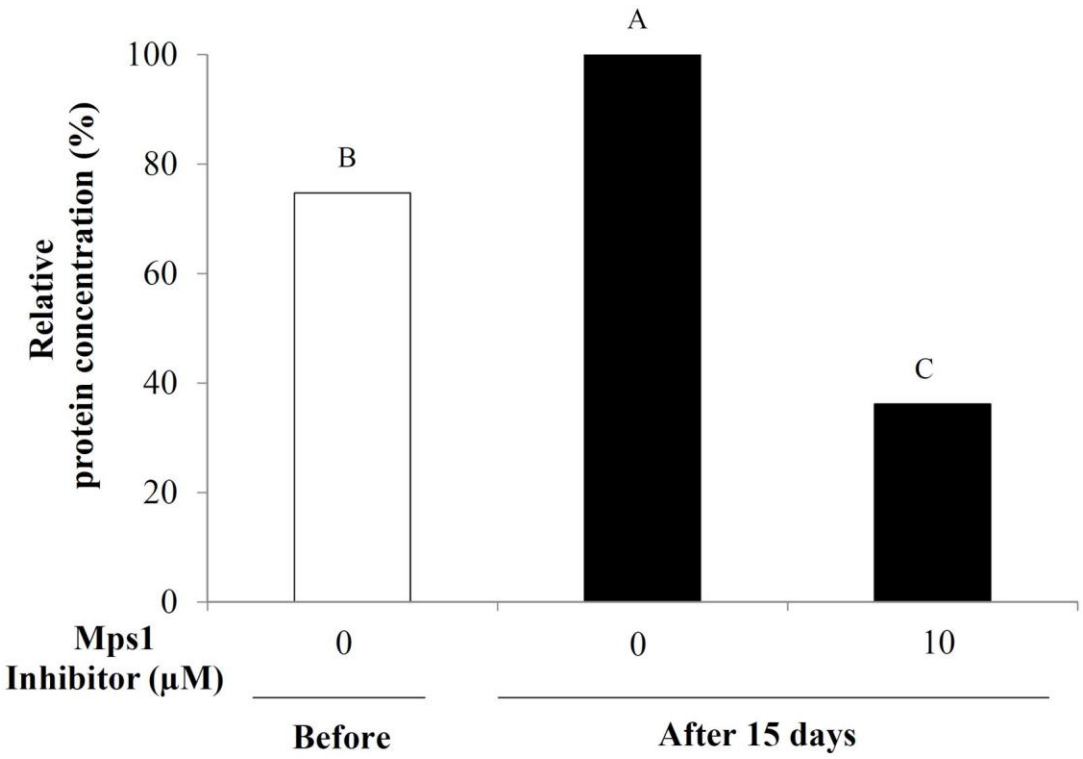

Fig 9. Quantification of the AaMps1 protein. Relative concentration (%) of AaMps1 protein by HDMS^E (data-independent acquisition, with ion mobility) mass spectrometry analysis in embryogenic suspension cultures of A. angustifolia before (0) and after 15 days of incubation in MSG basic culture medium with (10 μM) or without Mps1 inhibitor SP600125. Means followed by different letters are significantly different ($P < 0.01$) according to Tukey's test. (n = 3; Coefficient of variation = 14.1%).

doi:10.1371/journal.pone.0153528.g009

this protein kinase during cell cycle control in plants [18]. The inhibition of AaMps1 in A. angustifolia embryogenic suspension cultures reduces cellular growth, and it may be useful for understanding cell cycle control in gymnosperm somatic embryogenesis as well as for further studies on improving somatic embryo development.

Conclusions

This work has demonstrated the identification of Mps1 protein in A. angustifolia (AaMps1), showing that inhibition by the Mps1 inhibitor SP600125 affects the development of embryo-genic cultures, reducing cellular growth, PEM morphology, and the amount of AaMps1 pro-tein. Mass spectrometry analysis showed high homology with the AaMps1 predicted protein, obtained by in silico analyses with the Araucaria transcriptome database, and with the AtMps1 protein.

Supporting Information

S1 Fig. Multiple sequence alignment. Kinase domain in Mps1 proteins from A. angustifolia (AaMps1), A. thaliana (AtMps1), A. thicopoda (AbMps1), E. grandis (EgMps1), C. papaya (CpMps1), and M. truncatula (MtMps1). The black arrows indicate amino acids important for interaction with the inhibitor that are also conserved between hMps1, AaMps1 and other plant species. The blue arrow indicates the conserved DFG motifs. The red arrow indicates the con-served threonine residues.
(TIF)

S2 Fig. Tridimensional modeling and overlap of AaMps1 kinase domains and AtMps1. AaMps1 (cyan) in A. angustifolia and AtMps1 (green) in A. thaliana. (TIF)

S3 Fig. Tridimensional modeling and overlap of AaMps1 kinase domains and hMps1. AaMps1 (cyan) in A. angustifolia and hMps1 (pink) in humans. (TIF)

S1 Table. Sequence information.
(DOCX)

Author Contributions

Conceived and designed the experiments: JCDP MALC VS CSC. Performed the experiments: JCDP RSR ASH EAGO PME. Analyzed the data: JCDP MALC VS CSC. Contributed reagents/materials/analysis tools: EISF VS CSC. Wrote the paper: JCDP MALC CSC VS.

References

1. Fehér A. Somatic embryogenesis—Stress-induced remodeling of plant cell fate. Biochim Biophys Acta. 2015; 1849: 385–402. doi: 10.1016/j.bbagrm.2014.07.005 PMID: 25038583

2. Carrier DJ, Kendall EJ, Bock CA, Cunningham JE, Dunstan DI. Water content, lipid deposition, and (+)-abscisic acid content in developing white spruce seeds. J Exp Bot. 1999; 50: 1359–1364.

3. Ötvös K, Pasternak TP, Miskolczi P, Domoki M, Dorjgotov D, Szucs A, et al. Nitric oxide is required for, and promotes auxin-mediated activation of, cell division and embryogenic cell formation but does not influence cell cycle progression in alfalfa cell cultures. Plant Journal. 2005; 43: 849–860. doi: 10.1111/j. 1365-313X.2005.02494.x PMID: 16146524

4. Osti RZ, Andrade JBR, Souza JP, Silveira V, Balbuena TS, Guerra MP, et al. Nitrosyl ethylenediamine-tetraacetate ruthenium(II) complex promotes cellular growth and could be used as nitric oxide donor in plants. Plant Sci. 2010; 178: 448–453. doi: 10.1016/j.plantsci.2010.02.006

3. Attree SM, Fowke LC. Embryogeny of gymnosperms—advances in synthetic seed technology of coni-fers. Plant Cell Tiss Org. 1993; 35: 1–35. doi: 10.1007/bf00043936
4. Silveira V, Santa-Catarina C, Tun NN, Scherer GFE, Handro W, Guerra MP, et al. Polyamine effects on the endogenous polyamine contents, nitric oxide release, growth and differentiation of embryogenic suspension cultures of Araucaria angustifolia (Bert.) O. Ktze. Plant Sci. 2006; 171: 91–98. doi: 10.1016/ j.plantsci.2006.02.015
5. Santa-Catarina C, Silveira V, Scherer GFE, Floh EIS. Polyamine and nitric oxide levels relate with mor-phogenetic evolution in somatic embryogenesis of Ocotea catharinensis. Plant Cell Tiss Org. 2007; 90: 93–101. doi: 10.1007/s11240-007-9259-7
6. Vieira LDN, Santa-Catarina C, De Freitas Fraga HP, Wendt Dos Santos AL, Steinmacher DA, Schlogl PS, et al. Glutathione improves early somatic embryogenesis in Araucaria angustifolia (Bert) O. Kuntze by alteration in nitric oxide emission. Plant Sci. 2012; 195: 80–87. doi: 10.1016/j.plantsci.2012.06.011 PMID: 22921001
7. Santa-Catarina C, Silveira V, Balbuena TS, Viana AM, Estelita MEM, Handro W, et al. IAA, ABA, poly-amines and free amino acids associated with zygotic embryo development of Ocotea catharinensis. Plant Growth Regul. 2006; 49: 237–247. doi: 10.1007/s10725-006-9129-z
8. Farias-Soares FL, Steiner N, Schmidt EC, Pereira MLT, Rogge-Renner GD, Bouzon ZL, et al. The tran-sition of proembryogenic masses to somatic embryos in Araucaria angustifolia (Bertol.) Kuntze is related to the endogenous contents of IAA, ABA and polyamines. Acta Physiol Plant. 2014; 36: 1853– 1865. doi: 10.1007/s11738-014-1560-6
9. Planchais S, Glab N, Inzé D, Bergounioux C. Chemical inhibitors: a tool for plant cell cycle studies. Febs Lett. 2000; 476: 78–83. PMID: 10878255
10. Pasternak T, Asard H, Potters G, Jansen MA. The thiol compounds glutathione and homoglutathione differentially affect cell development in alfalfa (Medicago sativa L.). Plant Physiol Biochem. 2014; 74: 16–23. doi: 10.1016/j.plaphy.2013.10.028 PMID: 24246670
11. Inzé D, De Veylder L. Cell cycle regulation in plant development. Annu Rev Genet. 2006; 40: 77–105. PMID: 17094738
12. Dewitte W, Murray JA. The plant cell cycle. Annu Rev Plant Biol. 2003; 54: 235–264. PMID: 14502991
13. Liu X, Winey M. The MPS1 family of protein kinases. Annu Rev Biochem. 2012; 81: 561–585. doi: 10. 1146/annurev-biochem-061611-090435 PMID: 22482908
14. Musacchio A, Salmon ED. The spindle-assembly checkpoint in space and time. Nat Rev Mol Cell Bio. 2007; 8: 379–393.
15. Bennett BL, Sasaki DT, Murray BW, O'leary EC, Sakata ST, Xu W, et al. SP600125, an anthrapyrazo-lone inhibitor of Jun N-terminal kinase. Proc Natl Acad Sci USA. 2001; 98: 13681–13686. PMID: 11717429
16. De Oliveira EaG, Romeiro NC, Da Silva Ribeiro E, Santa-Catarina C, Oliveira AEA, Silveira V, et al. Structural and functional characterization of the protein kinase Mps1 in Arabidopsis thaliana. PloS One. 2012; 7: e45707. doi: 10.1371/journal.pone.0045707 PMID: 23049844
17. Steiner N, Vieira FDN, Maldonado S, Guerra MP. Effect of carbon source on morphology and histodif-ferentiation of Araucaria angustifolia embryogenic cultures. Braz Arch Biol Techn. 2005; 48: 895–903.
18. Steiner N, Farias-Soares F, Schmidt É, Pereira MT, Scheid B, Rogge-Renner G, et al. Toward estab-lishing a morphological and ultrastructural characterization of proembryogenic masses and early somatic embryos of Araucaria angustifolia (Bert.) O. Kuntze. Protoplasma. 2015: 1–15.
19. Altschul SF, Gish W, Miller W, Myers EW, Lipman DJ. Basic local alignment search tool. J Mol Biol. 1990; 215: 403–410. PMID: 2231712
20. Elbl P, Lira BS, Andrade SCS, Jo L, Dos Santos ALW, Coutinho LL, et al. Comparative transcriptome analysis of early somatic embryo formation and seed development in Brazilian pine, Araucaria angusti-folia (Bertol.) Kuntze. Plant Cell Tiss Org. 2015; 120: 903–915.
21. Elbl P, Campos R, Lira B, Andrade S, Jo L, Dos Santos A, et al. Erratum to: comparative transcriptome analysis of early somatic embryo formation and seed development in Brazilian pine, Araucaria angusti-folia (Bertol.) Kuntze. Plant Cell Tiss Org. 2015; 120: 917. doi: 10.1007/s11240-015-0730-6
22. Tamura K, Stecher G, Peterson D, Filipski A, Kumar S. MEGA6: molecular evolutionary genetics analy-sis version 6.0. Mol Biol Evol. 2013; 30: 2725–2729. doi: 10.1093/molbev/mst197 PMID: 24132122
23. Guindon S, Gascuel O. A simple, fast, and accurate algorithm to estimate large phylogenies by maxi-mum likelihood. Syst Biol. 2003; 52: 696–704. PMID: 14530136
24. Arnold K, Bordoli L, Kopp J, Schwede T. The SWISS-MODEL workspace: a web-based environment for protein structure homology modelling. Bioinformatics. 2006; 22: 195–201. PMID: 16301204

A. Biasini M, Bienert S, Waterhouse A, Arnold K, Studer G, Schmidt T, et al. SWISS-MODEL: modelling protein tertiary and quaternary structure using evolutionary information. Nucleic Acids Res. 2014; 42: W252–W258. doi: 10.1093/nar/gku340 PMID: 24782522

B. Kiefer F, Arnold K, Künzli M, Bordoli L, Schwede T. The SWISS-MODEL repository and associated resources. Nucleic Acids Res. 2009; 37: D387–D392. doi: 10.1093/nar/gkn750 PMID: 18931379

C. Dinkel H, Van Roey K, Michael S, Davey NE, Weatheritt RJ, Born D, et al. The eukaryotic linear motif resource ELM: 10 years and counting. Nucleic Acids Res. 2013; 42: gkt1047.

D. Fiser A, Sali A. ModLoop: automated modeling of loops in protein structures. Bioinformatics. 2003; 19: 2500–2501. PMID: 14668246

E. Šali A, Blundell TL. Comparative protein modelling by satisfaction of spatial restraints. J Mol Biol. 1993; 234: 779–815. PMID: 8254673

F. Chu ML, Chavas LM, Douglas KT, Eyers PA, Tabernero L. Crystal structure of the catalytic domain of the mitotic checkpoint kinase Mps1 in complex with SP600125. J Biol Chem. 2008; 283: 21495–21500. doi: 10.1074/jbc.M803026200 PMID: 18480048

G. Wang W, Yang Y, Gao Y, Xu Q, Wang F, Zhu S, et al. Structural and mechanistic insights into Mps1 kinase activation. J Cell Mol Med. 2009; 13: 1679–1694. doi: 10.1111/j.1582-4934.2008.00605.x PMID: 19120698

H. Chu ML, Lang Z, Chavas LM, Neres J, Fedorova OS, Tabernero L, et al. Biophysical and X-ray crystal-lographic analysis of Mps1 kinase inhibitor complexes. Biochemistry. 2010; 49: 1689–1701. doi: 10. 1021/bi901970c PMID: 20099905

I. Morris GM, Huey R, Lindstrom W, Sanner MF, Belew RK, Goodsell DS, et al. AutoDock4 and Auto-DockTools4: automated docking with selective receptor flexibility. J Comput Chem. 2009; 30: 2785– 2791. doi: 10.1002/jcc.21256 PMID: 19399780

J. Seeliger D, De Groot BL. Ligand docking and binding site analysis with PyMOL and Autodock/Vina. J Comput Aid Mol Des. 2010; 24: 417–422.

K. Lee T-Y, Bretaña NA, Lu C-T. PlantPhos: using maximal dependence decomposition to identify plant phosphorylation sites with substrate site specificity. BMC bioinformatics. 2011; 12: 261. doi: 10.1186/ 1471-2105-12-261 PMID: 21703007

L. Becwar MR, Noland TL, Wyckoff JL. Maturation, germination, and conversion of Norway spruce (Picea abies L.) somatic embryos to plants. In Vitro Cel Dev Biol Plant. 1989; 25: 575–580.

M. Balbuena TS, Silveira V, Junqueira M, Dias LLC, Santa-Catarina C, Shevchenko A, et al. Changes in the 2-DE protein profile during zygotic embryogenesis in the Brazilian Pine (Araucaria angustifolia). J Proteomics. 2009; 72: 337–352. doi: 10.1016/j.jprot.2009.01.011 PMID: 19367732

N. Reis RS, Vale EDM, Heringer AS, Santa-Catarina C, Silveira V. Putrescine induces somatic embryo development and proteomic changes in embryogenic callus of sugarcane. J Proteomics. 2016; 130: 170–179. doi: 10.1016/j.jprot.2015.09.029 PMID: 26435420

O. Amborella Genome Project. The Amborella genome and the evolution of flowering plants. Science. 2013; 342: 1241089. doi: 10.1126/science.1241089 PMID: 24357323

P. London N, Biggins S. Signalling dynamics in the spindle checkpoint response. Nat Rev Mol Cell Bio. 2014; 15: 736–748. doi: 10.1038/nrm3888

Q. Mattison CP, Old WM, Steiner E, Huneycutt BJ, Resing KA, Ahn NG, et al. Mps1 activation loop autop-hosphorylation enhances kinase activity. J Biol Chem. 2007; 282: 30553–30561. doi: 10.1074/jbc. M707063200 PMID: 17728254

R. Tipton AR, Ji W, Sturt-Gillespie B, Bekier ME, Wang K, Taylor WR, et al. Monopolar spindle 1 (MPS1) kinase promotes production of closed MAD2 (C-MAD2) conformer and assembly of the mitotic check-point complex. J Biol Chem. 2013; 288: 35149–35158. doi: 10.1074/jbc.M113.522375 PMID: 24151075

S. Zhao Y, Chen R-H. Mps1 phosphorylation by MAP kinase is required for kinetochore localization of spindle-checkpoint proteins. Curr Biol. 2006; 16: 1764–1769. PMID: 16950116

Anexo 2

bio-protocol
www.bio-protocol.org/e2031
Vol 6, Iss 23, Dec 05, 2016
DOI:10.21769/BioProtoc.2031

Isolating and Measuring the Growth and Morphology of Pro-Embryogenic Masses in *Araucaria angustifolia* (Bertol.) Kuntze (Araucariaceae)

Jackellinne Caetano Douétts-Peres[1], Vanildo Silveira[2, 3], Marco Antonio Lopes Cruz[4], Claudete Santa-Catarina[1, *]

[1]Laboratório de Biologia Celular e Tecidual, Centro de Biociências e Biotecnologia (CBB), Universidade Estadual do Norte Fluminense Darcy Ribeiro (UENF), Campos dos Goytacazes, Rio de Janeiro, Brazil; [2]Laboratório de Biotecnologia, CBB, UENF, Campos dos Goytacazes, Rio de Janeiro, Brazil; [3]Unidade de Biologia Integrativa, Setor de Genômica e Proteômica, UENF, Campos dos Goytacazes, Rio de Janeiro, Brazil; [4]Laboratório de Biotecnologia Vegetal, Núcleo em Ecologia e Desenvolvimento Sócio-ambiental de Macaé, Universidade Federal do Rio de Janeiro, Macaé, Rio de Janeiro, Brazil
*For correspondence: claudete@uenf.br

[Abstract] Embryogenic suspension cultures of *Araucaria angustifolia* (Bertol.) Kuntze (Araucariaceae) can be used as a model to test the effects of compounds added to the culture medium on the cellular growth and morphology of Pro-Embryogenic Masses (PEMs). PEMs are formed by embryogenic and suspensor-type cells. To measure changes in the cellular growth of embryogenic cultures, we performed sedimented cell volume (SCV) quantification, which is a non-destructive method. Morphological analysis by microscopy allowed for the observation of growth and development of PEMs and the alterations in embryogenic and suspensor-type cells. The methods used here provide an efficient means for monitoring the cellular growth of PEMs and identifying morphological changes during the development of embryogenic cultures. These studies can also be combined with biochemical and molecular analyses, such as proteomics, to further investigate embryo growth and morphology.

Keywords: Somatic embryogenesis, Size, Sedimented cell volume

[Background] Silveira *et al.* (2006) used SCV measurements to analyze the effects of exogenous polyamines on the morphological changes of *A. angustifolia* PEMs and Osti *et al.* (2010) tested the effect of different nitric oxide donors on cellular growth and PEM morphology. Recently, Douétts-Peres *et al.* (2016) studied the effect of a cellular growth inhibitor on cellular growth and PEM morphology using SCV, fresh and dry weight, PEM area, and individual diameters of embryogenic-type cells, including the length and width of the suspensor-type cells. In addition, alterations to cellular growth and morphology in response to endogenous compounds, such as polyamines, nitric oxide and specific proteins have been evaluated using this method (Silveira *et al.*, 2006; Osti *et al.*, 2010; Douétts-Peres *et al*., 2016).

Materials and Reagents

1. Falcon tube rack (Kasvi, catalog number: K30-1552)

Vol 6, Iss 23, Dec 05, 2016
DOI:10.21769/BioProtoc.2031

4. 12-well cell culture plates - disposable (TPP, catalog number: 92012)
5. Manual pipette 200 µl tips (Corning, Axygen®, catalog number: T-200-Y)
6. Manual pipette 1,000 µl tips (Corning, Axygen®, catalog number: T-1000-B)
7. Aluminum foil
8. Glass slides (Kasvi, catalog number: K5-7101)
9. Cover slips (Kasvi, catalog number: K5-2450)
10. Falcon tubes, 50 ml (Kasvi, catalog number: K19-0050)
11. Embryogenic suspension cultures of *A. angustifolia*, induced according to the methodology established by Steiner *et al.* (2005)
12. Cellulase (Sigma-Aldrich, catalog number: 22178)
13. Potassium nitrate (KNO_3) (Sigma-Aldrich, catalog number: V000944)
14. Calcium chloride dihydrate ($CaCl_2 \cdot 2H_2O$) (Sigma-Aldrich, catalog number: V000199)
15. Magnesium sulfate heptahydrate ($MgSO_4 \cdot 7H_2O$) (Sigma-Aldrich, catalog number: V001861)
16. Potassium chloride (KCl) (Sigma-Aldrich, catalog number: V000104)
17. Potassium dihydrogen phosphate (KH_2PO_4) (EMD Millipore, catalog number: 104873)
18. $MnSO_4 \cdot H_2O$ (Labsynth, catalog number: S2036)
19. $ZnSO_4 \cdot 7H_2O$ (Labsynth, catalog number: S1072)
20. Boric acid (H_3BO_3) (Sigma-Aldrich, catalog number: 31146)
21. Potassium iodide (KI) (Sigma-Aldrich, catalog number: V000130)
22. Cobalt(II) chloride hexahydrate ($CoCl_2 \cdot 6H_2O$) (Sigma-Aldrich, catalog number: V000213)
23. $CuSO_4 \cdot 5H_2O$ (Labsynth, catalog number: S1054)
24. Sodium molybdate dihydrate ($Na_2MoO_4 \cdot 2H_2O$) (Sigma-Aldrich, catalog number: M1651)
25. $FeSO_4 \cdot 7H_2O$ (Labsynth, catalog number: S1057)
26. Na_2EDTA (Labsynth, catalog number: E2005)
27. Myo-inositol (Sigma-Aldrich, catalog number: I17508)
28. Nicotinic acid (Labsynth, catalog number: A1043)
29. Pyridoxine (Sigma-Aldrich, catalog number: P9755)
30. Thiamine (Sigma-Aldrich, catalog number: T4625)
31. L-glutamine (Labsynth, catalog number: G1011)
32. Sucrose (Labsynth, catalog number: 2731)
33. MSG culture medium (see Recipes)

Equipment

5. Cell dissociation sieve-screens, 150 mesh (Sigma-Aldrich, catalog number: CD1-1KT) sterilized by autoclave (121 °C, 30 min)
6. Chamber flow (or its equivalent) (Pachame, model: PA 220)

Vol 6, Iss 23, Dec 05, 2016
DOI:10.21769/BioProtoc.2031

25. Adapted glass Erlenmeyer flasks (custom-made) (Figure 1), sterilized by autoclave (121 °C, 30 min). This adjustment to the flask can be performed by a company that produces laboratory glassware, fusing a glass tube to an Erlenmeyer flask
26. Ruler
27. Orbital shaker (or its equivalent) (Cientec Equipamentos para Laboratório, model: CT-165)
28. Analytical balance (or its equivalent) (Shimadzu, model: BL3200H)
29. Spatula sterilized by autoclave (121 °C, 30 min) (VWR, catalog number: 231-2233)
30. AxioPlan light microscope (Carl Zeiss, model: AxioPlan)
31. Manual pipettes (or their equivalent) (Eppendorf, catalog numbers: 3120000062 and 3120000054)
32. Forced air circulation drying oven (or its equivalent) (Ethik Technology, model: 420-6D)
33. AxioCam MRC5 digital camera (Carl Zeiss, model: AxioCam)
34. Desktop computer

Figure 1. Adapted Erlenmeyer flasks (100 and 50 ml) used in SCV analyses. For an adapted Erlenmeyer flask of 100 ml capacity, we used 25 ml of culture medium and 500 mg of fresh cells. For an adapted Erlenmeyer flask with 50 ml capacity, we used 10 ml of culture medium and 200 mg of fresh cells, with a ratio of 20 mg fresh cells to 1 ml of culture medium.

Software

1. AxioVision Rel. 4.8 software (Carl Zeiss, AxioVision)

Procedure

T. SCV analysis
   1. First, in the flow chamber, separate the embryogenic suspension cultures from the medium using the cell dissociation sieve (150 mesh screens) (Figure 2A).

Vol 6, Iss 23, Dec 05, 2016
DOI:10.21769/BioProtoc.2031

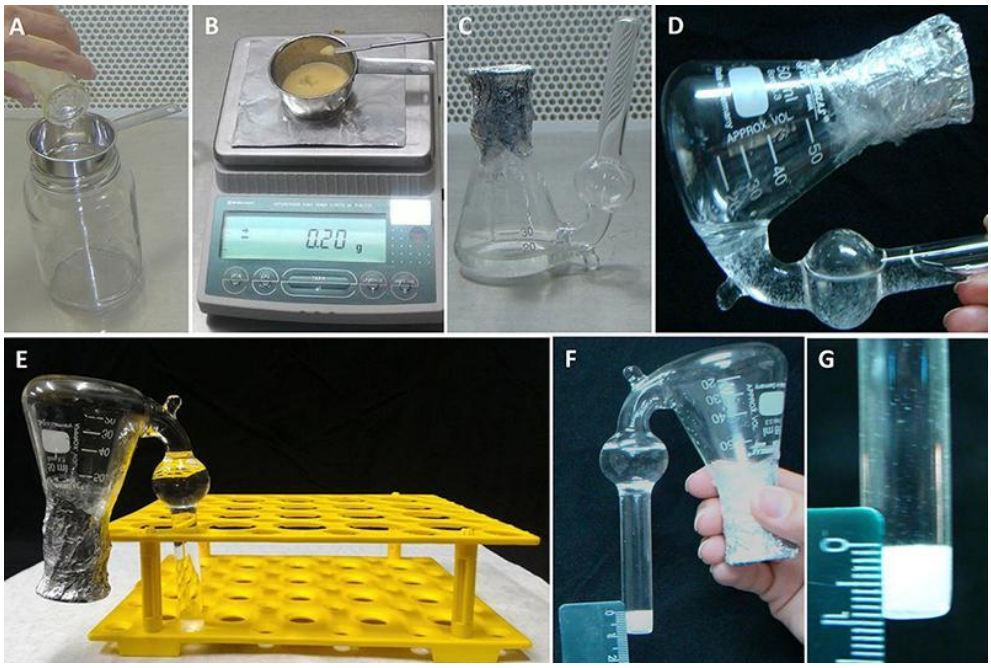

Figure 2. SCV analysis procedures. A. Separation of cells from the culture medium using the sieve; B. Sampling the cells (in terms of fresh weight) for the SCV analyses; C. Adapted Erlenmeyer flask containing the culture medium with inoculated cells; D. Transferring the cells and culture medium to the lateral side tube of the adapted Erlenmeyer flask for SCV measurement; E. Erlenmeyer flask held upright for 15 min; F and G. Details of SCV measurement using the ruler.

2. Then, place 200 mg of culture (fresh weight) consisting of separated cells in an adapted Erlenmeyer flask (Figure 1) containing 10 ml of the culture medium containing the required testing treatments (Figures 2B and 2C).
3. To measure the initial SCV, transfer the entire contents of the flask (culture medium and cells) to the adapted tube outside of the Erlenmeyer flask (Figure 2D). Keep upright in a Falcon tube rack (Figure 2E) for 15 min.
4. After this time, measure the initial SCV using a ruler (Figures 2F and 2G).
5. Later, return the entire contents (culture medium + cells) into the Erlenmeyer flask by carefully inverting to make sure to return most of the cells into the Erlenmeyer flask (Figure 2C). Keep the adapted Erlenmeyer flasks on a horizontal shaker (100 rpm in the dark at 25 ± 2 °C).
6. To determine PEM growth, repeat the measurement procedures every three days until the PEMs reach the decline phase.

Notes:

a. *A cellular growth curve (Figure 3) is performed to identify the phases of cellular growth of the embryogenic cultures in suspension. This identification can be used to establish the sampling points for the assessment of morphology and for biochemical studies.*
b. *If an Erlenmeyer flask of 100 ml capacity is used, we suggest the following proportion: 25 ml of*

Vol 6, Iss 23, Dec 05, 2016
DOI:10.21769/BioProtoc.2031

culture medium used for every 500 mg of fresh cells.

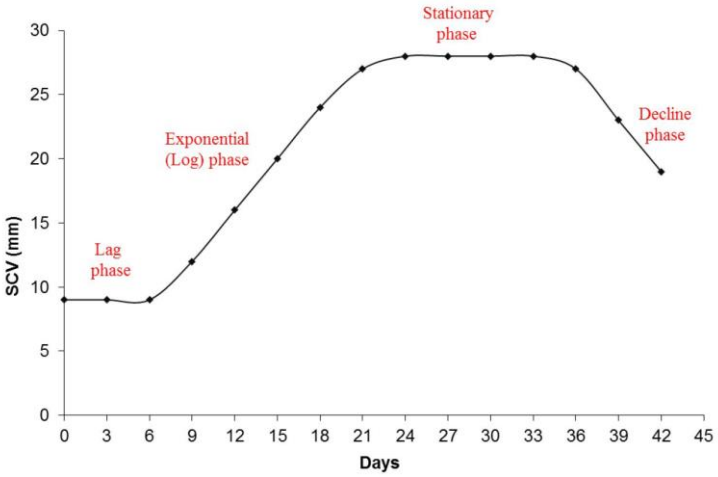

Figure 3. Graphic representation of the cellular growth by SCV. A cellular growth curve by SCV analysis from embryogenic suspension cultures of *A. angustifolia* in MSG culture medium showing the different phases during incubation.

B. Fresh and dry weight measurement
   1. Use 12-well cell culture plates for this analysis.
   2. In a flow chamber, separate the cells from the suspension cultures using a sieve to collect only the cells; discard the culture medium (Figure 2A).
   3. Next, use the analytical balance (Figure 2B) to weigh the cells and place 60 mg fresh cells into each well of the cell culture plate, which should contain 2 ml of culture medium per well (Figure 4A).
   4. Close the cell culture plates and keep on a horizontal shaker for incubation (100 rpm in the dark at 25 ± 2 °C).
   5. To measure the fresh weight on specific days (established by the growth curve, for example), take the cell culture plate and carefully remove the liquid culture medium using a pipette (Figure 4B). Repeat this procedure for each individual well.
   6. Use a spatula to collect all the solid contents of the cell culture from each well (Figure 4C), separately, on a piece of pre-weighed aluminum foil.
   7. Measure the fresh weight of cells using an analytical balance (Figure 4D). Dry the samples at 70 °C for 48 h. Then, measure the samples plus aluminum foil again on the analytical balance. It is necessary to subtract the weight of the aluminum foil (pre-weighed) to obtain the dry weight.

Vol 6, Iss 23, Dec 05, 2016
DOI:10.21769/BioProtoc.2031

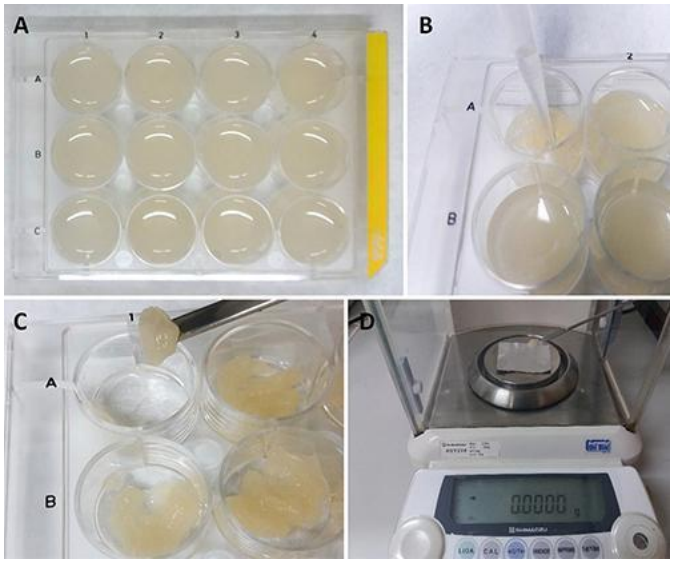

Figure 4. Measurement of fresh weight using 12-well cell culture plates. A. 12-well cell culture plates with cellular culture; B. Removal of liquid culture medium using a pipette; C. Collection of the cells from each well using a spatula; D. Measurement of the fresh weight with an analytical balance using pre-weighed aluminum foil.

C. Slide preparation for PEM morphology studies

1. First, in the flow chamber, separate the embryogenic suspension cultures from the medium using the cell dissociation sieve (150 mesh screens) (Figure 2A).
2. Then, 1,200 mg of separated cells, fresh weight (Figure 2B), should be placed into an Erlenmeyer flask (250 ml capacity) containing 60 ml of the culture medium containing the required testing treatments. Three flasks for each treatment should be maintained for three biological replicates.
3. Place the flasks on a horizontal shaker during incubation (100 rpm in the dark at 25 ± 2 °C).
4. For analyzing the incubation results on specific days, in a flow chamber, take a sample of PEMs from the liquid culture medium using the modified pipette tip. It is necessary to remove the end of the pipette tip (Figures 5A and 5B) to prevent the disruption of PEMs. The pipette tips must be sterilized before use.
5. Put a drop of the PEM culture on a glass slide (Figure 5C), and cover with a cover slip.
6. Observe under an optical microscope.

Notes:

a. *The remaining cells in the flask could be returned to the horizontal shaker for use on the next day of analysis. If you do not continue the incubation, and the cells will be discarded, it is not necessary to use a sterilized pipette tip for sampling.*
b. *The PEMs can alternatively be incubated in an Erlenmeyer flask with a smaller volume (keeping the ratio of 20 mg fresh cells for 1 ml of culture medium).*

Vol 6, Iss 23, Dec 05, 2016
DOI:10.21769/BioProtoc.2031

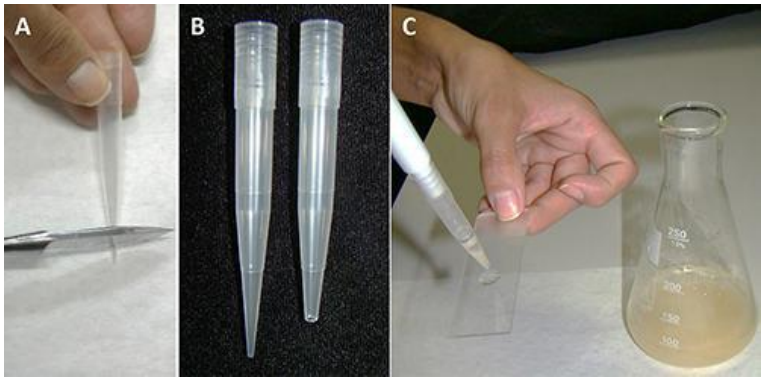

Figure 5. Slide preparation of PEMs from embryogenic suspension culture. A. Removal of the end of a tip; B. Comparison of the tip before and after cutting; C. Plating with a drop of PEMs in suspension culture.

D. Slide preparation for isolated embryogenic and suspensor-type cells

1. First, dissociate the PEMs to obtain embryogenic and suspensor-type cells by incubating the PEM suspension culture in culture medium with 0.1% (w/v) cellulase (Sigma-Aldrich).
2. Keep the samples incubating in cellulase for 3 h on a rotary shaker (100 rpm) in the dark at 25 ± 2 °C.
3. After incubation, transfer the cells to a Falcon tube and wash with a new culture medium that is cellulose free. Remove the culture medium carefully with a pipette and repeat this procedure three times.
4. To visualize the cells with an optical microscope, follow the procedure described in Procedure C used to prepare slides using a modified pipette tip.

E. Image capture

1. To capture images for morphological analysis, we use AxioVision Rel. 4.8 software according to the following procedures (other comparable image analysis software should suffice):
    a. Open the software AxioVision Rel. 4.8, and in the Tool Bar, select: View>Toolbars>Standard.
    b. To view the image on the screen: click the ‘Live’ option.
    c. Set in the software the specifications of the objective and ocular you are using to capture the image using the ‘Snap’ option.
    d. When saving the image, choose the .zvi format.

F. Procedure for morphological measurement and analysis

1. Area measurement
    a. Open the image in the microscope software.
    b. Choose the options: View>Toolbars>Measure.
    c. To measure the area, use the tool options, ‘outline’ or ‘outline spline’.
    d. Then, draw a closed shape around the embryonal head (Figures 6A and 7). When the form

Vol 6, Iss 23, Dec 05, 2016
DOI:10.21769/BioProtoc.2031

is closed, the area appears on the figure in μm^2. This value is used for area analyses.

e. Repeat this operation with several samples of embryonal head and suspensor-type cell images.

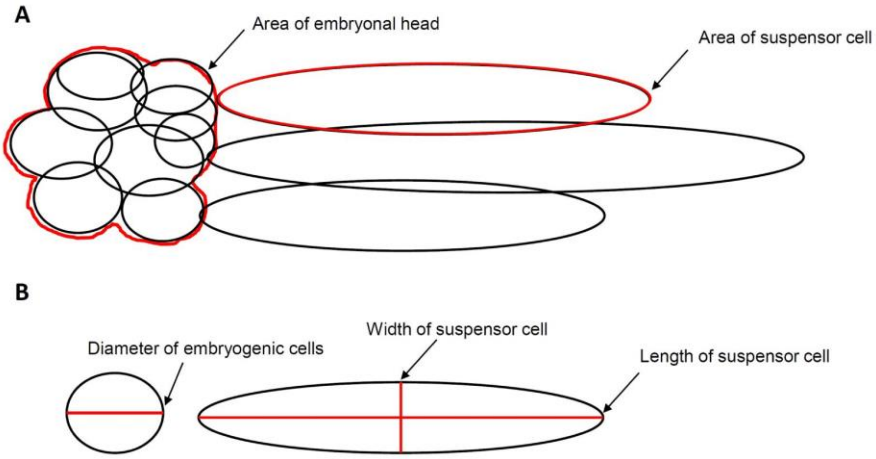

Figure 6. Measurement scheme of PEMs and isolated cells. A. Area analysis of embryonal head and suspensor-type cells from non-dissociated PEMs; B. Diameter, length and width analysis of dissociated embryogenic and suspensor-type cells.

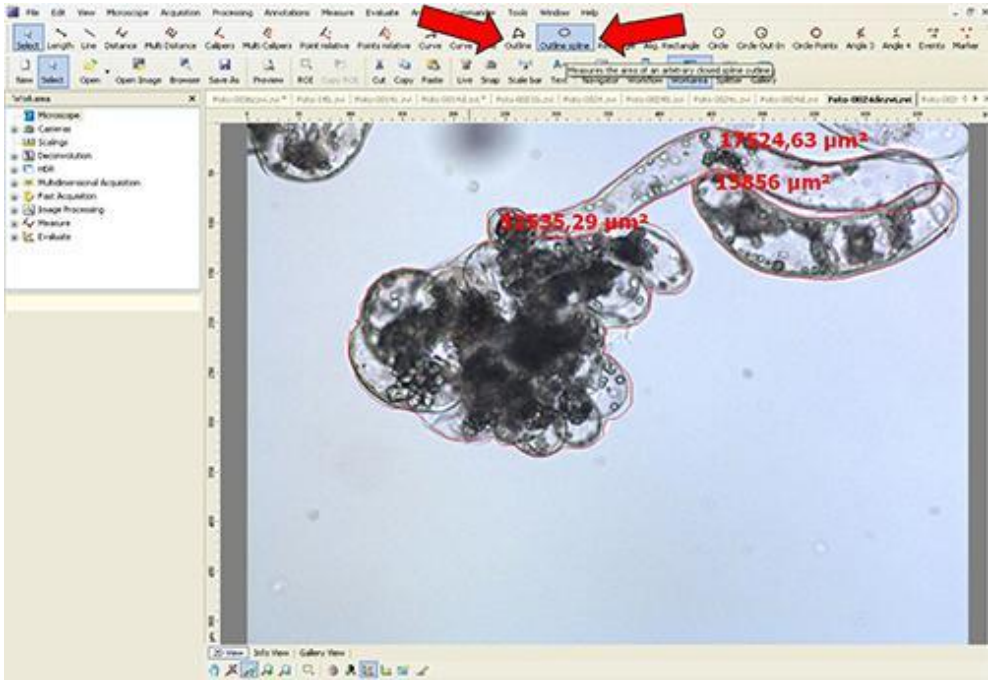

Figure 7. Area measurement procedure for non-dissociated PEMs using AxioVision software. Arrows (red) indicate the tool options used.

2. Diameter, width and length measurement
   a. Open the image in the microscope software.
   b. Choose the options: View>Toolbars>Measure

Vol 6, Iss 23, Dec 05, 2016
DOI:10.21769/BioProtoc.2031

c. To measure the area, use the tool option ‘length’.
d. Then, using the ‘length’ tool, measure the embryogenic-type cells to obtain the diameter data (see red line in Figure 6B and black line in Figure 8).
e. Using the ‘length’ tool, measure the length and width in suspensor-type cells, as shown by a black line in Figure 8.
f. Repeat this operation with several samples of dissociated embryogenic and suspensor cells.

Notes:

a. In Araucaria, as embryogenic-type cells are isodiametric, the size was measured based on the diameter, and as suspensor-type cells are elliptic and elongated, the size was measured using the length and width (at the middle of the cell) (Figure 8).
b. If the suspensor-type cells are curved, the ‘curve spline’ tool can be used as shown in Figure 9.

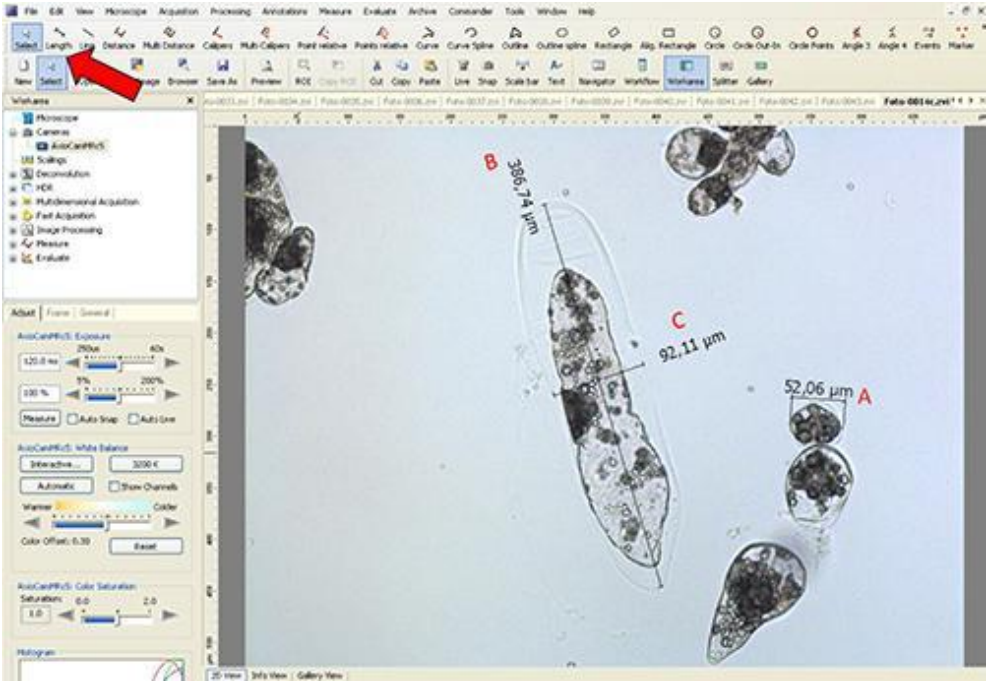

Figure 8. **Measurement of diameter, width and length of embryogenic and suspensor-type cells using AxioVision LE software.** The red arrow indicates the tool used for A. diameter analysis of embryogenic-type cells, B. length and C. width in suspensor-type cells.

Vol 6, Iss 23, Dec 05, 2016
DOI:10.21769/BioProtoc.2031

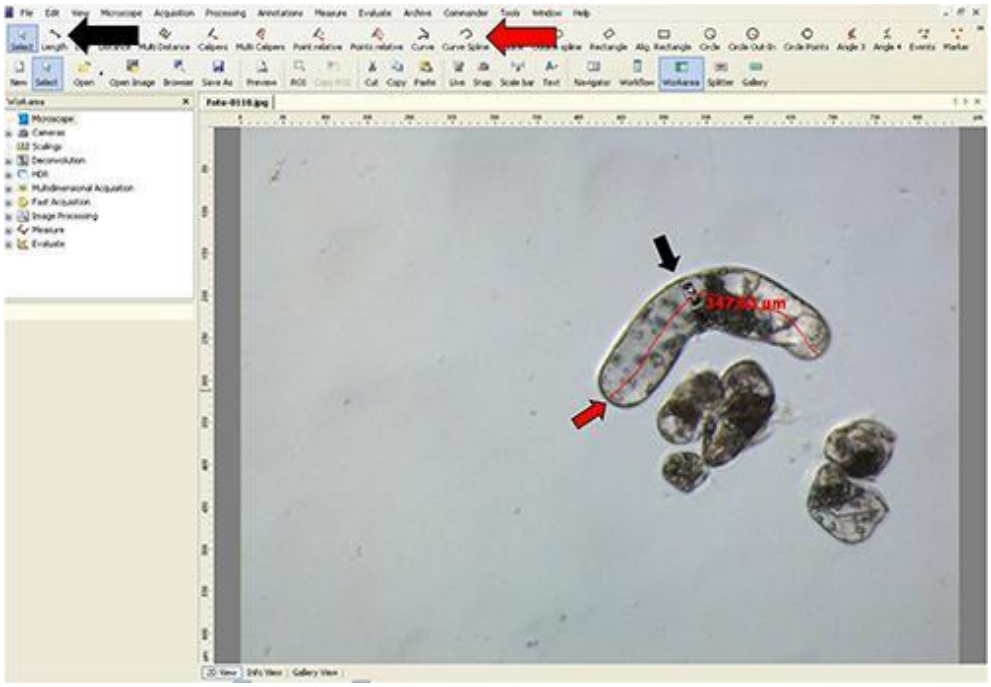

Figure 9. **Width and length measurements of suspensor-type cells using AxioVision software.** The red arrow indicates the 'Curve spline' tool used for length of curved suspensor-type cells, and the black arrow indicates the 'Length' tool used for width of these cells.

Data analysis

1. For the analysis of area, diameter, length and width, the values of different samples can be processed and presented in a graph format. Additionally, the data can be subjected to analysis of variance (ANOVA) and mean separation tests (such as Tukey or SNK) by using an appropriate statistical software.
2. SCV analysis: examples of results obtained from SCV analysis can be observed in Figure 1 of Silveira *et al.* (2006), Figure 2 of Osti *et al.* (2010) and Figure 4 of Douétts-Peres *et al.* (2016).
3. Fresh and dry weight analysis: Figure 5 of Douétts-Peres *et al.* (2016) is an example of fresh and dry weight measurement.
4. Cell size determination: Area measurement of the embryonal head and suspensor-type cells described here (Figure 6) can be observed in Figure 7 of Douétts-Peres *et al.* (2016). In addition, the diameter of embryogenic-type cells and the width and length of suspensor-type cells can be observed in Figure 8 of Douétts-Peres *et al.* (2016).

Vol 6, Iss 23, Dec 05, 2016
DOI:10.21769/BioProtoc.2031

Recipes

1. MSG culture medium (1 L) (Becwar *et al.*, 1989)

Reagents for making MSG culture medium	Final concentration in culture medium (/L)
KNO_3	100 mg
$CaCl_2 \cdot 2H_2O$	440 mg
$MgSO_4 \cdot 7H_2O$	320 mg
KCl	745 mg
KH_2PO_4	170 mg
$MnSO_4 \cdot H_2O$	22.3 mg
$ZnSO_4 \cdot 7H_2O$	8.6 mg
H_3BO_3	6.2 mg
KI	0.83 mg
$CoCl_2 \cdot 6H_2O$	0.025 mg
$CuSO_4 \cdot 5H_2O$	0.025 mg
$Na_2MoO_4 \cdot 2H_2O$	0.25 mg
$FeSO_4 \cdot 7H_2O$	27.8 mg
Na_2EDTA	37.3 mg
Nicotinic acid	0.5 mg
Pyridoxine	0.5 mg
Thiamine	1 mg
Myo-Inositol	100 mg
L-glutamine	1,460 mg
Sucrose	30 g

a. Preparation of liquid MSG culture medium
   i. To prepare 1 L of liquid MSG culture medium, weigh 30 g of sucrose and dissolve in ~500 ml of distilled water.
   ii. Add 100 ml solution A, 5 ml solution B, 10 ml solution C and 2 ml solution D. Add 1,460 mg of L-glutamine.
   iii. Dissolve all reagents. Adjust the volume with distilled water to 1 L. Mix the culture medium and adjust the pH to 5.7. Sterilize in an autoclave for 15 min at 121 °C.

b. Preparation of stock solutions
   i. To prepare stock solutions A, B and D, weigh the reagents in an analytical balance, dissolve in distilled water, and make up the final volume with distilled water.
   ii. To prepare stock solution C, weigh each reagent and add separately to ~150 ml of heated distilled water (~45 °C). Then, mix the two solutions and adjust the final volume to 500 ml. Protect this solution from light.

Reagents for Solution A	For 500 ml of stock solution A
KNO_3	500 mg
$CaCl_2 \cdot 2H_2O$	2,200 mg
$MgSO_4 \cdot 7H_2O$	1,600 mg
KCl	3,730 mg
KH_2PO_4	850 mg

Reagents for Solution B	For making 200 ml of stock solution B
$MnSO_4 \cdot H_2O$	892 mg
$ZnSO_4 \cdot 7H_2O$	344 mg
H_3BO_3	248 mg
KI	33 mg
$CoCl_2 \cdot 6H_2O$	1 mg
$CuSO_4 \cdot 5H_2O$	1 mg
$Na_2MoO_4 \cdot 2H_2O$	10 mg

Reagents for Solution C	For 500 ml of stock solution C
$FeSO_4 \cdot 7H_2O$	1,390 mg
Na_2EDTA	1,865 mg

Reagents for Solution D	For 500 ml of stock solution D
Nicotinic acid	25 mg
Pyridoxine	25 mg
Thiamine	50 mg
Myo-Inositol	5,000 mg

Acknowledgments

This work was supported by FAPERJ (Foundation for Research Support of the State of Rio de Janeiro) and CNPq (National Counsel of Technological and Scientific Development). The VCS method presented was derived from Silveira *et al*. (2006).

References

1. Becwar, M. R., Noland, T. L. and Wyckoff, J. L. (1989). Maturation, germination, and conversion of Norway spruce (*Picea abies* L.) somatic embryos to plants. *In vitro Cell Dev* 25(6): 575-580.
2. Douétts-Peres, J. C., Cruz, M. A., Reis, R. S., Heringer, A. S., de Oliveira, E. A., Elbl, P. M., Floh, E. I., Silveira, V. and Santa-Catarina, C. (2016). Mps1 (Monopolar Spindle 1) protein inhibition affects cellular growth and pro-embryogenic masses morphology in embryogenic cultures of *Araucaria angustifolia* (Araucariaceae). *PLoS One* 11(4): e0153528.
3. Osti, R. Z., Andrade, J. B. R., Souza, J. P., Silveira, V., Balbuena, T. S., Guerra, M. P., Franco, D. W., Floh, E. I. S. and Santa-Catarina, C. (2010). Nitrosyl ethylenediaminetetraacetate ruthenium(II)

Vol 6, Iss 23, Dec 05, 2016
DOI:10.21769/BioProtoc.2031

complex promotes cellular growth and could be used as nitric oxide donor in plants. *Plant Sci* 178(5): 448-453.

4. Silveira, V., Santa-Catarina, C., Tun, N. N., Scherer, G. F. E., Handro, W., Guerra, M. P. and Floh, E. I. S. (2006). Polyamine effects on the endogenous polyamine contents, nitric oxide release, growth and differentiation of embryogenic suspension cultures of *Araucaria angustifolia* (Bert.) O. Ktze. *Plant Sci* 171(1): 91-98.
5. Steiner, N., Vieira, F. D. N., Maldonado, S. and Guerra, M. P. (2005). Effect of carbon source on morphology and histodifferentiation of *Araucaria angustifolia* embryogenic cultures. *Braz Arch of Bio Technol* 48(6): 895-903.